COMPUTATIONAL FLUID DYNAMICS MODELING OF THERMAL QUENCHING IN SONIC PROBE FLOW

by

JOSIAH BREDA-NIXON

(Under the Direction of Brandon Rotavera)

ABSTRACT

Computational fluid dynamics (CFD) modeling was conducted on flow inside of three different sonic probes used for sampling gases from a combustion reactor. The effects of inlet temperature and pressure were analyzed to quantify thermal quenching rates resulting from expansion cooling. Gas-phase nitrogen was used to simulate flows occurring in jet-stirred reactors, which commonly utilize >97% (vol.) N_2. The process was modeled as adiabatic (i.e. wall heat transfer is neglected because of the probe material (quartz) and short residence time) and boundary conditions were: (1) P_{inlet} = 1, 10, and 25 atm; (2) P_{outlet} = 0.08 atm; (3) T_{inlet} = 500, 750, 1000 K; (4) T_{outlet} = 300 K. The major outcomes are computed temperature and pressure gradients in space and time and over the length of the sonic probe (0.85 m), which provided comprehensive understanding of sonic probe flow.

INDEX WORDS: Computational fluid dynamics, sonic probe, aerodynamic quench

COMPUTATIONAL FLUID DYNAMICS MODELING OF THERMAL QUENCHING IN SONIC PROBE FLOW

by

JOSIAH BREDA-NIXON

B.S., Tuskegee University, 2019

A Thesis Submitted to the Graduate Faculty of The University of Georgia in Partial Fulfillment of the Requirements for the Degree

MASTER OF SCIENCE

ATHENS, GEORGIA

2021

COMPUTATIONAL FLUID DYNAMICS MODELING OF THERMAL QUENCHING IN SONIC PROBE FLOW

by

JOSIAH BREDA-NIXON

Major Professor:	Brandon Rotavera
Committee:	C. Brock Woodson
	Rawad Saleh

Electronic Version Approved:

Ron Walcott
Vice Provost for Graduate Education and Dean of the Graduate School
The University of Georgia
August 2021

DEDICATION

I am dedicating the thesis to both my parents, Daray Breda and Charles Nixon, for pushing me to endure the struggles along the way because everyday isn't going to be a breeze. Some days aren't as good as others and that's okay. They have guided me and helped mold me into the person that I am today. They're available when I need them and I know they want the best for me, so I'm glad they were able to be with me through this process. I am proud to be their son.

ACKNOWLEDGEMENTS

I would like to thank Dr. Rotavera for first, giving me the opportunity to be a part of his research group. Additionally, I'd like to thank him for the boundless knowledge that he has shared with me over my two yeas here at UGA. He is not only a great teacher, but also a great mentor that is very logical and precise with the information he gives. I feel exceptionally ready to transition into my career as an engineer because of my experiences with him.

I would also like to thank my girlfriend, Morgan Brathwaite, for helping me reach this milestone as well. She has supported and pushed me along through this process and I couldn't thank her enough. Having her with me day in and day out has been a relief, especially with the recent pandemic. She is currently going into her third year of vet school here at UGA and I aim to support her just as she has me through the rest of her process.

Lastly, I would like to thank the support staff and engineers over at Convergent Science for really helping me along through this process as well.

TABLE OF CONTENTS

Page

LIST OF TABLES

Page

LIST OF FIGURES

Page

CHAPTER 1

INTRODUCTION AND BACKGROUND

Combustion drives the global economy and today, transportation is almost entirely (>99%) powered by internal combustion engines (ICE) [1]. This is important because society continues to rely heavily on ICE for transportation, commerce, and power generation [2]. A study from 2012 by Reitz showed that there were about 750 million passenger cars worldwide with 250 million in the U.S. alone [2]. This number only includes the passenger cars that are considered internal combustion engine vehicles (ICEV) and the number has only increased since then. Even with the rise in interest for battery electric vehicles (BEV) and plug-in hybrid electric vehicles (PHEV), it is unlikely that they will surpass ICE any time soon. Current sales of electric vehicles in the United States are <1%. While this electrification route may come across as appealing because the world is moving towards a future in transportation with cleaner emissions and lower fuel consumption while still achieving the same reliability of vehicles today, many barriers, technological and otherwise, exist. However, certain barriers prevent such alternatives from coming to fruition in the next 10-20 years; these barriers include an overwhelming cost and a current power infrastructure which is unlikely to be able to support such a large demand of energy to support a full transition from ICEV to BEV and PHEV. By focusing more research towards improving ICE efficiency, the same goals can be met in a similar way and, importantly, on a shorter time scale [3].

Low-temperature combustion

One major research area for ICE is low-temperature combustion (LTC). Our group performs experiments and quantum chemical calculations in this LTC range to produce chemical insight used in experimental models that support the development of computer models used to design high combustion efficiencies and lower fuel consumption and emissions. The operating temperatures for LTC range between 500 K and 1200 K which is significantly lower than a diesel engine or a spark-ignition engine which operates around 2000 K. Operating with LTC directly affects fuel emissions and the emissions from these combustion processes have a large influence on air quality, environment, climate, and health [4]. By performing combustion research in the LTC range there will be a significant reduction in toxic emissions such as NOx and particulate matter; this is depicted in Figure 1. Additionally, by using LTC conditions in laboratory experiments, combustion conditions can mimic that of a homogenous charge compression ignition (HCCI) engine which is an ideal combustion process for internal combustion engines, since it can deliver high fuel and thermal efficiencies [5]. Another benefit of using LTC is that a variety of fuel mixtures can be used and resources are not limited to gasoline or diesel fuel. However, some challenges that come with operating with these different fuel mixtures in the LTC range are knowing how these fuels will react under LTC conditions and what parameters would be considered optimal for these fuels. This is important because the fuels will breakdown into different components under lower temperatures compared to higher temperatures [6]. Another challenge is that these processes rely on autoignition of the fuel so, not every fuel will combust in the same amount of time. With these challenges, data must be collected and recorded under these low temperatures to develop profiles for how different fuel mixtures act.

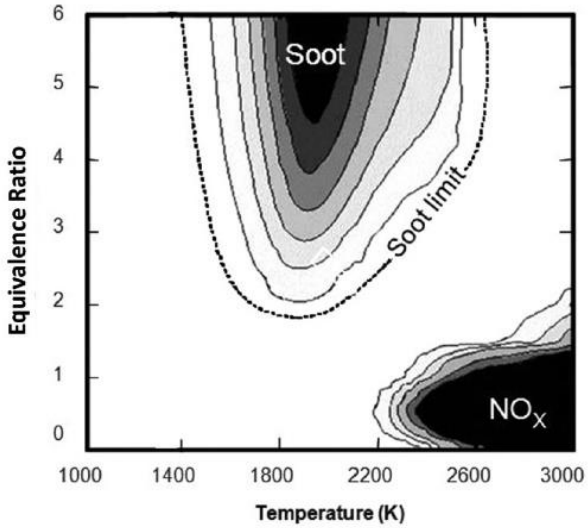

Figure 1: Temperature vs. equivalence ratio graph showing the soot and NOx islands. The equivalence ratio is a metric for quantifying the amount of fuel relative to the ideal amount of air required for complete combustion.

Jet-stirred reactors

In order to help achieve high thermal and combustion efficiencies, a jet-stirred reactor (JSR) is employed by the Rotavera Group for LTC experiments; an image of the JSR is shown in Figure 2. This JSR is a spherical flow reactor that is 30 cm^3 in volume, with jets that extend towards the center and support continuous, homogenous flow used to study chemical kinetics [7]. The JSR produces homogenous conditions, which is essential for the proper air and fuel mixing experimentally. It was designed and constructed to produce control dilute reactive flows with precise control over variables that are important to combustion experiments, such as temperature and pressure [7]. Another benefit of the JSR is that it can be paired well with analytical techniques, including gas chromatography, mass spectrometry, and VUV spectroscopy, for the identification and quantification of species in the gas phase [7].

Figure 2: Jet-stirred reactor used in experimentation with four turbulent jets used for secondary mixing. Sonic probes sample from the reactor by translating from left to right in the image above.

Historical overview of combustion reactors and sonic probe sampling

Sampling the fuel post-combustion is essential to properly show the benefits of what implementing LTC can achieve. Gas sampling is a reliable method to evaluate combustion performance, such as combustion temperature and efficiency [8]. For this purpose, sonic probes are used to extract samples from these reacting environments. This is made possible by creating conditions inside of the probe to halt all reactions that were taking place because of the combustion. Creating such conditions is achieved by introducing an aerodynamic quench which is defined as a rapid reduction in temperature and pressure by accelerating the flow to supersonic speeds [9]. To accelerate the flow into the probe, the pressure inside the probe is made significantly lower than the pressure inside of the reacting environment; for instance, a pressure of 100,000 Pa (≈ 760 Torr ≈ 1 atm) would be the pressure in the combustion chamber while the pressure inside of the probe is 8,000 Pa (≈ 60 Torr ≈ 0.08 atm). A visual of this can be seen below in Figure 3.

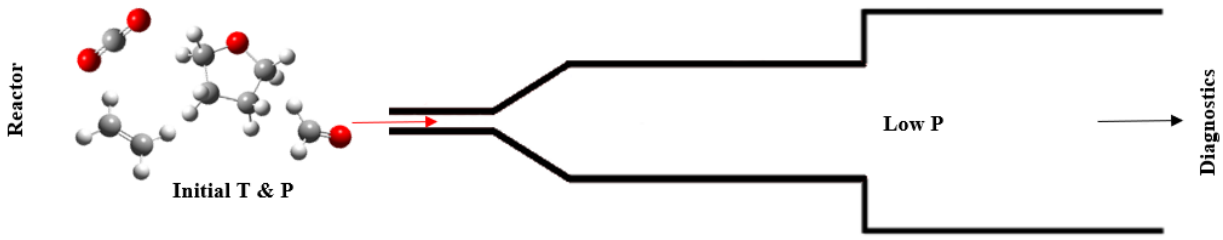

Figure 3: Diagram of combustion products moving through the inlet of a probe where the initial pressure would be significantly higher than the pressure inside of the probe. This allows for the aerodynamic quench to occur and the sample can then be analyzed by the diagnostics systems.

A aerodynamic quench is the most desirable method for quenching temperature and pressure-dependent chemical reactions due to the exceptionally high quenching rates [9]. This is important because it ensures that the sample that is being extracted from the reactor is being delivered to the diagnostics systems without changing composition.

Opportunity for research

While previous research on sonic probe sampling has provided ample evidence for sonic probes being capable of quenching gases in reactive flows [10], it has not yet been identified using CFD how long it takes for the aerodynamic quench to happen and where the changes are happening in the probe. To improve upon previous findings, the focus of this research was primarily on what happens inside of the probe as samples are extracted from the combustion chamber. The primary objective is to quantify how the temperature and pressure change over time. This would reveal the quenching rate, defined herein as the time required to reach 1% of equilibrium temperature, of a specific gas flow because I would see where the temperature and pressure stop changing. Next, I wanted to see where in the probe these changes were happening by showing how the temperature and pressure change along the length of the probe. Finally, I wanted to show whether or not the probe dimensions had an effect on that quenching rate or where the changes happened in the probe. Three different probes with varying geometry were

used to determine the effect of the probe geometry on quenching rates; probes 1-3 are shown in Figures 4-6.

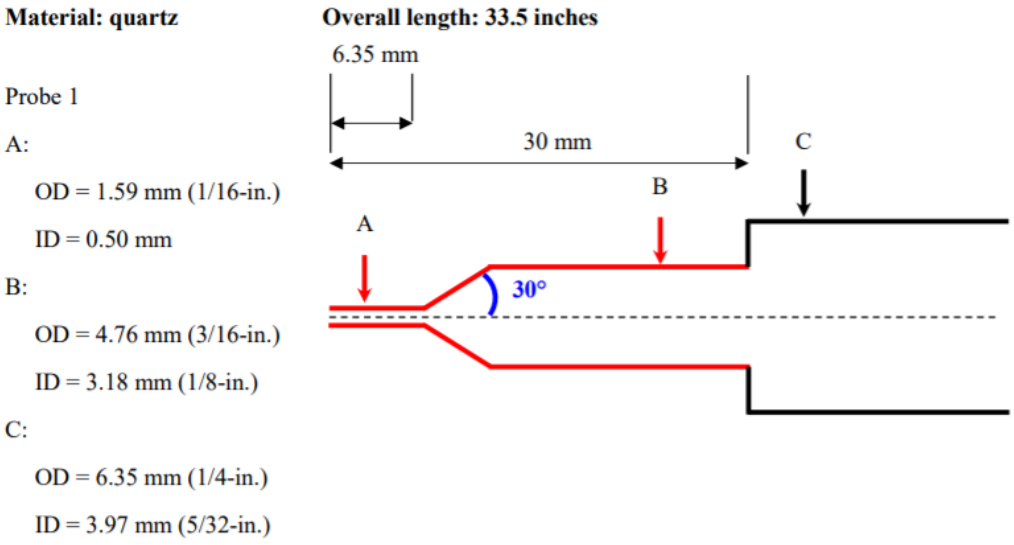

Figure 4: Geometry measurements for the design of probe 1 used in the research; not drawn to scale

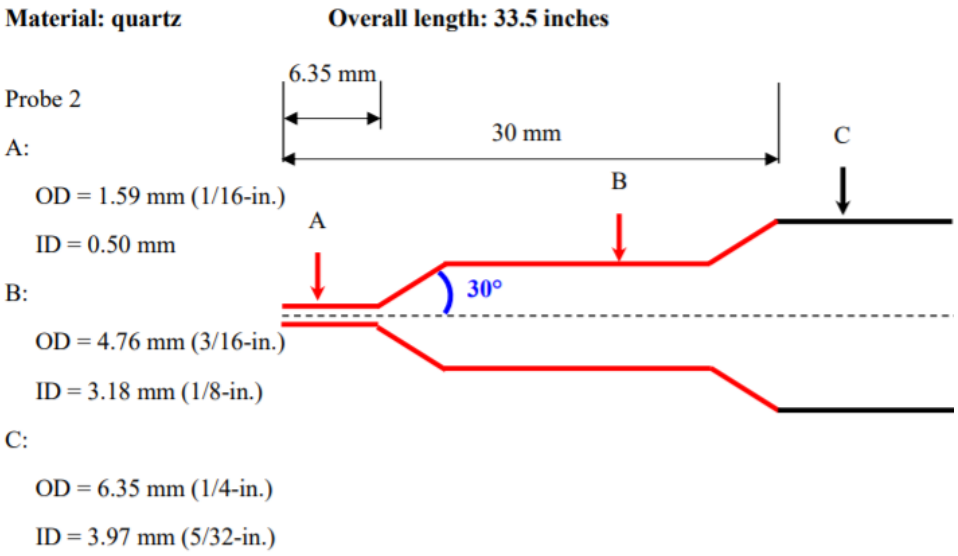

Figure 5: Geometry measurements for the design of probe 2 used in the research; not drawn to scale

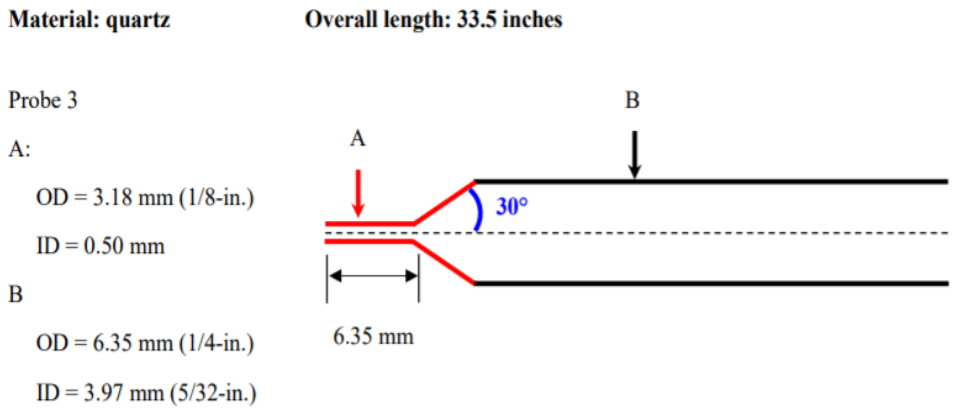

Figure 6: Geometry measurements for the design of probe 3 used in the research; not drawn to scale

Experimentally testing this would require taking an intrusive approach. This is because sensors would be needed to track how the temperature and pressure were changing and placed along multiple points in each of the probes. This presents challenges that would introduce significant errors in the data that is collected, and this would be due to the probes' small size. The sensors placed inside of the probe would create disturbances in the flow of the fluid and cause discrepancies in the data. A non-intrusive approach was decided upon to address this issue, involving the use of computational fluid dynamics (CFD) software.

CHAPTER 2

BACKGROUND OF CFD

CFD is a computational methodology used to study science that, with the help of digital computers, produces quantitative predictions of fluid-flow phenomena based on an equation of state and the conservation laws; The conservation of mass, momentum, and energy [11]. These predictions describe physical properties which can be used to find mass flow rates, heat transfer rates, pressure drops, etc. This allows for the performance of designs to be optimized with the data collected, which saves time and ultimately lowers the costs that come with testing designs experimentally. The most important benefit of using CFD is that real conditions can be simulated and then verified experimentally.

Methodologies of CFD modeling

CFD can describe the changes of all physical properties for both the fluid flow and heat transfer, such as velocity, pressure, temperature, density, and viscosity [12]. Below is the conservation of mass equation for steady-state flow:

$$\frac{\partial u}{\partial x} + \frac{\partial v}{\partial y} + \frac{\partial w}{\partial z} = 0 \qquad 1$$

This equation essentially accounts for the movement of a fluid in all directions within a control volume. Understanding how the fluid moves is a key component in making sure the other physical properties can be calculated correctly as well. Next, the conservation of momentum equation is listed below:

$$\rho \frac{Du}{Dt} = -\nabla p + \mu \nabla^2 u + \rho F \qquad 2$$

This equation is derived from Newton's second law, where force = mass * acceleration. On the left side, the mass term is directly related to the density term because fluids are the focus here; density = mass/volume. The acceleration term is where the velocity term is held with respect to time. On the right side of the equation, all the forces acting on the fluid are accounted for, including the pressure, viscosity, and external forces. Finally, the conservation of energy equation is listed below:

$$\frac{\partial}{\partial t}[\rho\,(e+\tfrac{1}{2}\upsilon^2)] + \nabla[\rho v\,(e+\tfrac{1}{2}\upsilon^2)] = -\nabla q + \nabla(\sigma v) + \rho v F \qquad 3$$

This equation accounts for the rate of increase of energy per unit volume, the convection of energy into a point by flow, the net heat flux, and the work of surface and body forces of a fluid in a given control volume. Finally, CFD software utilizes the Navier-Stokes equations, which are listed below:

$$\rho\left(\frac{\partial u}{\partial t} + u\frac{\partial u}{\partial x} + v\frac{\partial u}{\partial y} + w\frac{\partial u}{\partial z}\right) = \rho g_x - \frac{\partial P}{\partial x} + \mu\left(\frac{\partial^2 u}{\partial x^2} + \frac{\partial^2 u}{\partial y^2} + \frac{\partial^2 u}{\partial z^2}\right) \qquad 4$$

$$\rho\left(\frac{\partial v}{\partial t} + u\frac{\partial v}{\partial x} + v\frac{\partial v}{\partial y} + w\frac{\partial v}{\partial z}\right) = \rho g_y - \frac{\partial P}{\partial y} + \mu\left(\frac{\partial^2 v}{\partial x^2} + \frac{\partial^2 v}{\partial y^2} + \frac{\partial^2 v}{\partial z^2}\right) \qquad 5$$

$$\rho\left(\frac{\partial w}{\partial t} + u\frac{\partial w}{\partial x} + v\frac{\partial w}{\partial y} + w\frac{\partial w}{\partial z}\right) = \rho g_z - \frac{\partial P}{\partial z} + \mu\left(\frac{\partial^2 w}{\partial x^2} + \frac{\partial^2 w}{\partial y^2} + \frac{\partial^2 w}{\partial z^2}\right) \qquad 6$$

These equations are broken into three parts to describe the fluid in the x, y, and z directions. Fundamentally, these equations are the same and describe how the inertial forces are equal to the external forces acting on the fluid. On the left side of the equation, the fluid motion is accounted for, the density of the fluid, and the time as well. On the right side of the equation, the first term describes gravity, the second term describes the pressure, and the last term describes the viscosity or friction.

Some challenges with CFD stem from these equations because of how dependent the equations are on the input parameters. Certain assumptions are made within a problem to account for this, but the setup of initial parameters must be input correctly; to do this, boundary conditions have to be applied properly. First, these boundaries must be identified in order to specify the parameters at that boundary.

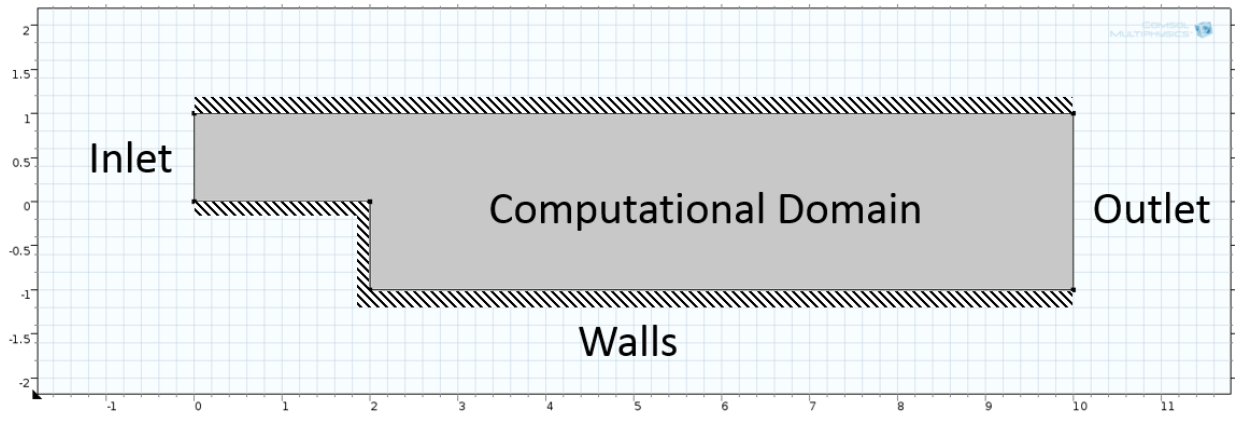

Figure 7: Diagram of boundaries in CFD software where the inlet, outlet, and walls are specified

With the boundaries identified, the CFD software can then establish a computational domain so that the problem can be solved. However, before the software can solve the equations for geometry, a mesh must be created on the geometry so that smaller control volumes are made within your geometry.

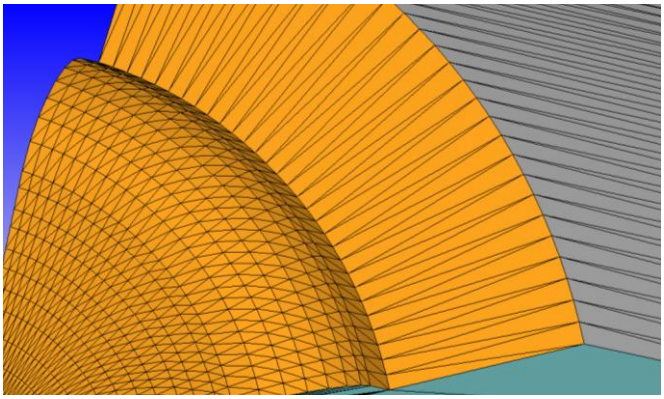

Figure 8: Example of meshing in a CFD software

Inside of these control volumes is where the equations are applied in your geometry. In Figure 8, there is an example of this meshing, and one thing that is shown is the differences in some control volumes. This meshing process affects the speed and accuracy of all simulations that are running. These control volumes will vary based on specifications and are normally smaller for more complex areas in a geometry. This can be a downside with CFD because in really complex geometries, smaller meshing will be needed, and this will dramatically increase the simulation run time in a problem. In some cases, simulations need to be run in parallel on multiple processors to get the best results.

With the boundaries identified and the mesh applied to the geometry, the next steps are to set the boundary conditions. The inlet and outlet boundary conditions will specify the inlet and outlet conditions, respectively, such as the pressure, temperature, and the species of the fluid. The walls can be modeled based on what material is being used and can be specified as moving or stationary. Next, the simulation parameters must be set where the simulation time and solver parameters are specified. In this section, the time steps, simulation run time, and how the software will solve the problem are specified. Once the setup of the problem is completed, the simulation can be executed, and the output data can be collected and interpreted.

Converge CFD software

In this research, Converge CFD software was used to run the CFD simulations for the probes. Converge is a commercially used software for some big companies such as Honeywell and Caterpillar. It is one of the leading CFD software for simulating three-dimensional flow. The reason it was chosen over other software, however, is because of the autonomous meshing feature. Since the meshing process is crucial, having the automatic meshing feature saves ample time because usually, a secondary software or script is needed to apply the mesh which is less convenient. The Converge software has an integrated chemistry feature where chemical models can be applied to simulations as well. With this feature, Converge has an option where thermodynamic data can be imported into the software so that chemical models match the models that are specific to certain research. The software is user-friendly and allows for automatic meshing on geometries created in the software as well as imported geometries that were previously made using CAD software.

Impact of simulations

Converge CFD software is 3D but, the focus of this research is 1D. With the results from Converge, the goal was to determine what the effect of inlet temperature and pressure in the reactor had on dT/dt, dP/dt, and dT/dx, respectively. This is important because it will show how the pressure and temperature change with respect to time and along the length of the probe. By knowing how the temperature and pressure are changing in the probe, the effectiveness of sonic probes under different conditions can be analyzed. Additionally, the most important part will be confirming that the chemicals extracted into the probe don't undergo further chemical reactions. By using different probes, the effectiveness of each probe design can be looked at individually, and this can potentially reveal what probe is better suited for specific conditions.

CHAPTER 3

SIMULATION APPROACH

The simulation software used to run the simulations was Converge CFD software. Firstly, the different probes were created in Converge using the specifications provided in Figures 4-6. Then, once the geometry was finished, the case setup began where boundaries and conditions were set.

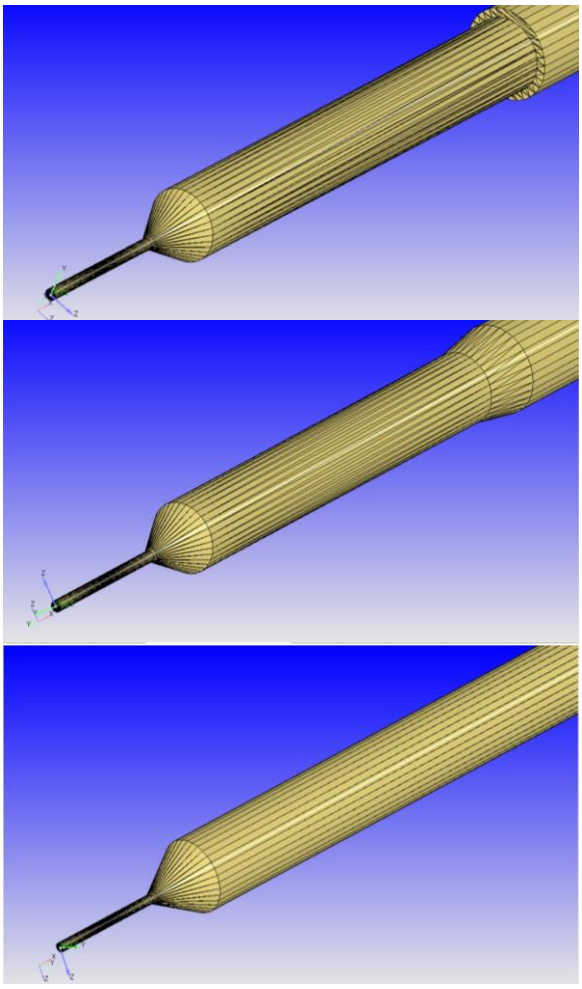

Figure 9: Meshed version of probes after being created in Converge CFD software. Top: Probe 1; Middle: Probe 2; Bottom: Probe 3

Setup of computational domain/model

The first step is to assign the boundaries, i.e., inlet, wall, and outlet. With the boundaries assigned to a section of the geometry, the initial boundary conditions were input along with the simulation time and solver parameters. Pure nitrogen was chosen for the gas composition at the inlet to represent a 'non-reacting flow.' The process is modeled as adiabatic (i.e., neglect wall heat transfer because of material (quartz) and short residence time) and will have fixed boundary conditions of (1) P_{inlet} = 1, 10, and 25 atm; (2) P_{outlet} = .08 atm; (3) T_{inlet} = 500, 750, 1000 K; (4) T_{outlet} = 300 K. The velocity at the inlet was 448 m/s which is equal to a volumetric flow rate of 5.2 L/min. The experiments are conducted using flow rates between 0.5 – 50 L/min; the 5.2 L/min value was chosen as a middle value. This parameter was constant in all the simulations because the inlet diameter was consistent in all probes. Diagrams of where the inlet, outlet, and wall boundary conditions were set in the Converge software are shown below in Figures 10-12.

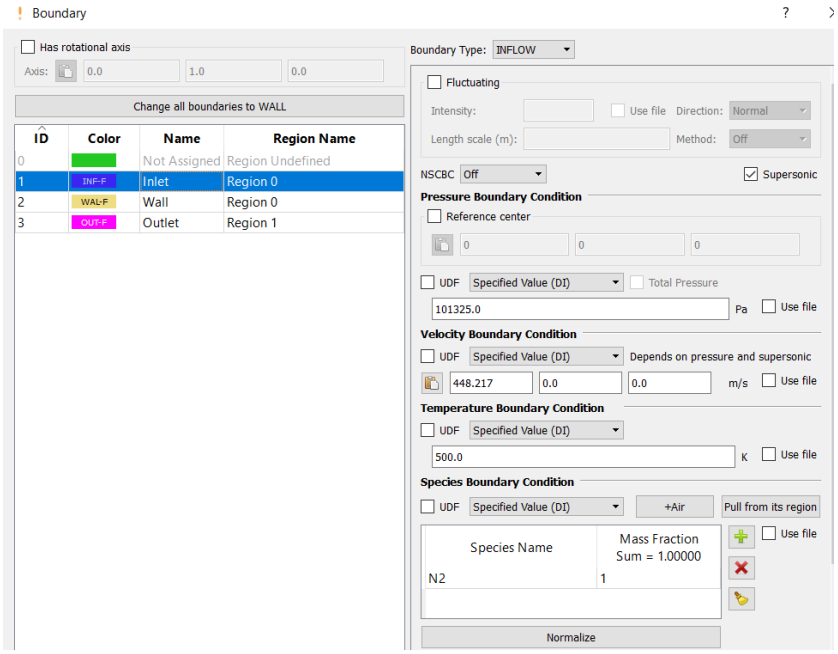

Figure 10: Inlet boundary conditions tab in Converge CFD software; inlet pressure/temperature conditions changed here for different cases: (1) P_{inlet} = 1, 10, and 25 atm; (2) T_{inlet} = 500, 750, 1000 K

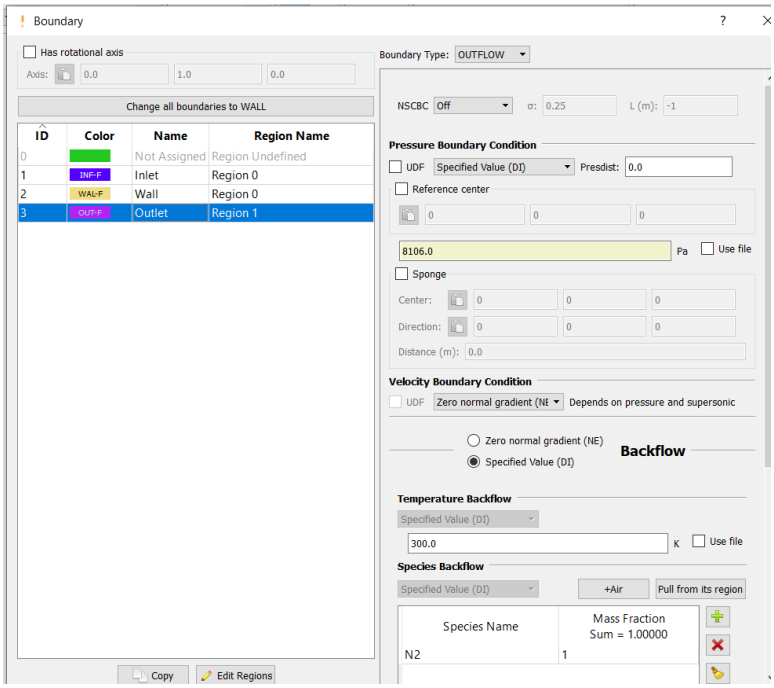

Figure 11: Outlet boundary conditions tab in Converge CFD software; outlet pressure/temperature stayed constant in simulations: (1) P_{outlet} = .08 atm; (2) T_{outlet} = 300 K

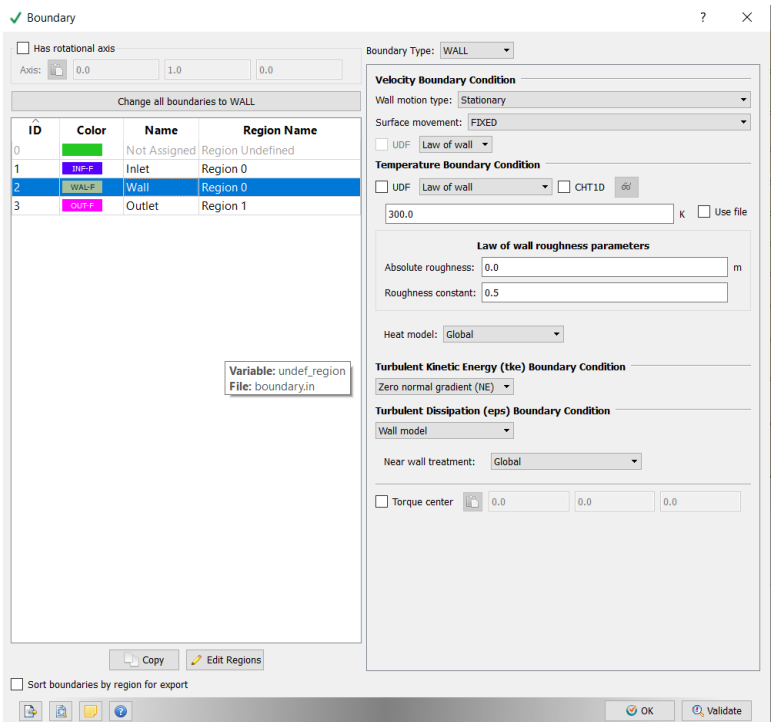

Figure 12: Boundary conditions of the wall for the simulations.

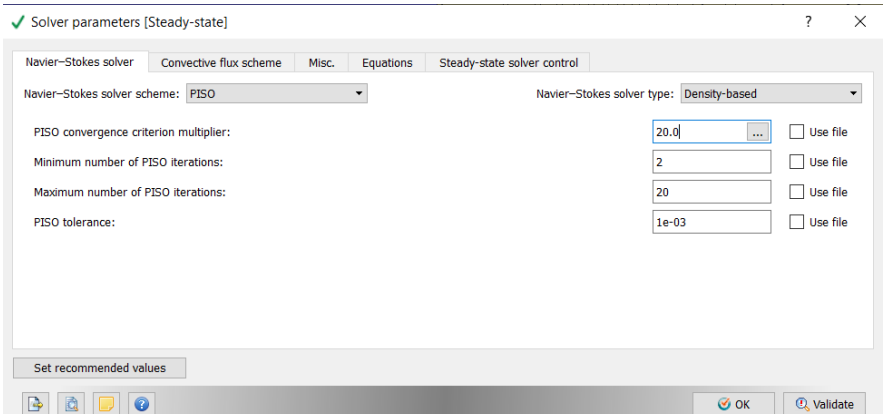

Figure 13: Solver parameters tab in Converge CFD software.

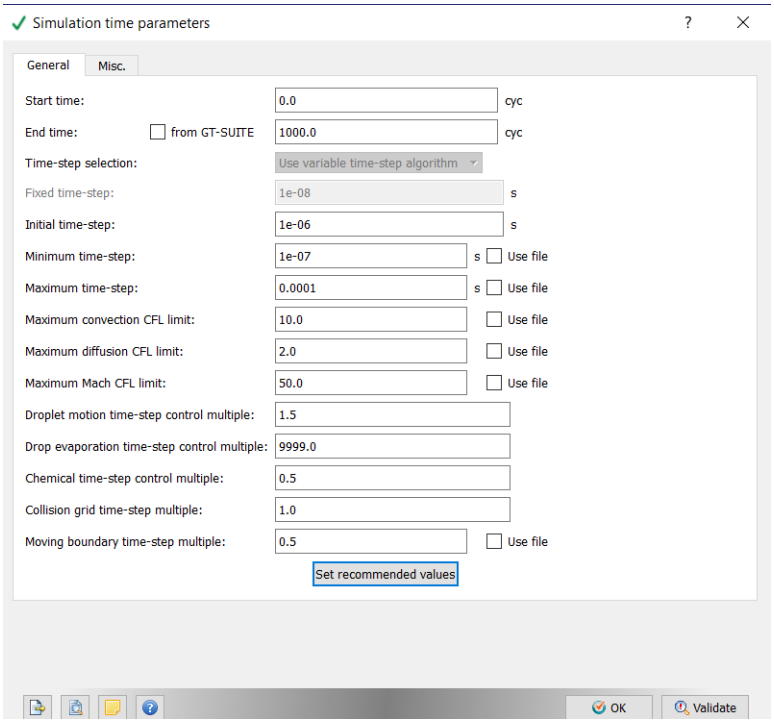

Figure 14: Simulation time parameters tab in Converge CFD software.

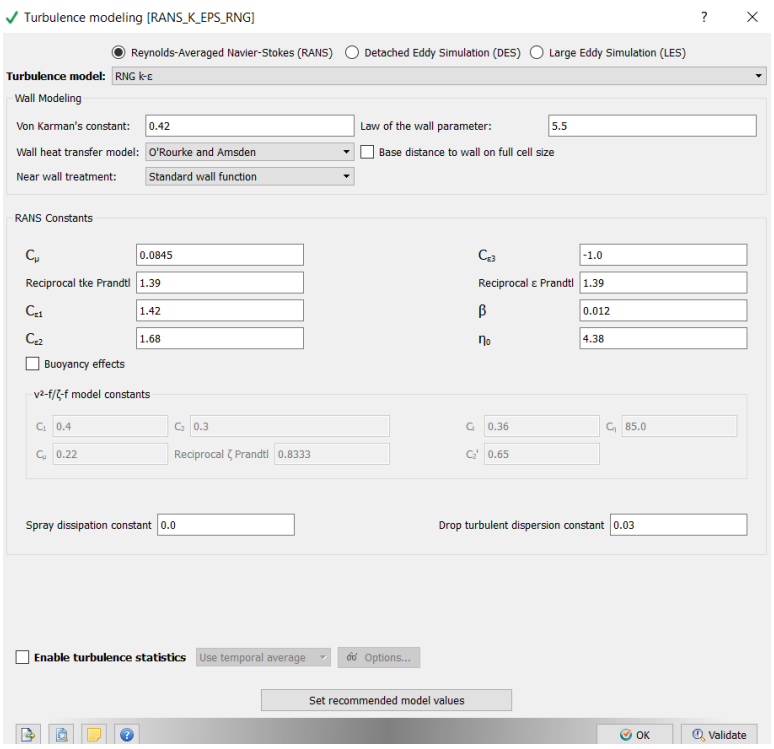

Figure 15: Physical model tab in Converge CFD software where a turbulence model was chosen.

After the boundary conditions were set, setting the simulation parameters was the next phase. The solver was specified to solve the problem using a density-based method, and the assumption was made that the flow would be at steady state. With the simulation time parameters, an initial guess was made to begin the simulations and was adjusted accordingly as the simulations progressed. The physical model of the flow was modeled as turbulent, so the solver used the Reynolds-averaged Navier-Stokes model. Finally, after the case setup was completed and the simulations were running properly, the post-processing was the next step.

CHAPTER 4

RESULTS OF CFD SIMULATIONS

In these results, ‘quenching’ is defined by the point at which the temperature stops changing and reaches ‘equilibrium.’ Because temperature and pressure have a direct correlation, the timeframe will be the same. So, the temperature was used to describe this quenching since the chemical reactions in the combustion chamber are temperature-dependent. Based on this equilibrium temperature, an equation was developed to identify when the temperature becomes sufficiently quenched; this equation is shown below:

$$.01 * T_{equlibrium} = x \quad (7)$$

$$.001 * T_{equlibrium} = y \quad (8)$$

In solving for x and y, x is the point where the temperature is changing within 1% of $T_{equlibrium}$, while y is the point where the temperature is changing within .01% of $T_{equlibrium}$. Consequently, the time it takes for the temperature to be quenched can be shown with these error margins.

The expectations with these results were to see the time it takes to quench the temperature take longer as the inlet temperature and pressure were increased. Another expectation was to see the final changes for the temperature and pressure happen after the geometry changes. This was important because if the aerodynamic quench happened before that, the different probe data wouldn’t show a change. The last expectation was that quenching would be fastest in probe 1 because of the sudden expansion region, which could help with the quenching speed. This assumption was made because the shockwaves inside the probe would help increase the flow of the fluid through the probe with the most abrupt geometry change.

Effect of gas temperature at probe inlet on quenching rates

In Figures 16-18, the temperature vs. time plots clearly show that the aerodynamic quench is being achieved by the sudden drop in temperature in a short amount of time (dT/dt). In these plots, $T_{equilibrium}$ gets higher as the inlet temperature is increased at the same inlet pressure. Also, as the inlet pressure is increased, the variance between the $T_{equilibrium}$ at the different inlet temperatures increases as well. This is shown better in data Table 1 because of how close the data is. Another trend that is easier to see with the data Table 1 is that as the inlet pressure and temperature increase, the quenching time gets faster. This is true for every case except for when the .01% tolerance is used for the 1 atm data where instead, the quenching time doesn't change. One thing that is interesting to see as well is that the quenching time took the longest in probe 1 with an inlet pressure of 10 atm when compared to the other inlet pressures. The same trends are shown, but the quenching time is slightly higher. Finally, the dT/dt vs. time graphs show that the quenching rate is extremely high in the first 10 μs. This also reveals that the quenching rate is higher as the inlet temperature increases, which explains why at higher inlet temperatures, the time it takes to reach $T_{equilibrium}$ is lower.

Table 1: Overview of time it takes for temperature to be quenched

P_{inlet} (atm)	**T_{inlet} (K)**	**Time (s)**	**1% of $T_{equilibrium}$ (K)**	**Time (s)**	**.01% of $T_{equilibrium}$ (K)**
1	500	.016	316	.021	319
	750	.014	333	.021	336
	1000	.01	333	.021	336
10	500	.018	336	.022	339
	750	.015	384	.018	387
	1000	.013	418	.016	422
25	500	.017	339	.02	342
	750	.014	397	.016	401
	1000	.012	444	.013	448

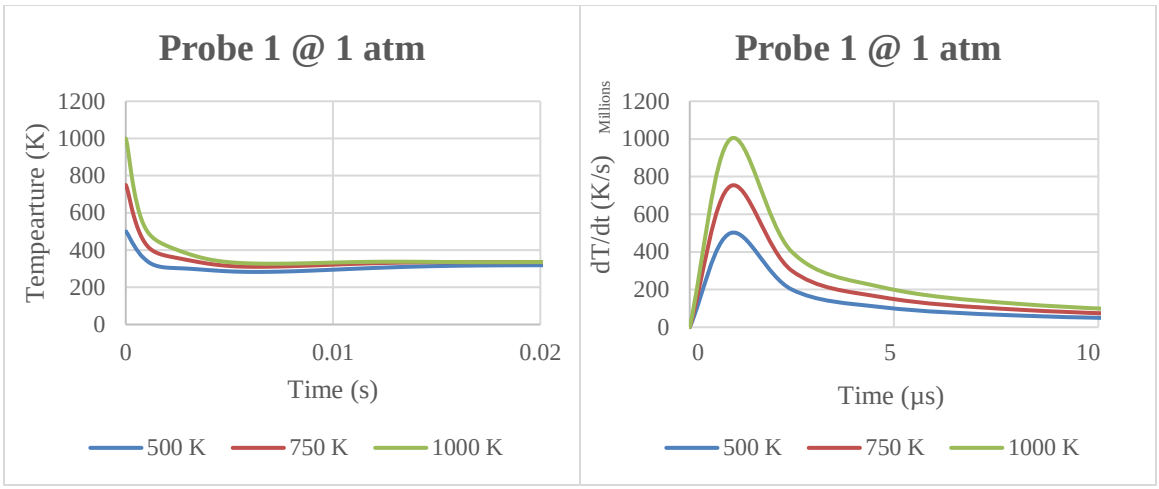

Figure 16: Temperature change in probe 1 at 1 atm with different inlet temperatures. Left: ΔT over time; Right: quenching rate over time

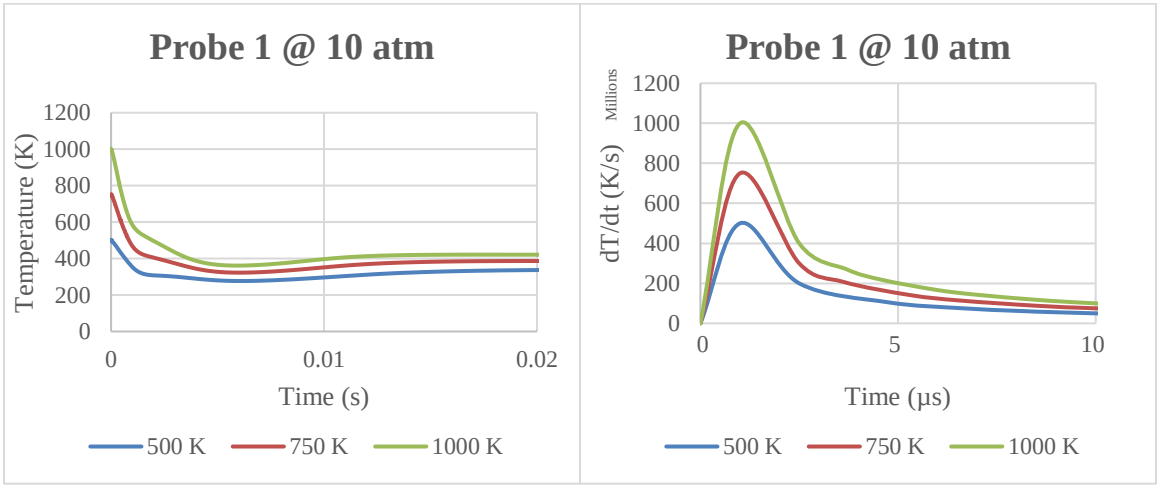

Figure 17: Temperature change in probe 1 at 10 atm with different inlet temperatures. Left: ΔT over time; Right: quenching rate over time

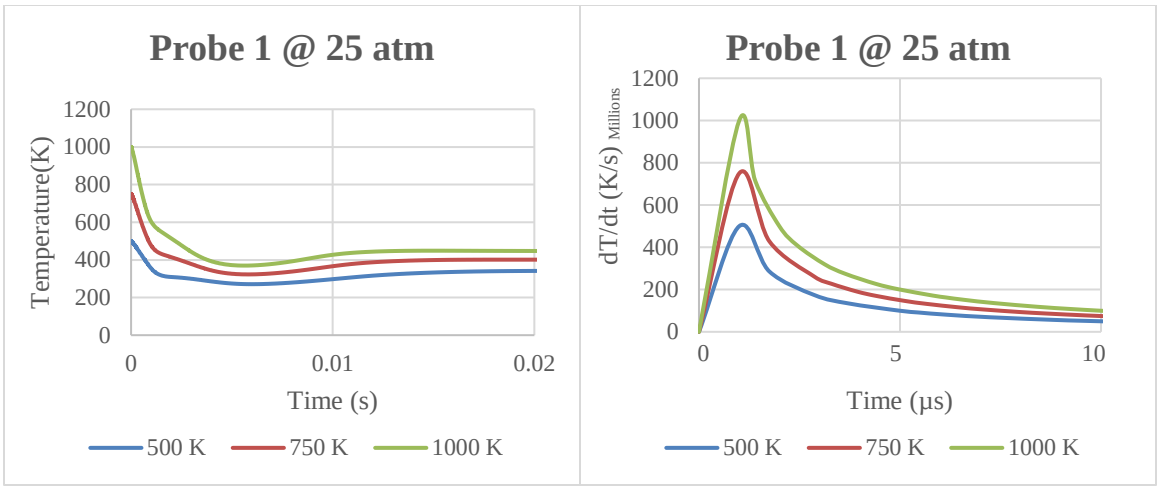

Figure 18: Temperature change in probe 1 at 25 atm with different inlet temperatures. Left: ΔT over time; Right: quenching rate over time

Effect of gas pressure at probe inlet on quenching rates

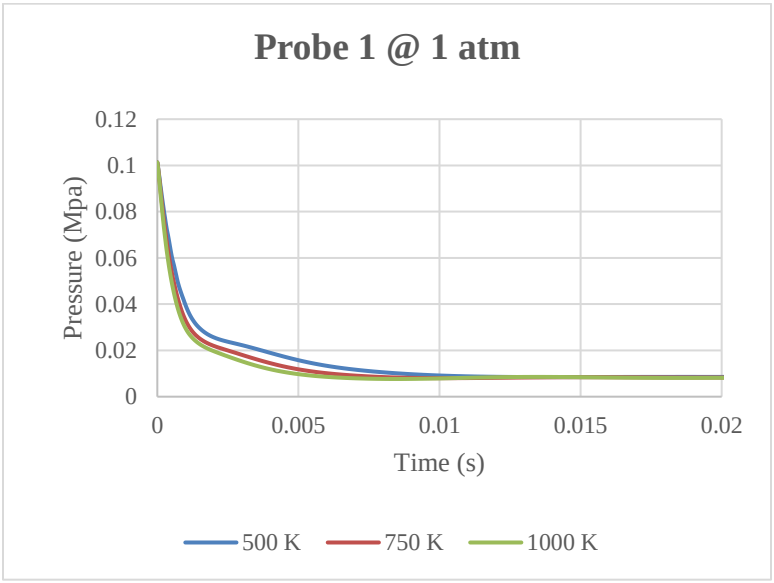

Figure 19: Pressure change over time in probe 1 at 1 atm with different inlet temperatures.

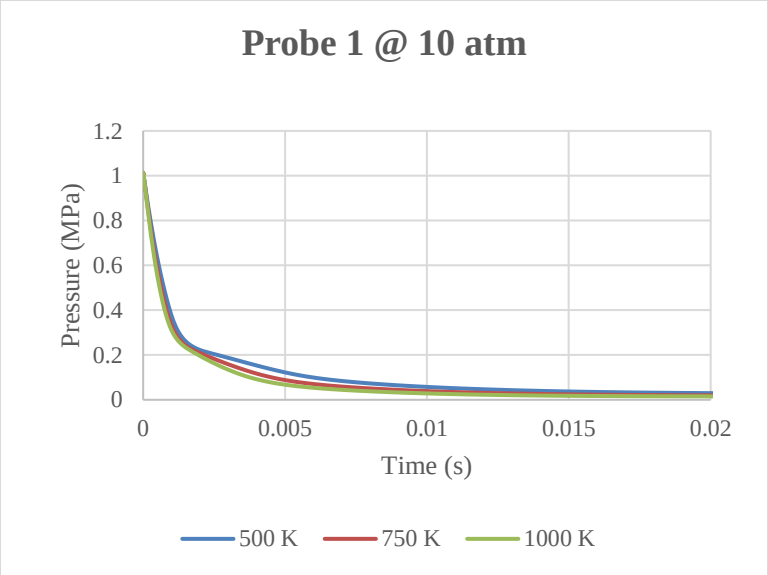

Figure 20: Pressure change over time in probe 1 at 10 atm with different inlet temperatures.

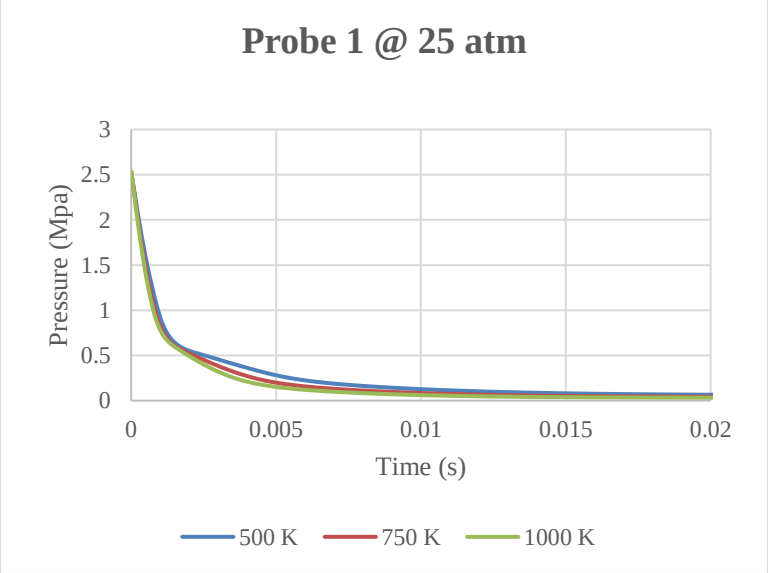

Figure 21: Pressure change over time in probe 1 at 25 atm with different inlet temperatures.

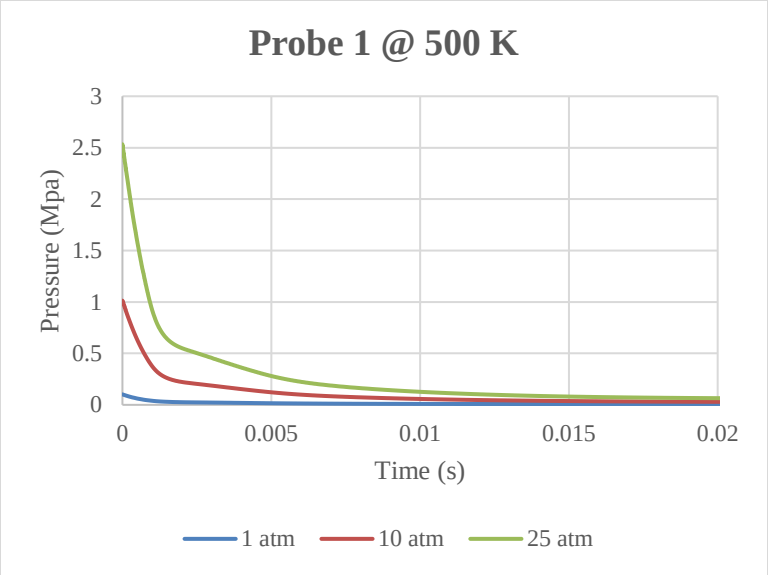

Figure 22: Pressure change over time in probe 1 at 500 K with different inlet pressures.

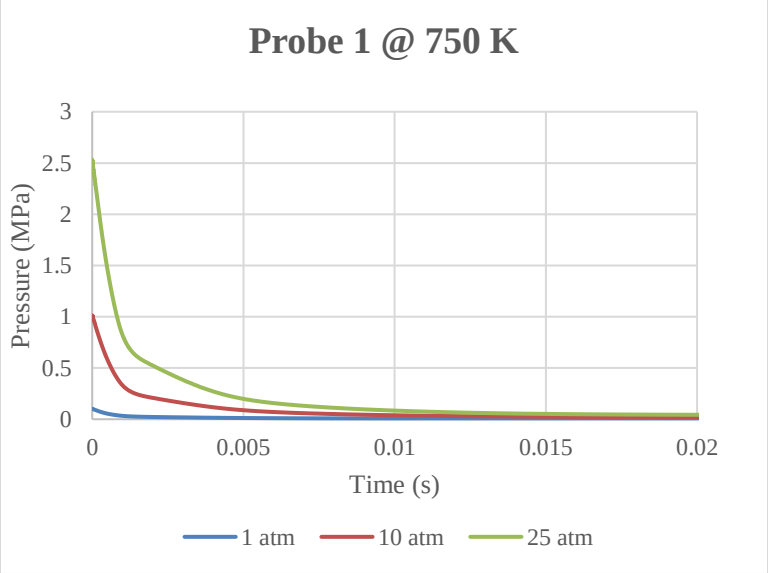

Figure 23: Pressure change over time in probe 1 at 750 K with different inlet pressures.

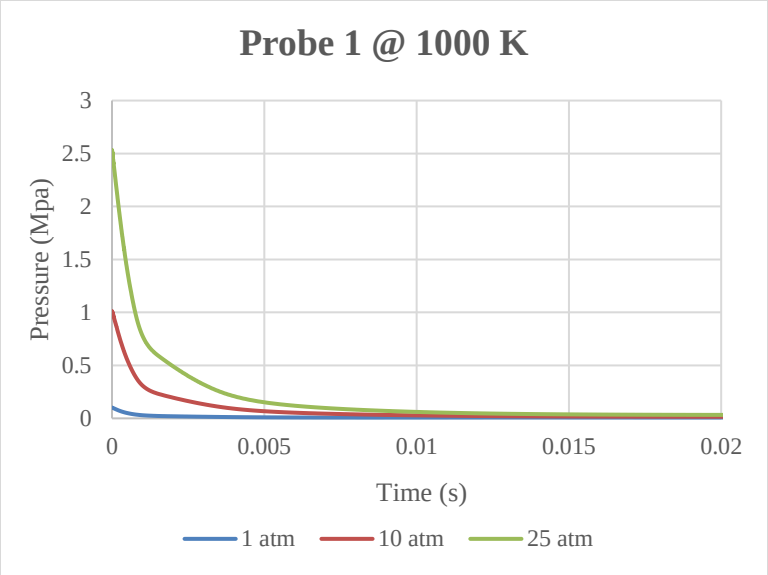

Figure 24: Pressure change over time in probe 1 at 1000 K with different inlet pressures.

The first thing to notice from Figures 19-21 is that the aerodynamic quench is able to be seen in the same timeframe as the dT/dt data because of the direct correlation of temperature and pressure so, this data confirms what was gathered by the effect of inlet temperature data on the quenching rate (dP/dt). In Figures 16-18, a trend that can be shown with the dT/dt vs. time plots is depicted in Figures 19-21 where, at higher temperatures with the same inlet pressure, the quenching rate is higher. Finally, by analyzing Figures 22-24, as pressure increases, the time needed for quenching increases as well. However, based on the data from Table 1, that is not the case; the data clearly shows that the 10 atm simulations had the longest quenching time, which is almost impossible to see graphically. The only trend that is shown in Figures 16-18 that isn't shown in Figures 19-21 is the dip in temperature before the simulations reach $T_{equilibrium}$. This may be due to the pressure acclimating to the equilibrium conditions more gradually than the temperature does in such a short time span.

Temperature/Pressure gradients along length of probe

Table 2: Overview of where quenching is completed in probe 1

P_{inlet} (atm)	**T_{inlet} (K)**	**Length (m)**	**1% of $T_{equilibrium}$ (K)**	**Length (m)**	**.01% of $T_{equilibrium}$ (K)**
1	500	.1	316	.13	319
	750	.09	333	.13	336
	1000	.07	333	.13	336
10	500	.22	336	.24	339
	750	.21	384	.23	387
	1000	.2	418	.21	422
25	500	.4	339	.42	342
	750	.34	397	.35	401
	1000	.34	444	.35	448

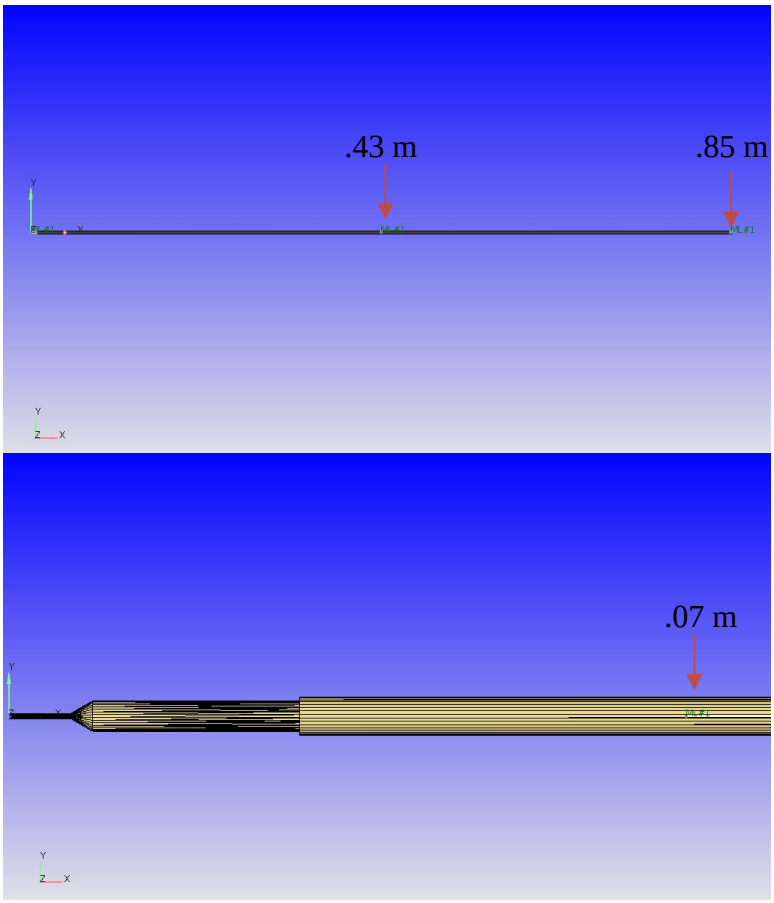

Figure 25: Diagram of specific points in probe 1. Top: Full length of probe; Bottom: Shortest length in probe 1 where $T_{equilibrium}$ is reached

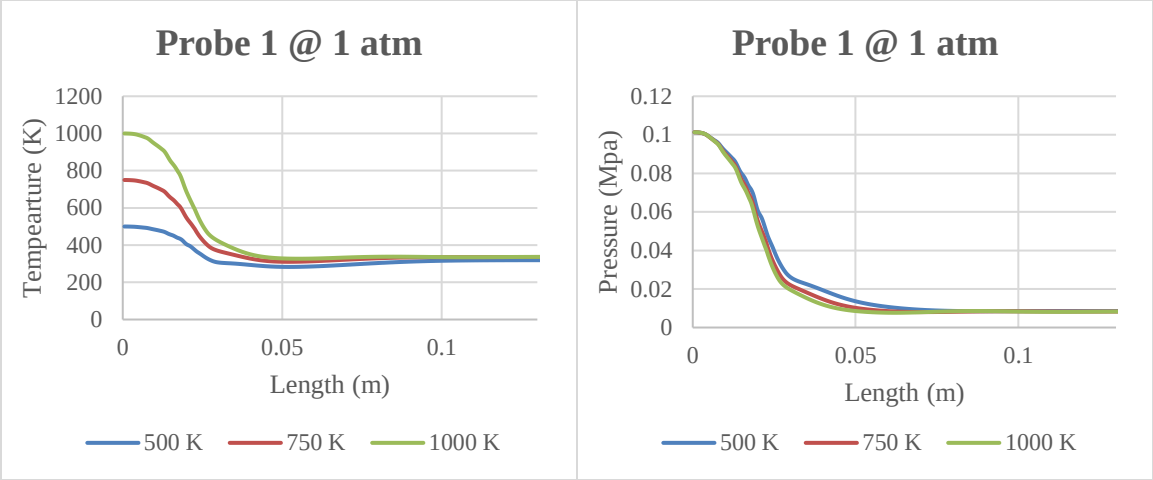

Figure 26: Temperature/pressure change in probe 1 at 1 atm with different inlet temperatures. Left: ΔT along length of probe 1; Right: ΔP along length of probe 1

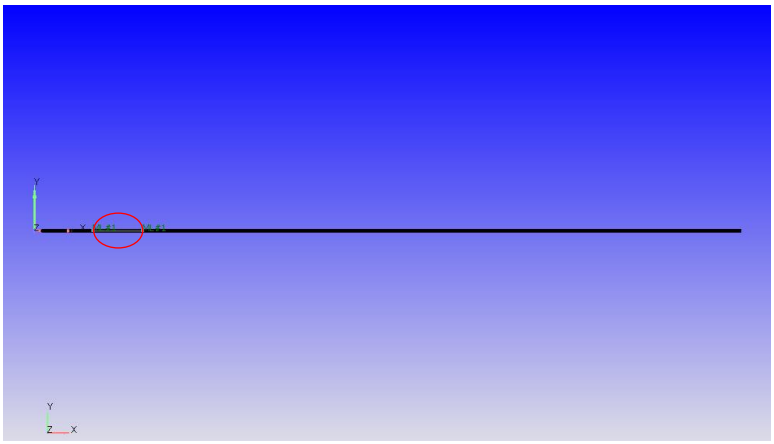

Figure 27: Region where temperature and pressure have been quenched in probe 1 at 1 atm; .07 m - .13 m /.85 m

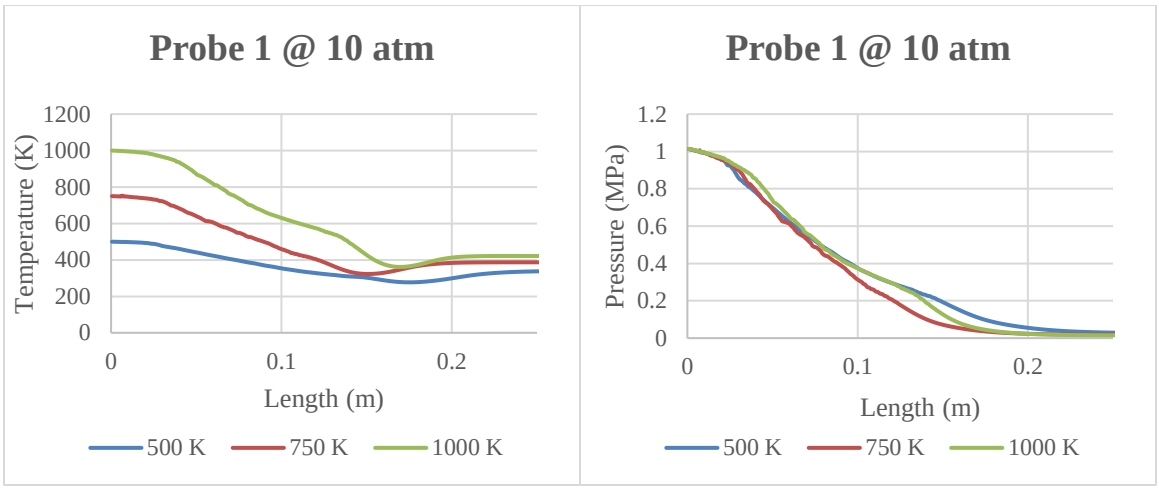

Figure 28: Temperature/pressure change in probe 1 at 10 atm with different inlet temperatures. Left: ΔT along length of probe 1; Right: ΔP along length of probe 1

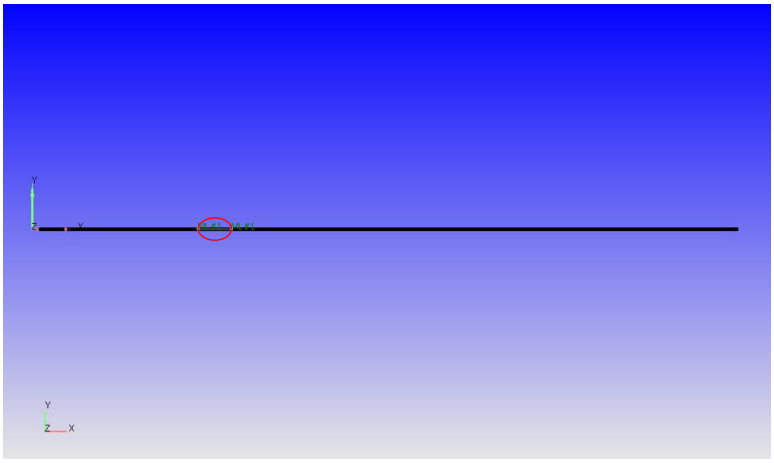

Figure 29: Region where temperature and pressure have been quenched in probe 1 at 10 atm; .2 m - .24 m / .85 m

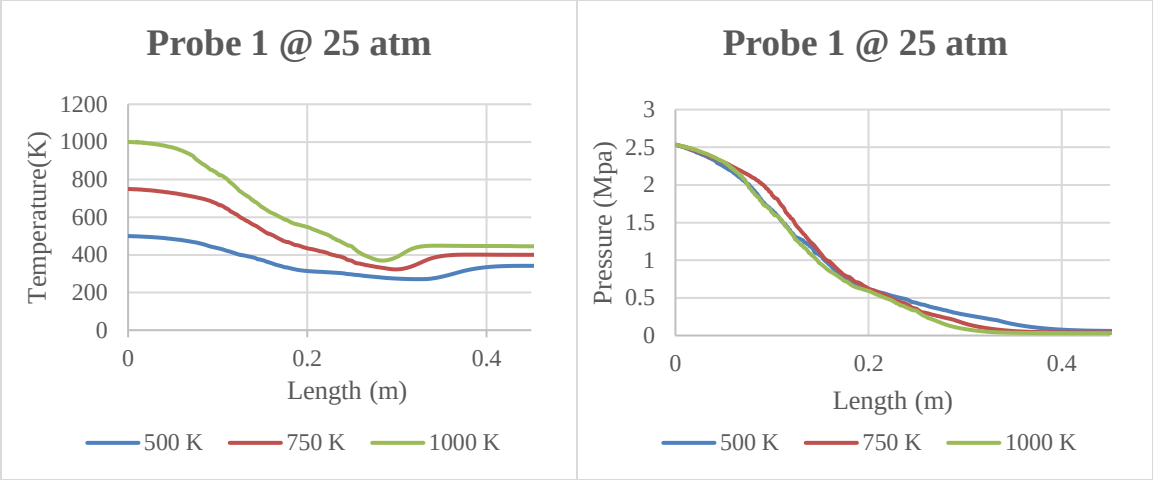

Figure 30: Temperature/pressure change in probe 1 at 25 atm with different inlet temperatures. Left: ΔT along length of probe 1; Right: ΔP along length of probe 1

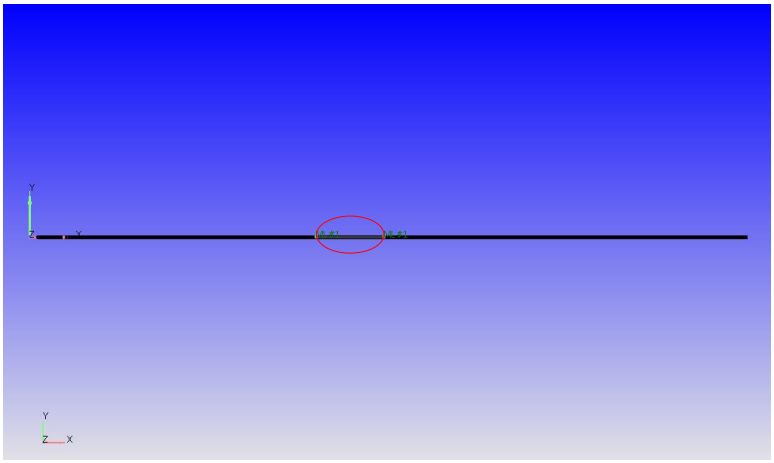

Figure 31: Region where temperature and pressure have been quenched in probe 1 at 25 atm; .34 m - .42 m / .85 m

In Figures 26-31, the change in temperature and pressure with respect to the length of the probe can clearly be shown (dT/dx, dP/dx). The diagrams in Figures 27, 29, and 31 help to give a visual of what is being described in Table 2. One trend that can be seen with the data in Table 2 is that as the temperature increases for a given inlet pressure, the quenching is happening at an earlier point in the probe. Conversely, as the pressure increases, the overall quenching range in

the probe increases as well. This means that as the pressure increases, dT/dx and dP/dx become smaller because the distance the fluid needs to travel before it reaches $T_{equilibrium}$ is increased.

Effect of probe geometry on quenching rates

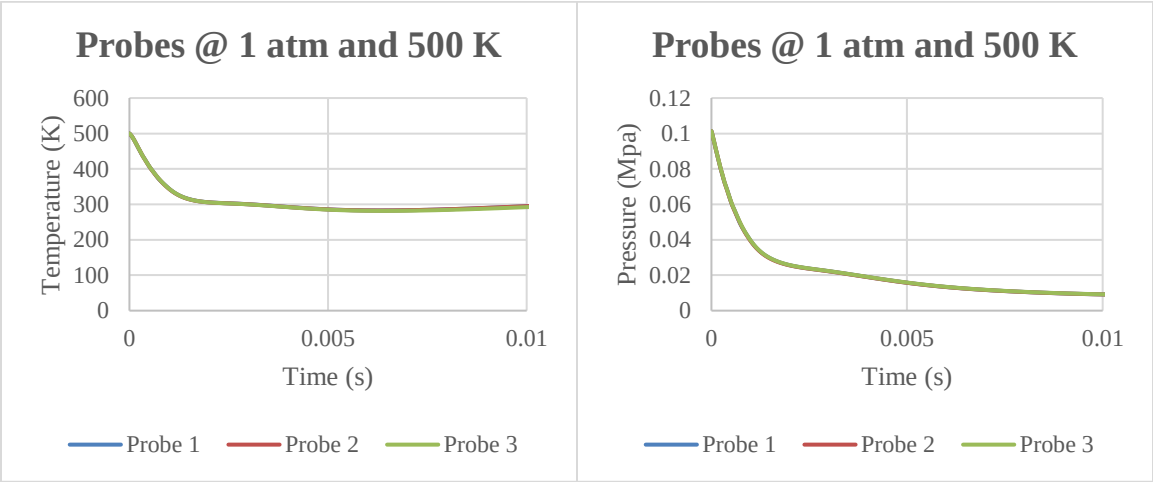

Figure 32: Quenching rate in each probe at 1 atm and 500 K. Left: ΔT over time; Right: ΔP over time

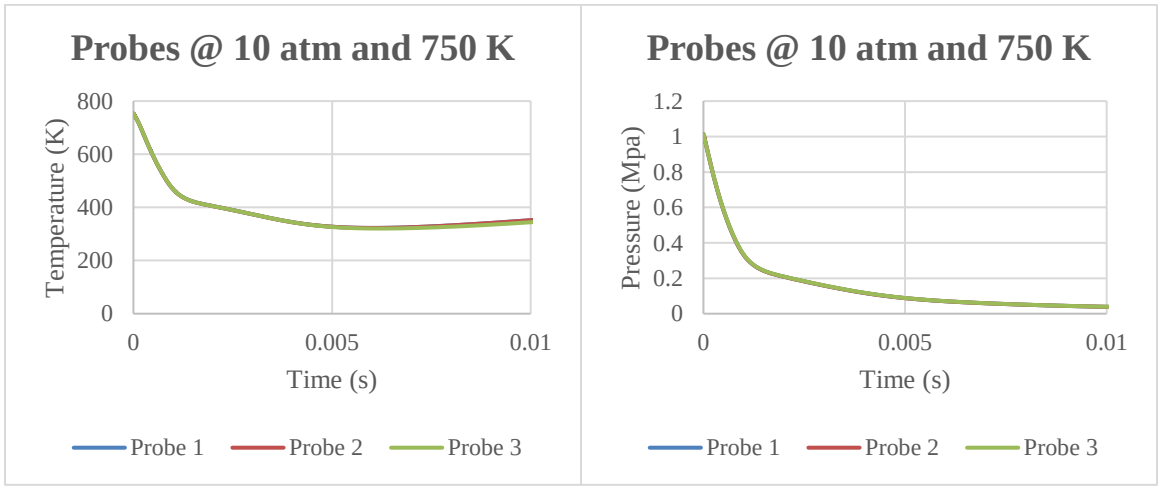

Figure 33: Quenching rate in each probe at 10 atm and 500 K. Left: ΔT over time; Right: ΔP over time

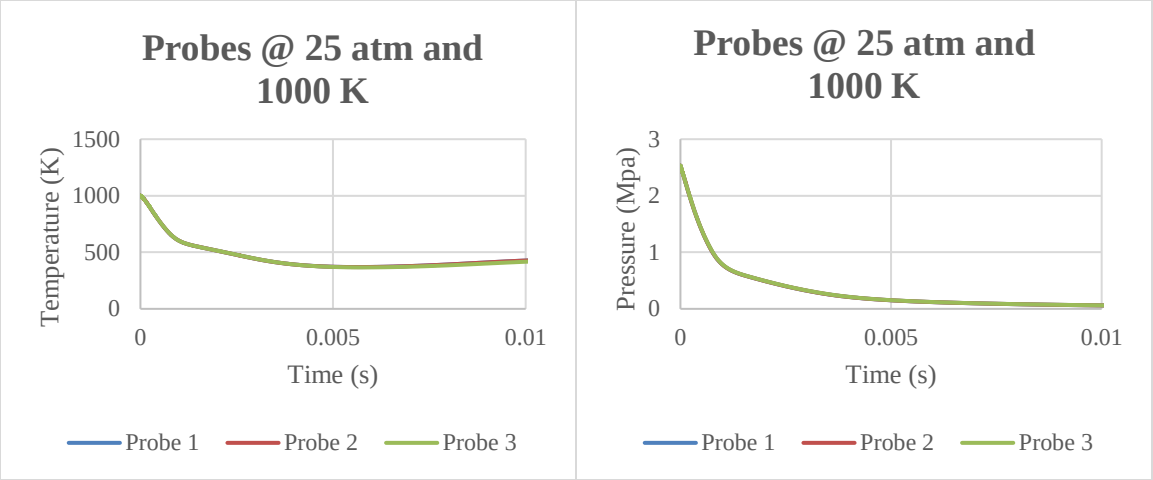

Figure 34: Quenching rate in each probe at 25 atm and 500 K. Left: ΔT over time; Right: ΔP over time

The results from Figures 32-34 were fairly straightforward and showed that the data for each of the probes aligned seamlessly. Although it has been shown that the quenching process is happening after the geometry changes, the different probe geometries had no effect on the quenching rate inside the probes. This means that changes made downstream of the inlet can be neglected.

Summary and discussion

In summary, computed temperature and pressure gradients in space-time (e.g., dT/dx and dP/dx) as a function of the conditions over the length of the sonic probe (.085 m) are provided, which give a comprehensive understanding of sonic probe flow using CFD modeling. Probe data modeled under the specified conditions (i.e. (1) P_{inlet} = 1, 10, and 25 atm; (2) P_{outlet} = .08 atm; (3) T_{inlet} = 500, 750, 1000 K; (4) T_{outlet} = 300 K) was able to reveal trends among the different sets of data at a given inlet temperature/pressure.

CHAPTER 5

FUTURE WORK AND CONCLUSIONS

With this work, a comprehensive understanding of the effect of quenching rates for temperature and pressure inside of the probes was able to be determined. I was successfully able to find how the temperature and pressure change with time and along the length of the probe (dT/dt, dP/dt, dT/dx, dP/dx). Additionally, I was able to identify key trends with each set of data that was confirmed by subtle differences that could be shown with the graphical and quantitative data. Finally, I was also able to conclude that the probe geometry downstream of the inlet can be neglected. The major takeaways from this research were:

- Increasing the inlet pressure will cause dT/dx and dP/dx to be smaller
- Increasing the inlet temperature will cause the $T_{equilibrium}$ to be slightly higher
- Probe geometry can be neglected downstream of the inlet
- The quenching rate is higher as inlet temperature is increased at a set inlet pressure
- Overall, quench is achieved in less than .021 s and in .42 m

In the future, simulations can be run for similar probe designs that have different orifice diameters at the inlet of the probes to see if this will have an effect on the quenching rates that were shown. Geometry changes were only made downstream of the inlet, but consistent diameters were used. Changing some of these parameters may increase or decrease the speed of the flow, which can have some effect on the quenching rates. Additionally, this can also be achieved by taking a closer look at the effect of volumetric flow rate at the inlet on quenching

rates. With the experiments being run between 0.5 – 50 L/min, this allows for a wide testing range for simulations.

Another study that can be done in the future requires the use of the chemistry feature in Converge CFD software. We want to see the effect of gas composition on dT/dx by analyzing if there is any effect on the predicted dT/dx if we used pure nitrogen in the simulations as compared to a more reactive mixture. This is a way we can compare these simulation results to experimental results. In Figure 35 below, we want to make sure that the chemical composition of our combustion products doesn't change as it travels through the probe. This will be done using these simulation models and adding on chemical models of fuels that have been produced in the lab.

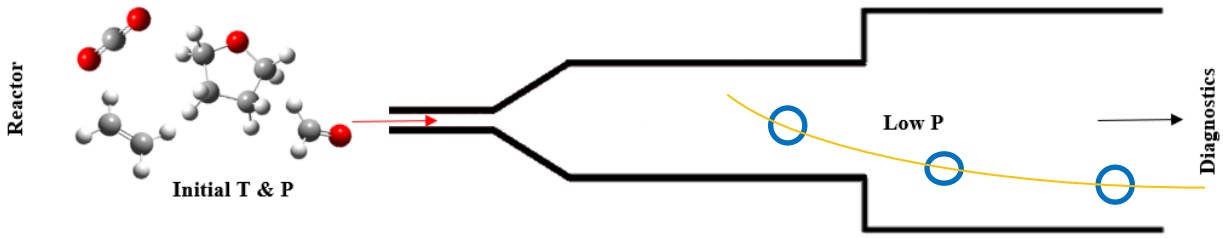

Figure 35: Diagram of gas sampled from a combustion experiment moving through a sonic sampling probe. The orange line depicts the temperature decrease in space and time through the probe. Future work will examine the potential for changing chemical composition inside of the probe along the thermal and pressure gradients computed herein.

REFERENCES

1) Kalghatgi, Gautam. “Is It Really the End of Internal Combustion Engines and Petroleum in Transport?” *Applied Energy*, vol. 225, 2018, pp. 965–974., doi:10.1016/j.apenergy.2018.05.076.
2) Reitz, Rolf D. “Directions in Internal Combustion Engine Research.” *Combustion and Flame*, vol. 160, no. 1, 2013, pp. 1–8., doi:10.1016/j.combustflame.2012.11.002.
3) Senecal, Kelly, and Felix Leach. *Racing Toward Zero: The Untold Story of Driving Green*. SAE International, 2021.
4) Kohse-Höinghaus, Katharina. “Clean Combustion: Chemistry and Diagnostics for a Systems Approach in Transportation and Energy Conversion.” *Progress in Energy and Combustion Science*, vol. 65, 2018, pp. 1–5., doi:10.1016/j.pecs.2017.10.001.
5) Dec, John E. “Advanced Compression-Ignition Engines—Understanding the in-Cylinder Processes.” *Proceedings of the Combustion Institute*, vol. 32, no. 2, 2009, pp. 2727–2742., doi:10.1016/j.proci.2008.08.008.
6) Rotavera, Brandon, and Craig A. Taatjes. “Influence of Functional Groups on Low-Temperature Combustion Chemistry of Biofuels.” *Progress in Energy and Combustion Science*, 2021, p. 100925., doi:10.1016/j.pecs.2021.100925.
7) Davis, Jacob C. (2019) *“*Design of a High-Pressure Jet-Stirred Reactor Facility for gas-phase chemical kinetics.*” University of Georgia*

8) Mitani, Tohru. “Quenching of Reaction in Gas-Sampling Probes to Measure Scramjet Engine Performance.” *Symposium (International) on Combustion*, vol. 26, no. 2, 1996, pp. 2917–2924., doi:10.1016/s0082-0784(96)80133-0.
9) Chiappetta, L., and M. B. Colket. “Design Considerations for Aerodynamically Quenching Gas Sampling Probes.” *Journal of Heat Transfer*, vol. 106, no. 2, Jan. 1984, pp. 460–466., doi:10.1115/1.3246694.
10) Davani, Abbasali, et al. “CFD Deign of Jet-Stirred Reactors.” *AIAA Scitech 2019 Forum*, June 2019, doi:10.2514/6.2019-2146.
11) “Computational Fluid Dynamics.” *Computational Fluid Dynamics - an Overview | ScienceDirect Topics*, www.sciencedirect.com/topics/materials-science/computational-fluid-dynamics.
12) “What Is Computational Fluid Dynamics (CFD)?: SimScale.” *SimScale*, 28 May 2021, www.simscale.com/docs/simwiki/cfd-computational-fluid-dynamics/what-is-cfd-computational-fluid-dynamics/.
13) Biswas, Gautam, and Somenath Mukherjee. *Computational Fluid Dynamics*. Alpha Science International Ltd., 2014. Biswas, Gautam, and Somenath Mukherjee. *Computational Fluid Dynamics*. Alpha Science International Ltd., 2014.
14) Colket, M.b., et al. “Internal Aerodynamics of Gas Sampling Probes.” *Combustion and Flame*, vol. 44, no. 1-3, 1982, pp. 3–14., doi:10.1016/0010-2180(82)90058-x.
15) Davani, Abbasali A., and Paul D. Ronney. “A Jet-Stirred Chamber for Turbulent Combustion Experiments.” *Combustion and Flame*, vol. 185, 2017, pp. 117–128., doi:10.1016/j.combustflame.2017.07.009.

16) The Editors of Encyclopaedia Britannica. “Chain Reaction.” *Encyclopædia Britannica*, Encyclopædia Britannica, Inc., 2 May 2017, www.britannica.com/science/chain-reaction#ref173571..1016/j.jqsrt.2019.106603.

17) Gross, Jurgen H. *Mass Spectrometry: a Textbook*. Springer International PU, 2018.

18) R D Reitz, H Ogawa. “IJER Editorial: The Future of the Internal Combustion Engine - R D Reitz, H Ogawa, R Payri, T Fansler, S Kokjohn, Y Moriyoshi, AK Agarwal, D Arcoumanis, D Assanis, C Bae, K Boulouchos, M Canakci, S Curran, I Denbratt, M Gavaises, M Guenthner, C Hasse, Z Huang, T Ishiyama, B Johansson, TV Johnson, G Kalghatgi, M Koike, SC Kong, A Leipertz, P Miles, R Novella, A Onorati, M Richter, S Shuai, D Siebers, W Su, M Trujillo, N Uchida, B M Vaglieco, RM Wagner, H Zhao, 2020.” *SAGE Journals*, journals.sagepub.com/doi/full/10.1177/1468087419877990.

19) Jianchen, Wang, and Lin Yuzhen. “Design Analysis of the Sampling Probe for Supersonic Combustion.” *50th AIAA/ASME/SAE/ASEE Joint Propulsion Conference*, 2014, doi:10.2514/6.2014-3948.

20) Kajishima, Takeo, and Kunihiko Taira. *Computational Fluid Dynamics Incompressible Turbulent Flows*. Springer International Publishing, 2018.

21) Kohse-Höinghaus, Katharina. “Combustion Chemistry Diagnostics for Cleaner Processes.” *Chemistry - A European Journal*, vol. 22, no. 38, 2016, pp. 13390–13401., doi:10.1002/chem.201602676.

22) Koritzke, Alanna L., et al. “QOOH-Mediated Reactions in Cyclohexene Oxidation.” *Proceedings of the Combustion Institute*, vol. 37, no. 1, 2019, pp. 323–335., doi:10.1016/j.proci.2018.05.029.

23) Lelevic, Aleksandra, et al. “Gas Chromatography Vacuum Ultraviolet Spectroscopy: A Review.” *Journal of Separation Science*, vol. 43, no. 1, Oct. 2019, pp. 150–173., doi:10.1002/jssc.201900770.

24) Manley, Dawn K., et al. “Research Needs for Future Internal Combustion Engines.” *Physics Today*, vol. 61, no. 11, 2008, pp. 47–52., doi:10.1063/1.3027991.

25) Mass Spectrometry :: Introduction, Principle of Mass Spectrometry, Components of Mass Spectrometer, Applications, http://premierbiosoft.com/tech_notes/mass-spectrometry.html

26) “Multiphysics Cyclopedia.” *COMSOL*, www.comsol.com/multiphysics/heat-transfer-conservation-of-energy?parent=fluid-flow-heat-transfer-and-mass-transport-0402-442.

27) Munson, Bruce R., et al. *Fundamentals of Fluid Mechanics*. Wiley, 1998.

28) Poole, Colin F. “Packed Columns for Gas–Liquid and Gas–Solid Chromatography.” *Gas Chromatography*, 2012, pp. 97–121., doi:10.1016/b978-0-12-385540-4.00004-3.

29) Radionica - Chem.bg.ac.rs. https://www.chem.bg.ac.rs/zf/lect/ZF2018_Ljesevic_GCxGC_Theory.pdf.

30) Wang, Zhi, et al. “Knocking Combustion in Spark-Ignition Engines.” *Progress in Energy and Combustion Science*, vol. 61, 2017, pp. 78–112., doi:10.1016/j.pecs.2017.03.004.

31) Wendt, John F., and John D. Anderson. *Computational Fluid Dynamics: an Introduction*. Springer, 2010.

32) Westbrook, Charles K, and W.j. Pitz. “Computer Modeling of Engine Knock Chemistry.” *Proceedings Supercomputing Vol.II: Science and Applications*, doi:10.1109/superc.1988.74137.

APPENDICES

Additional probe data

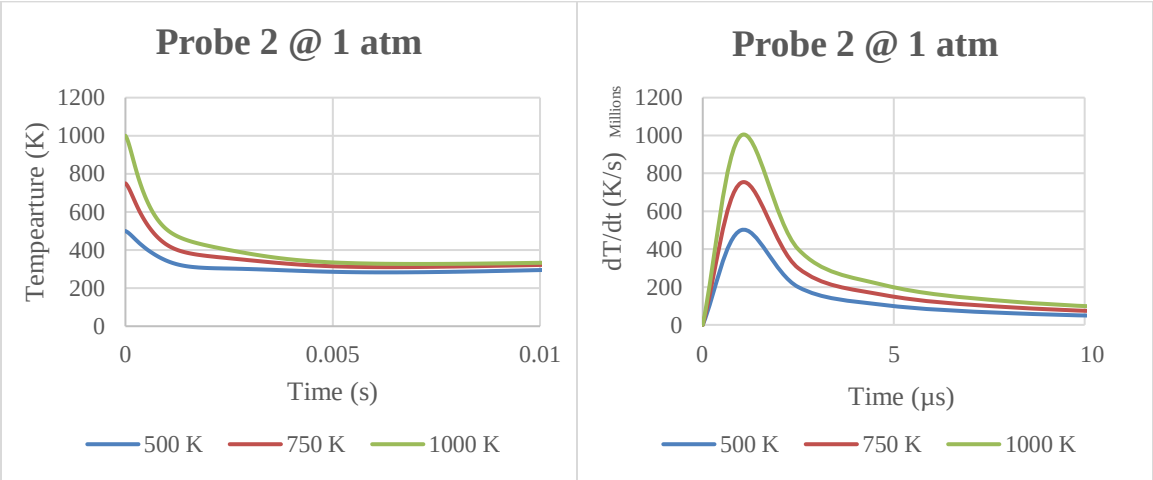

Figure 36: Temperature change in probe 2 at 1 atm with different inlet temperatures. Left: ΔT over time; Right: quenching rate over time

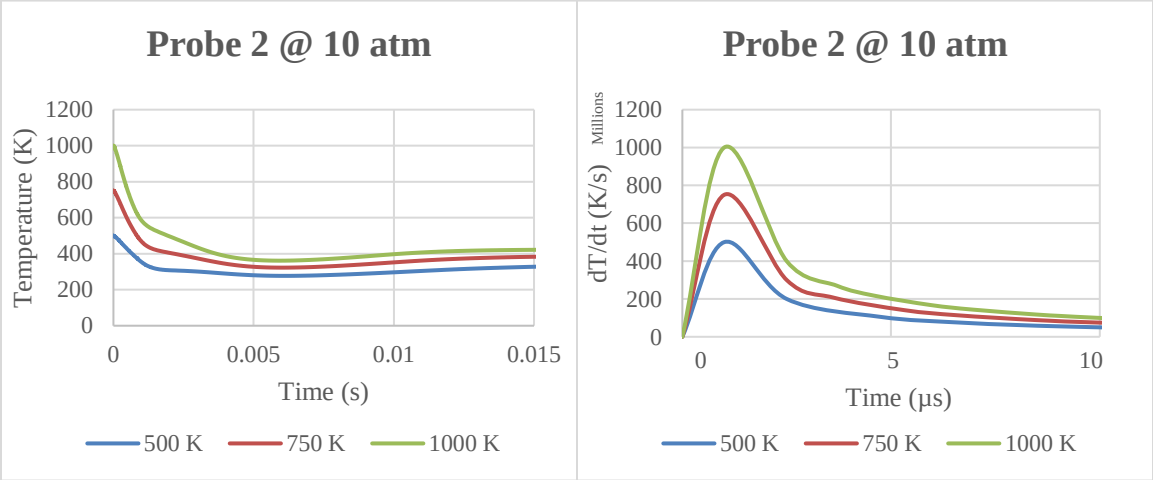

Figure 37: Temperature change in probe 2 at 10 atm with different inlet temperatures. Left: ΔT over time; Right: quenching rate over time

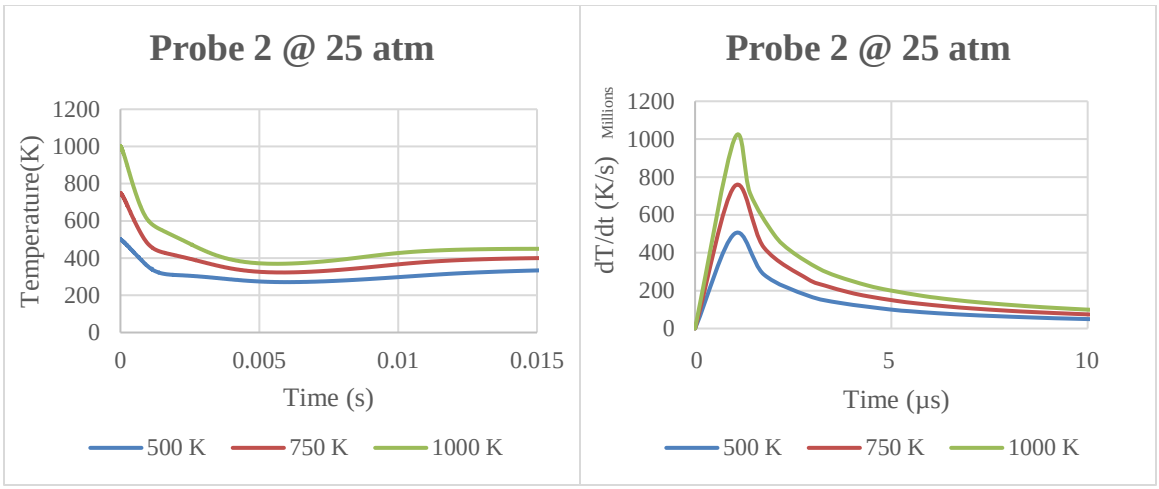

Figure 38: Temperature change in probe 2 at 25 atm with different inlet temperatures. Left: ΔT over time; Right: quenching rate over time

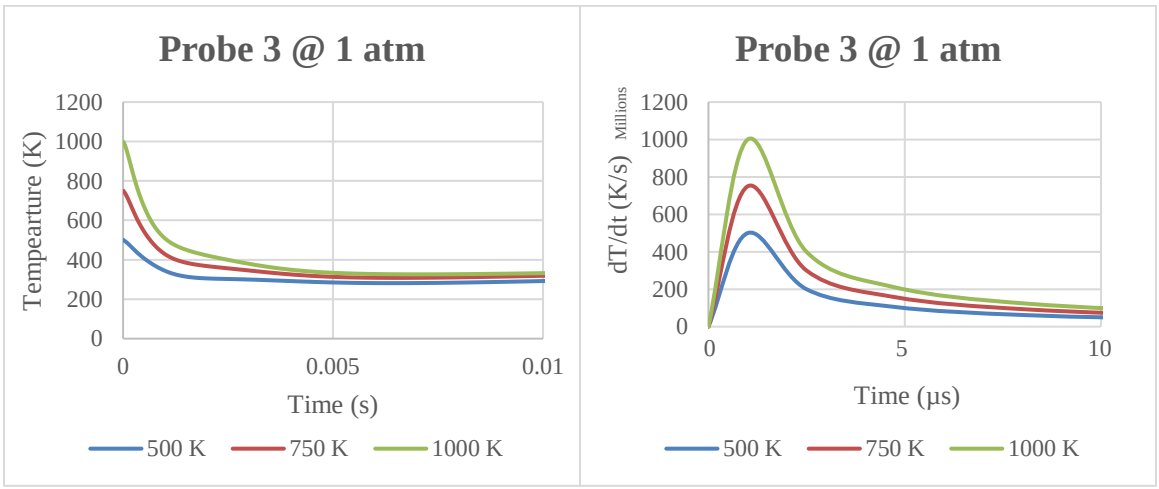

Figure 39: Temperature change in probe 3 at 1 atm with different inlet temperatures. Left: ΔT over time; Right: quenching rate over time

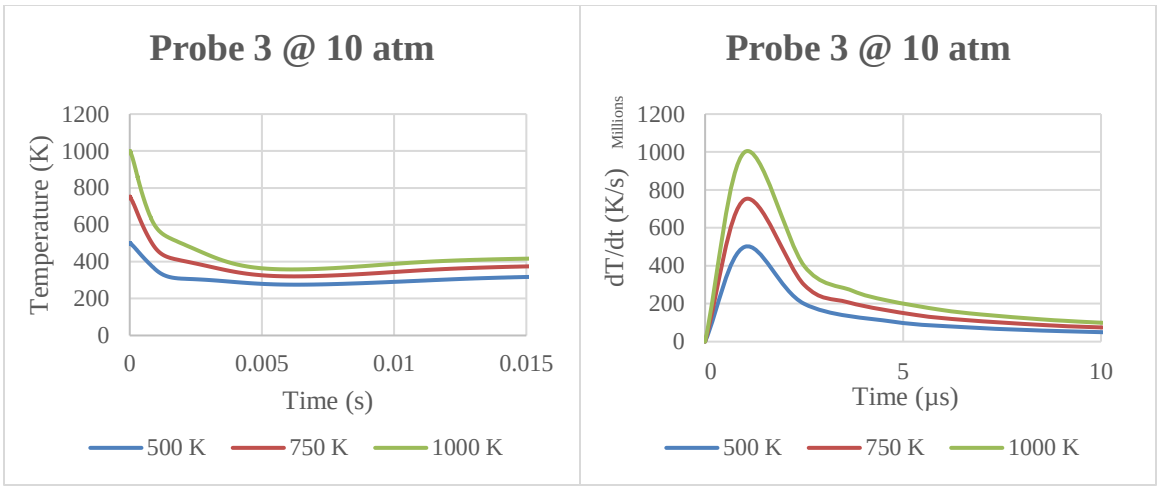

Figure 40: Temperature change in probe 3 at 10 atm with different inlet temperatures. Left: ΔT over time; Right: quenching rate over time

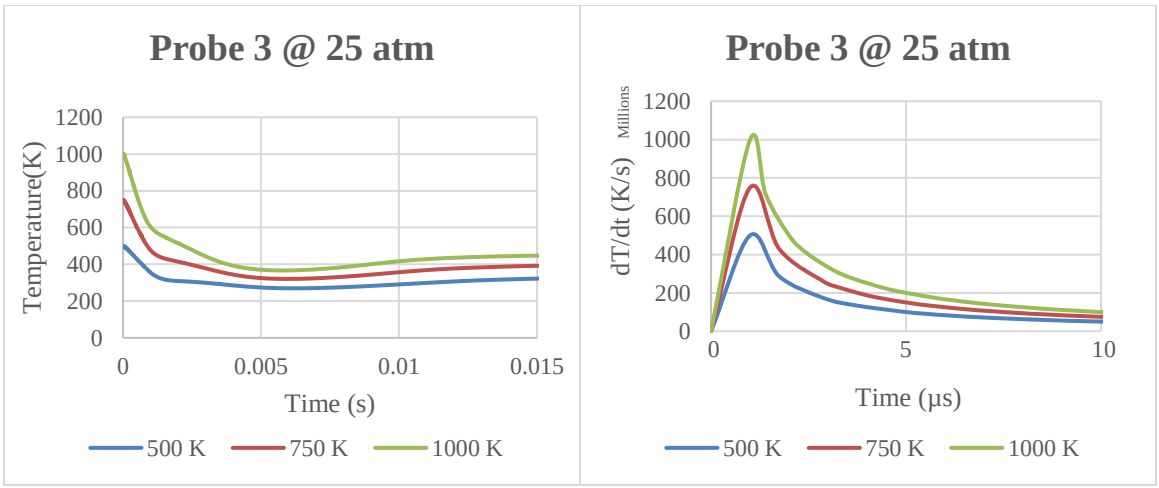

Figure 41: Temperature change in probe 3 at 25 atm with different inlet temperatures. Left: ΔT over time; Right: quenching rate over time

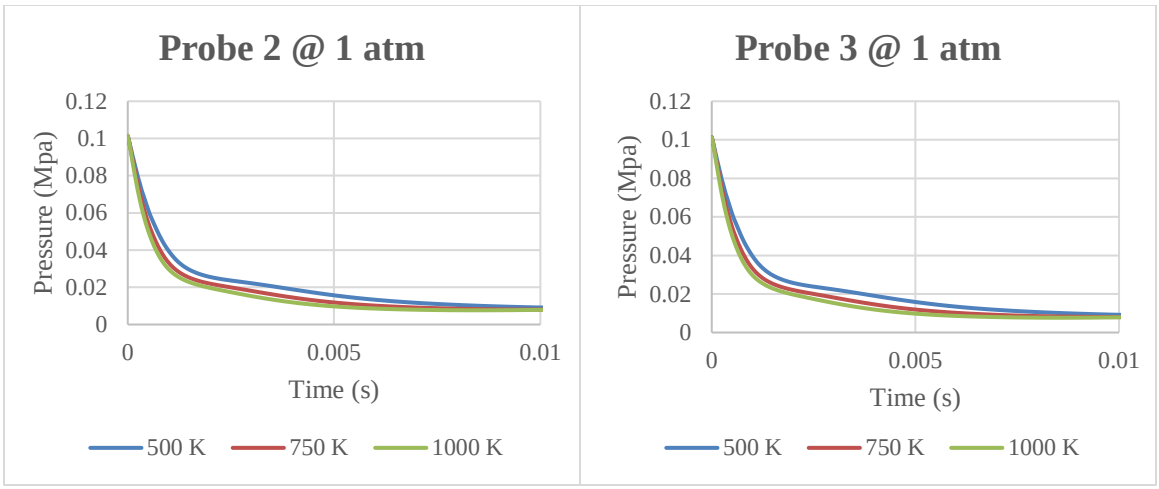

Figure 42: Pressure change over time in probes 2 and 3 at 1 atm with different inlet temperatures.

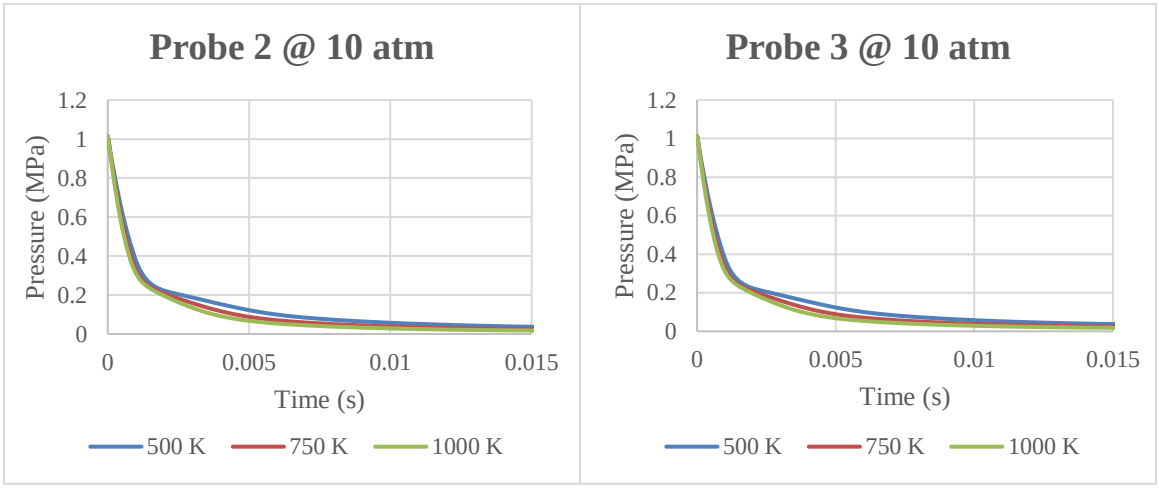

Figure 43: Pressure change over time in probes 2 and 3 at 10 atm with different inlet temperatures.

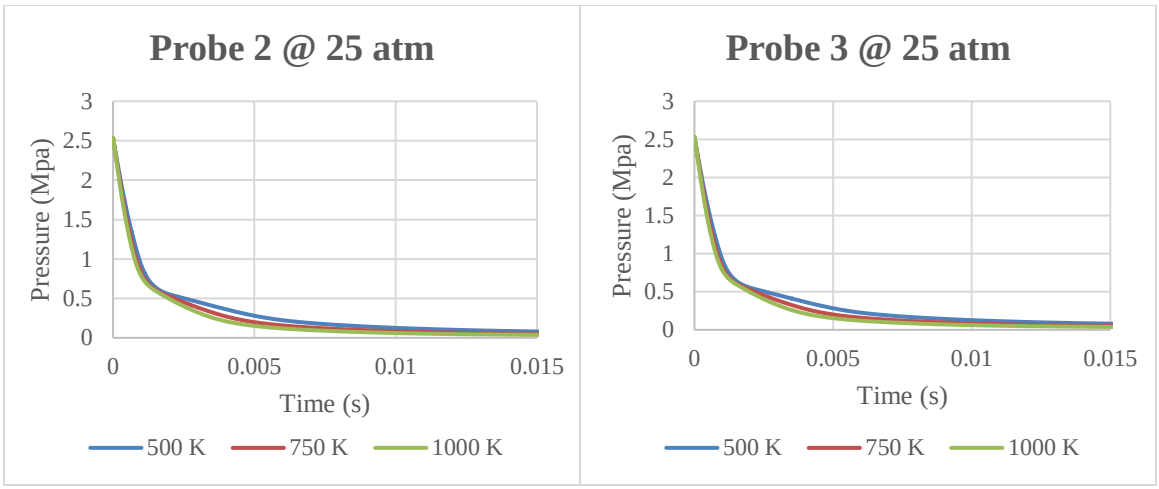

Figure 44: Pressure change over time in probes 2 and 3 at 25 atm with different inlet temperatures.

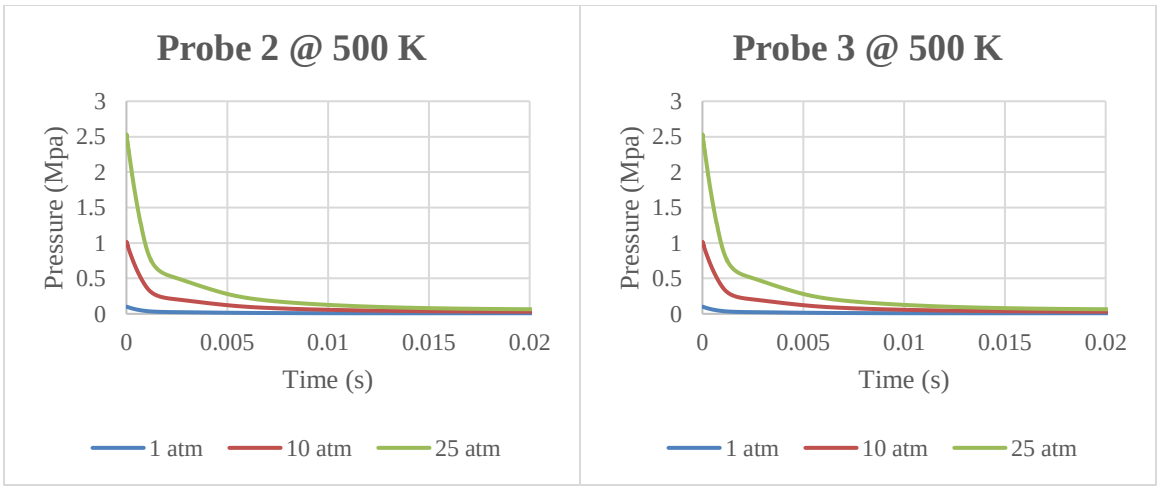

Figure 45: Pressure change over time in probes 2 and 3 at 500 K with different inlet pressures.

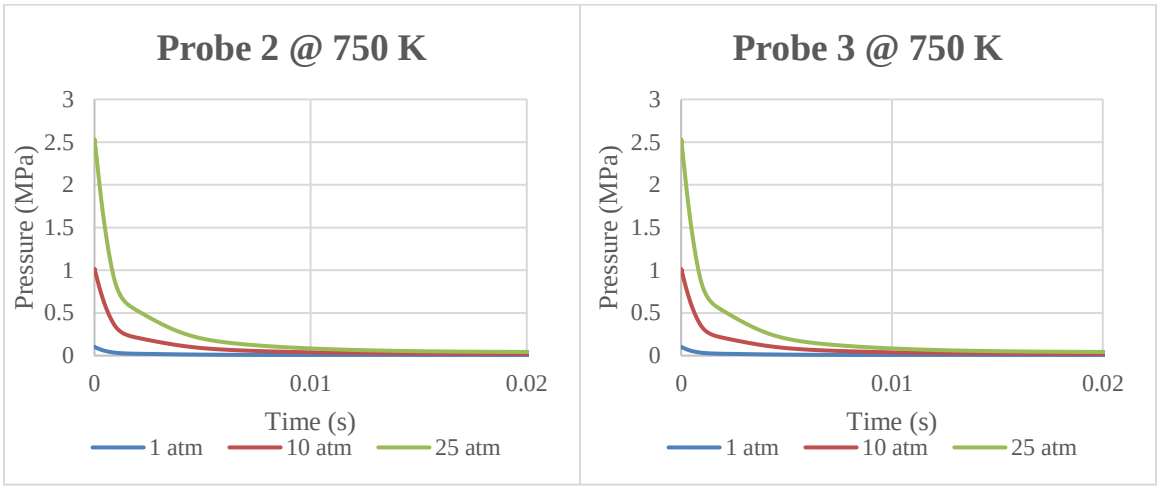

Figure 46: Pressure change over time in probes 2 and 3 at 750 K with different inlet pressures.

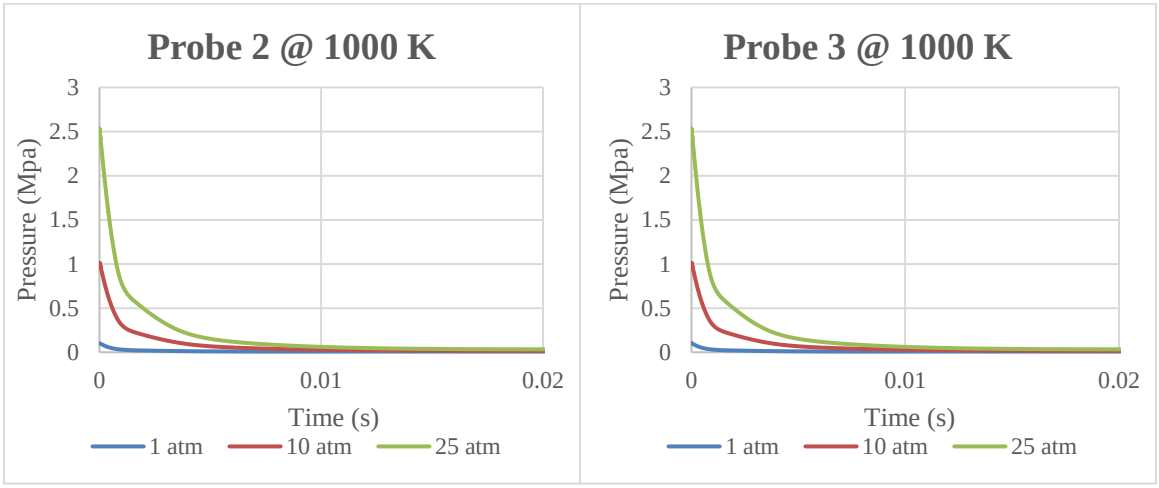

Figure 47: Pressure change over time in probes 2 and 3 at 1000 K with different inlet pressures.

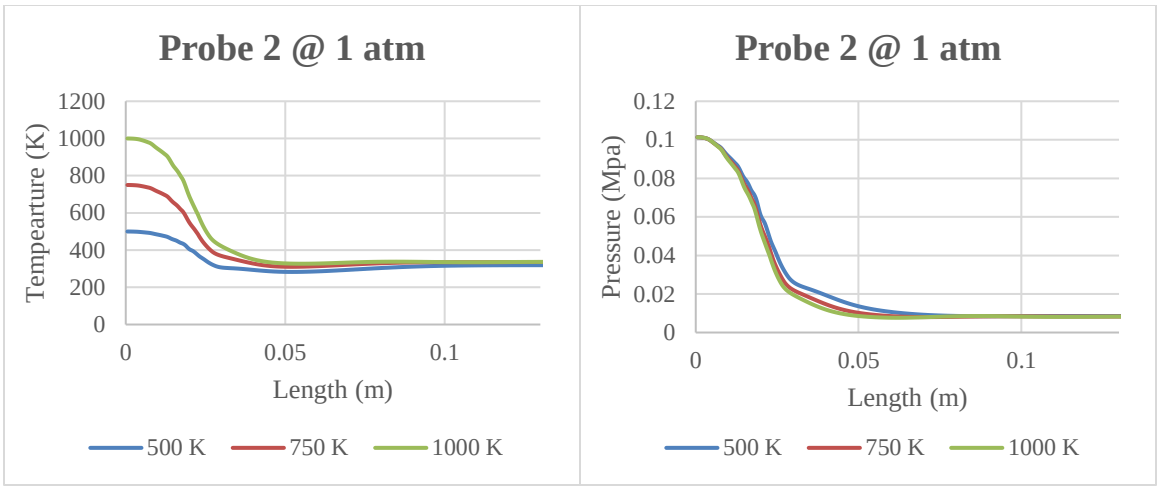

Figure 48: Temperature/pressure change in probe 2 at 1 atm with different inlet temperatures. Left: ΔT along length of probe 2; Right: ΔP along length of probe 2

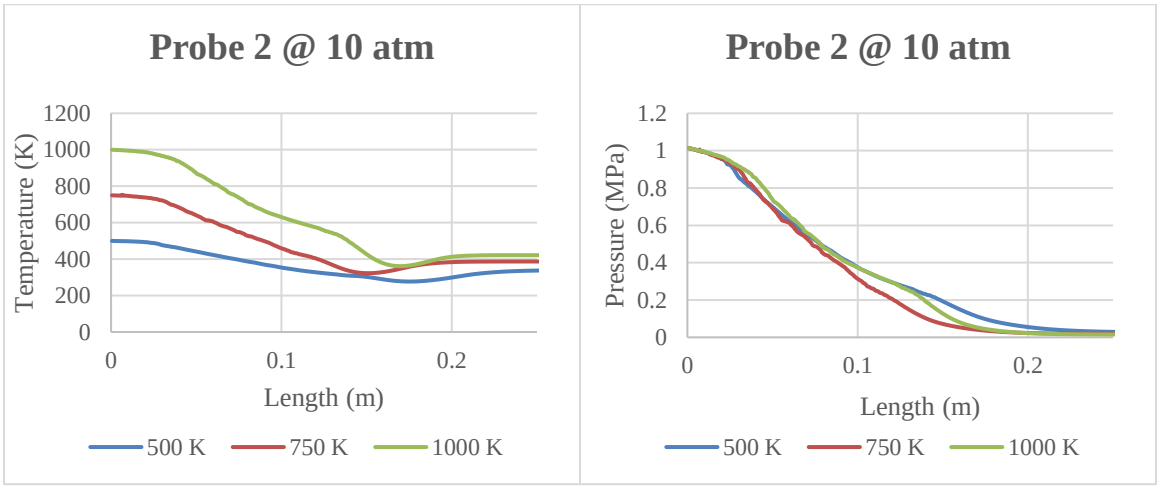

Figure 49: Temperature/pressure change in probe 2 at 10 atm with different inlet temperatures. Left: ΔT along length of probe 2; Right: ΔP along length of probe 2

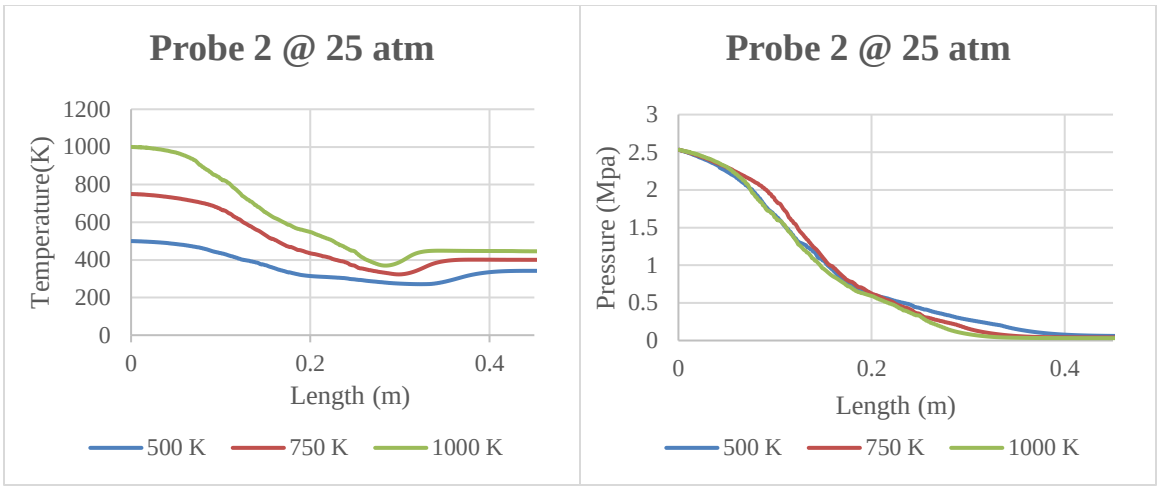

Figure 50: Temperature/pressure change in probe 2 at 25 atm with different inlet temperatures. Left: ΔT along length of probe 2; Right: ΔP along length of probe 2

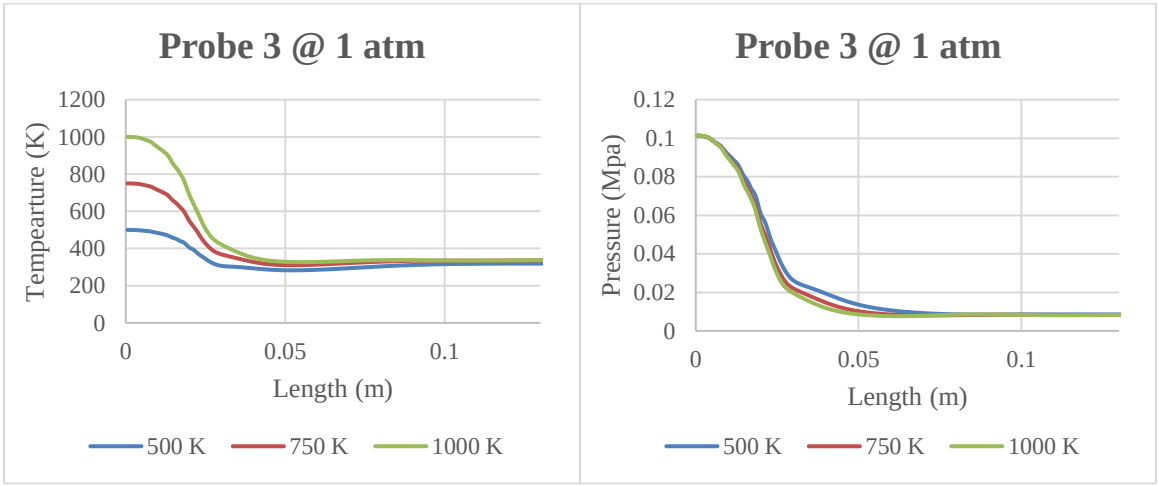

Figure 51: Temperature/pressure change in probe 3 at 1 atm with different inlet temperatures. Left: ΔT along length of probe 3; Right: ΔP along length of probe 3

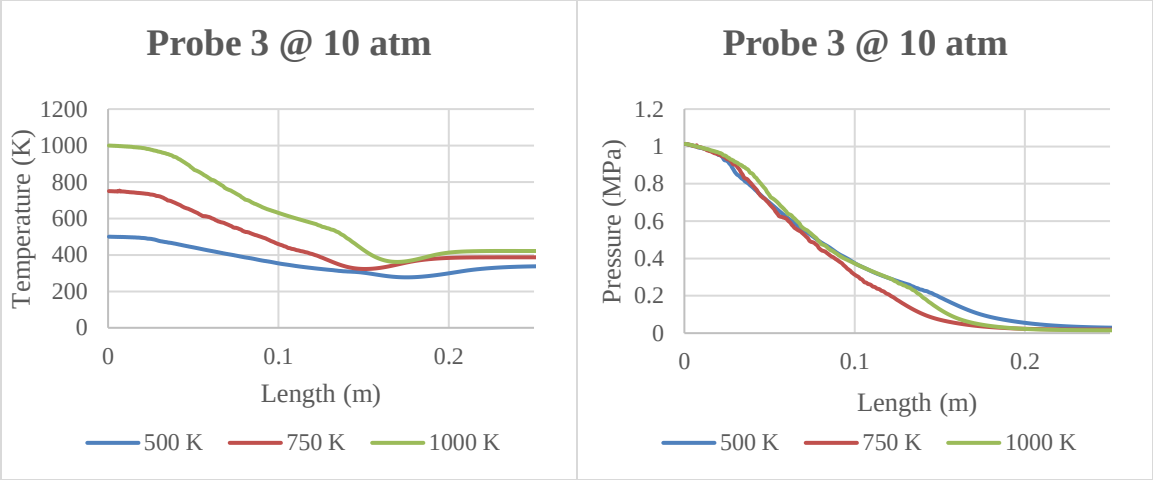

Figure 52: Temperature/pressure change in probe 3 at 10 atm with different inlet temperatures. Left: ΔT along length of probe 3; Right: ΔP along length of probe 3

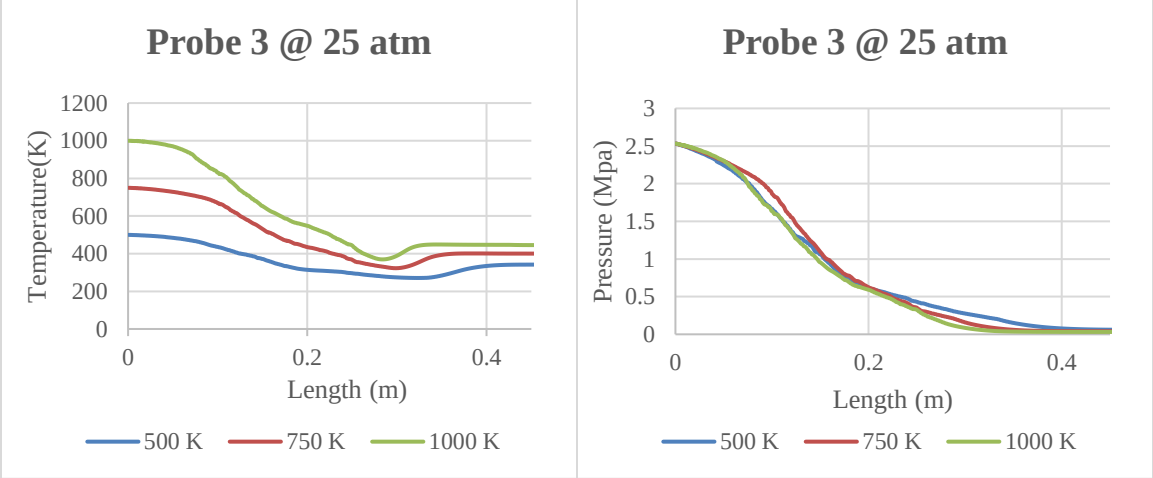

Figure 53: Temperature/pressure change in probe 3 at 25 atm with different inlet temperatures. Left: ΔT along length of probe 3; Right: ΔP along length of probe 3

Guide on how to setup a simulation in Converge CFD software

By using screenshots and detailed steps, a walkthrough on how to properly use Converge CFD software to setup a simulation is shown below. By following this step-to-step guide, a fully functional simulation can be setup for modeling fluid flow in a sonic probe.

1. Once in the Converge_studio application, select ‘New project’ on the pop-up menu. *please note that if you have a CAD model of your geometry, you can import the geometry from this menu as well*

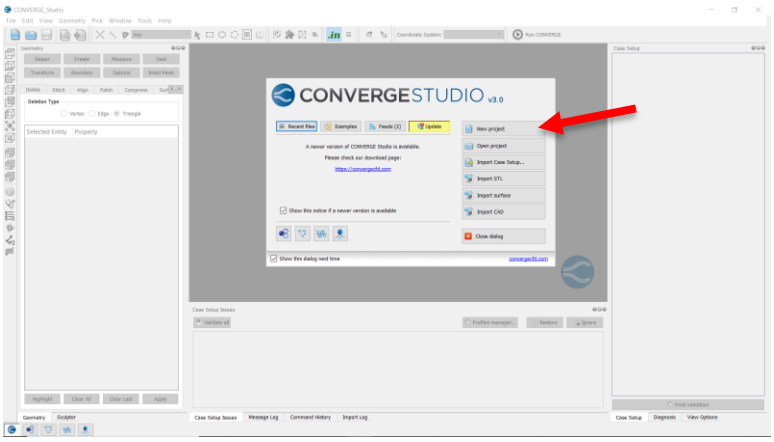

2. If this pop-up menu doesn’t come up, then find the ‘File’ button in the upper left hand of the screen and select ‘new project’ from there.

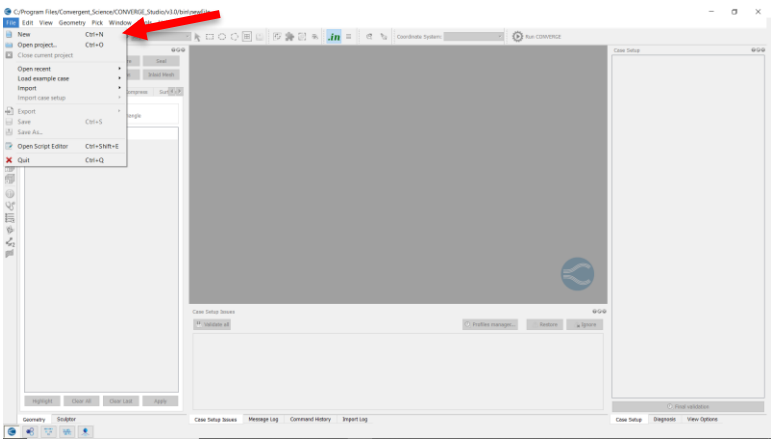

3. If you choose to create your geometry in Converge, then select the ‘Create’ tab on the left and click on the ‘Shape’ tab below that. (if you chose to import a geometry instead, skip to step 7)

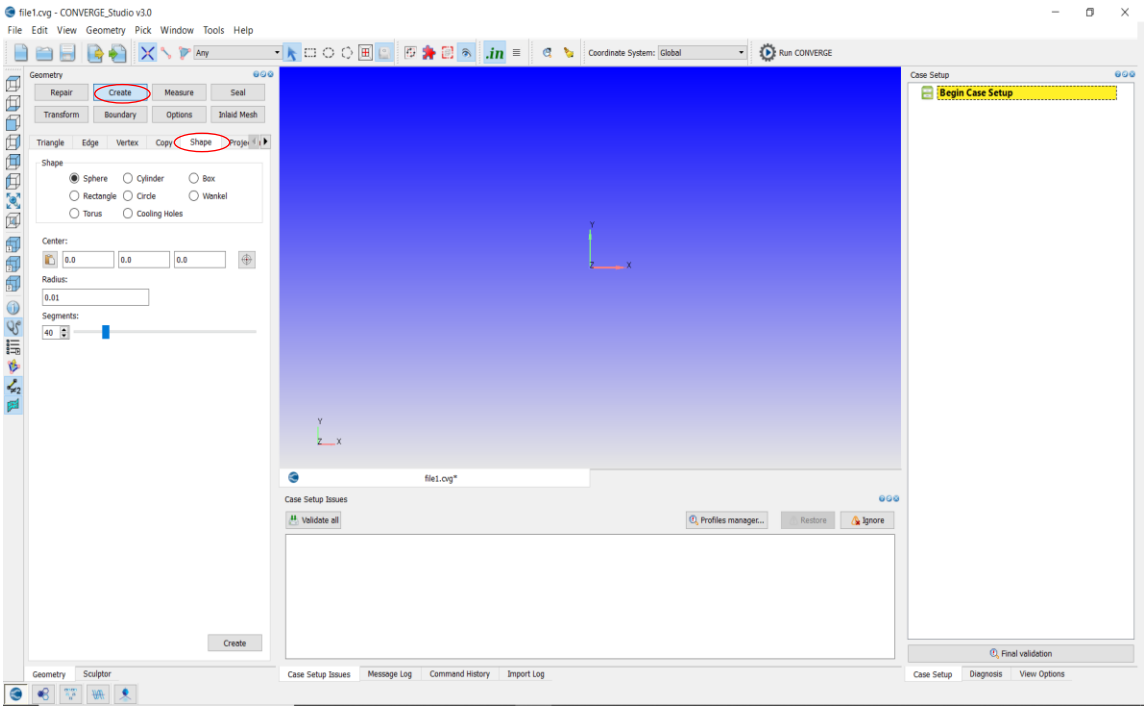

4. Once under the ‘Shape’ tab, choose the shape needed for your geometry (here I will show an arbitrary design for a probe). In this case, select ‘Cylinder’ and specify your 1st and 2nd diameter/radius size. *NOTE: the units are in meters so make sure to adjust accordingly* Next, identify how long the cylinder is and make sure to specify the direction (here, the probe will be designed along the x-axis so, ensure that the y and z-axis values are set to 0. Once, your specifications are complete, click ‘Create’ at the bottom left and the 1st portion of the geometry should come up. To move the geometry, hold the ctrl button on the keyboard along with left or right mouse clicks to adjust the view accordingly. To view specific sides of the geometry, different view points can be chosen by clicking the corresponding cube face on the far left panel in the software. Additionally, to undo some changes made, ctrl + z can be used.

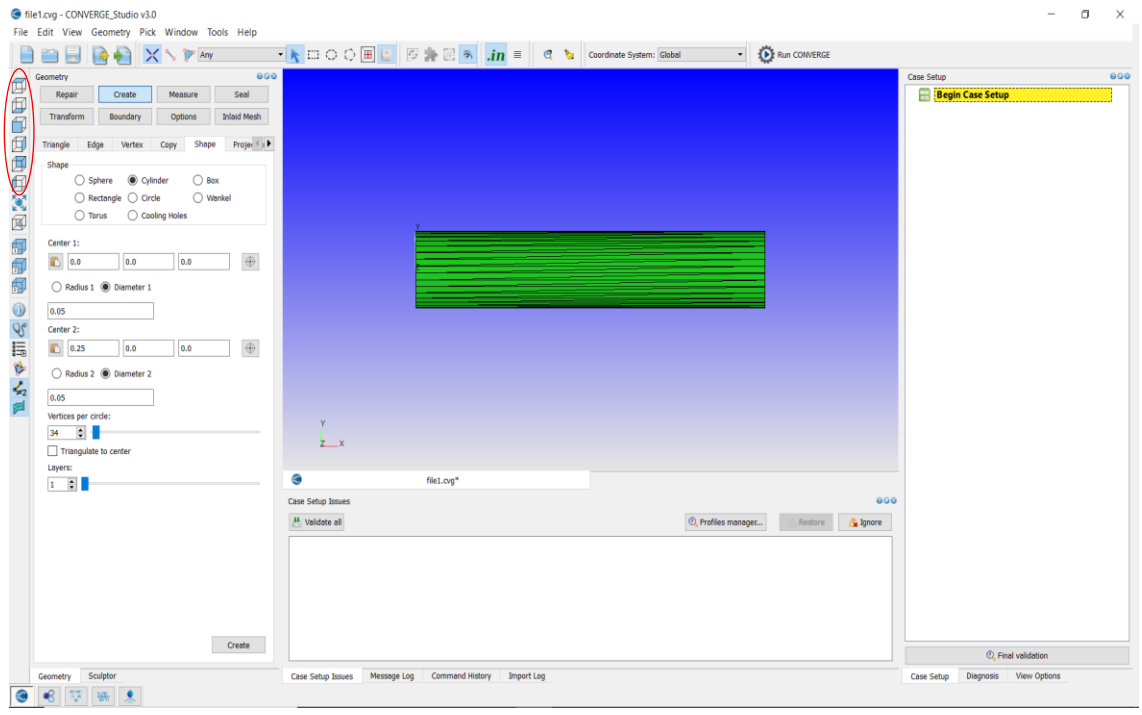

5. Using the ‘Cylinder’ option also allows for different angles to be created based on the length and diameter of your geometry. Specify, the 1st and 2nd diameter here and make sure to start this portion of your geometry where the last portion ended. Then, specify how long this portion of the geometry is and click ‘Create’ in the bottom left. This should add the second piece of the geometry.

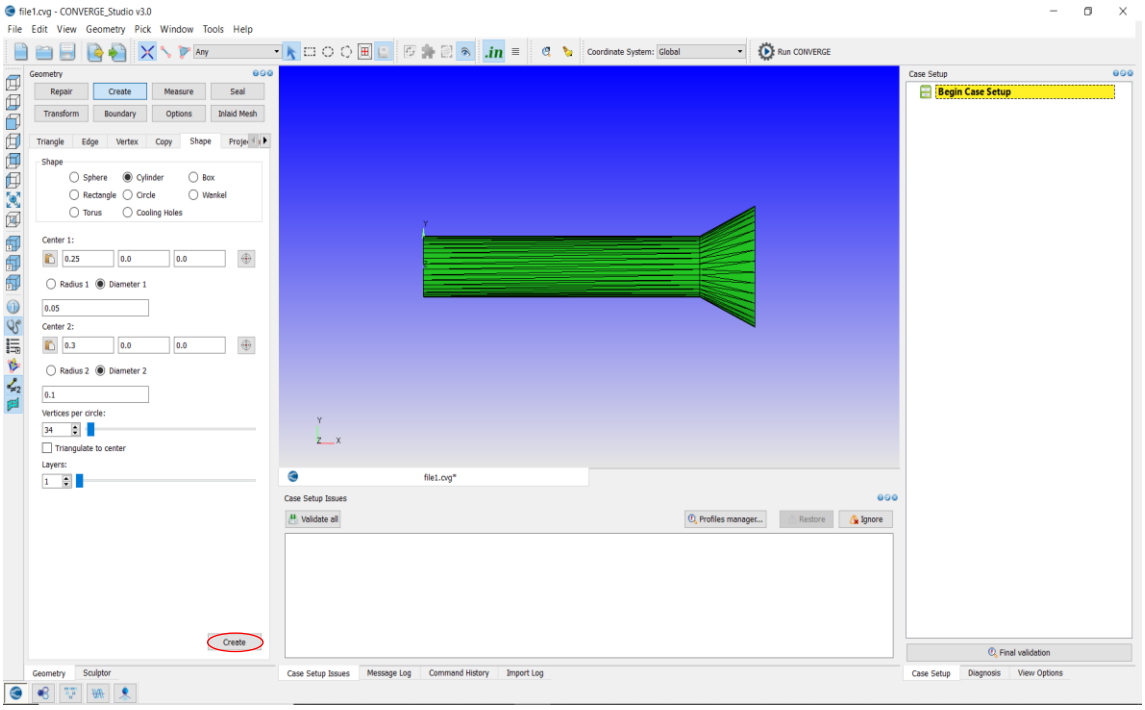

6. Repeat step 5 until the geometry is finished and the design properly shown in the software. This is probably a good step to save the file so choose ‘File’ in the upper left and choose ‘Save as’ to save your file. Save your file under the name you like and I find it best to create a folder so that all the input and output data can be sorted through easily.

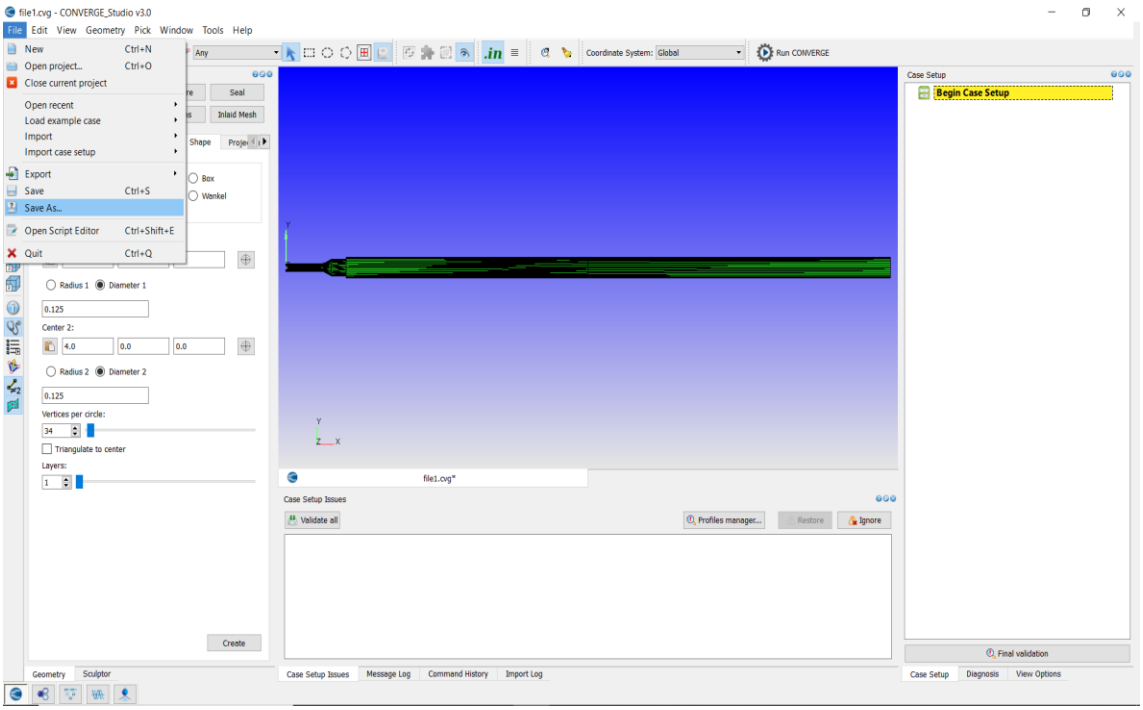

7. Click the ‘Repair’ option and scroll to the ‘Polygonica’ tab. Once here, click ‘Coarsen the whole surface’ option to fix most, if not all major issues in the geometry. To check and see if the geometry is correct, select ‘diagnosis’ in the bottom right. Then select the box for ‘Check that all normals are pointing to the interior’. Without checking this box, the simulation will not run if there are proplems with the normal orientation. Finally press the ‘Find’ option in the bottom right.

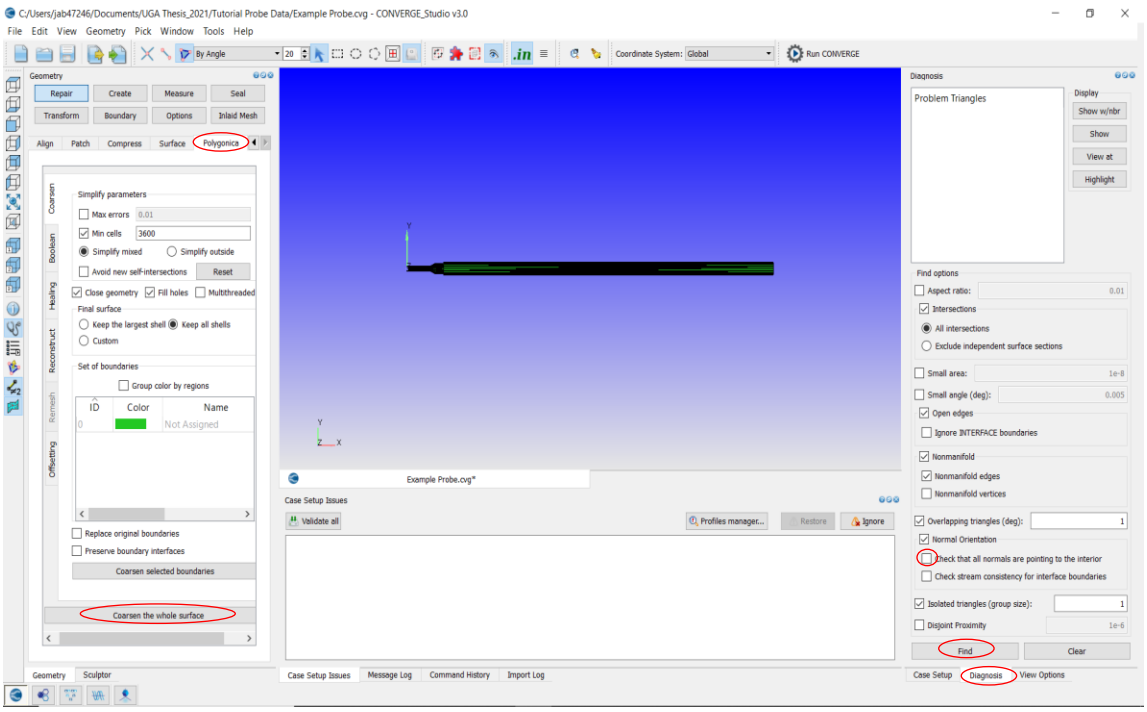

8. After that, a diagnosis box will show what problems there are in the geometry. Normal orientation should be the only issue here. If, more errors in the geometry exist, checkout the Converge training materials (located on the group drive under common files and Converge CFD software.*The manual is located here as well*) for a more detailed explanation for how to fix geometry issues. If the only issue shown is with Normal orientation, then select ‘Transform’ on the upper left and select the ‘Normal’ tab. Once there, select the ‘Attempt to fix all normals’ option. Finally, select the ‘Apply’ button in the bottom left.

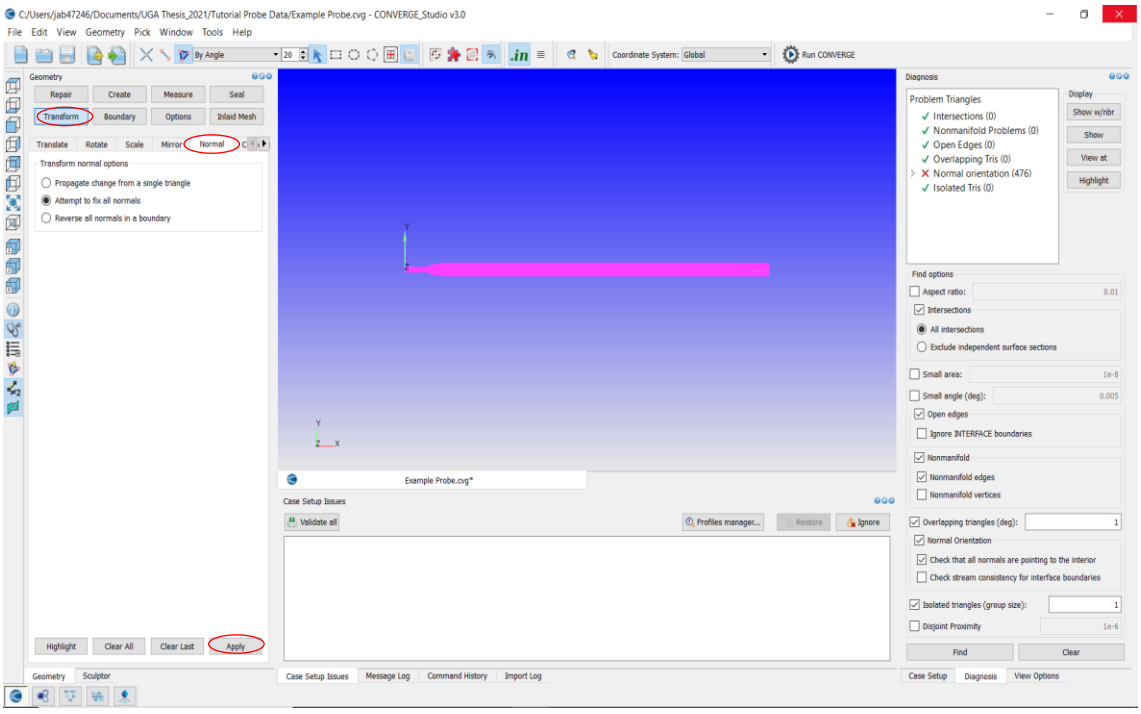

9. Now, press the ‘Find’ button again in the bottom right corner under the ‘Diagnosis’ tab. This should fix all the issues with the geometry and complete the 1st phase. At this point, it might be a good time to save the file again (can be done with ctrl + s).

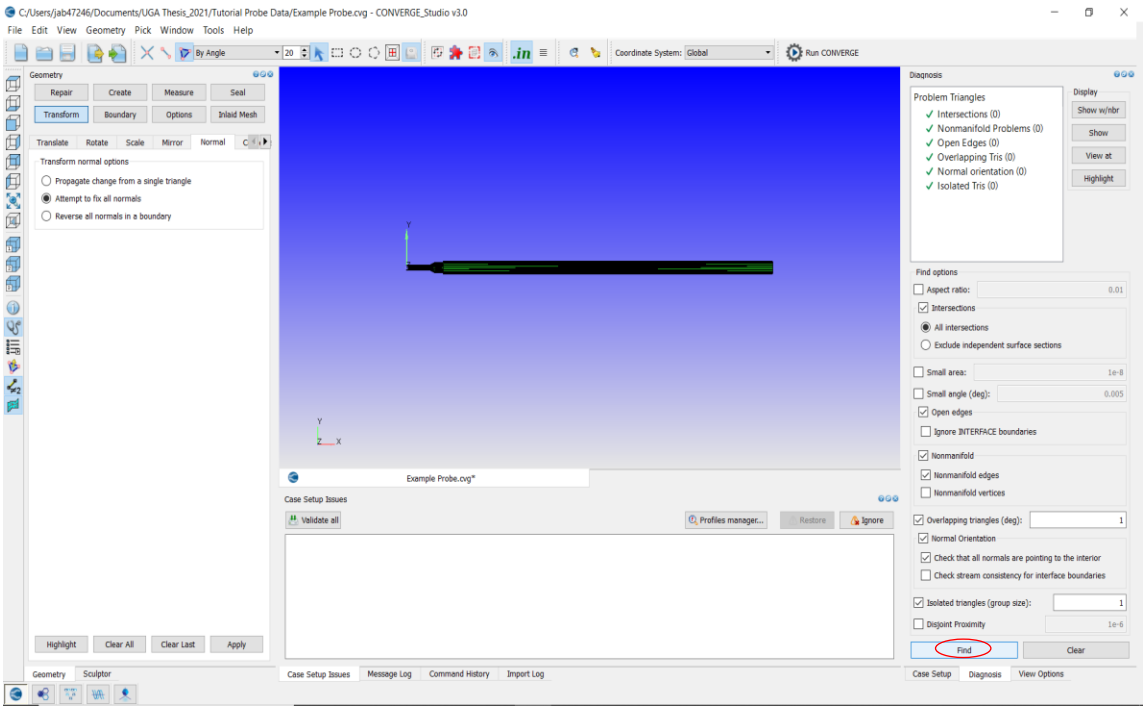

10. To begin the next phase, select ‘Boundary’ on the upper left and click the green plus slightly below that. This is where the boundaries of your geometry are identified (in this case, 3 boundaries will be used i.e. inlet, walls, outlet). Once the Boundary definition tab comes up, specify the name of the boundary and the color. Once completed, press ‘ok’ and the first boundary will show on the left. Repeat steps beginning with pressing the green button for the remainder of the boundaries.

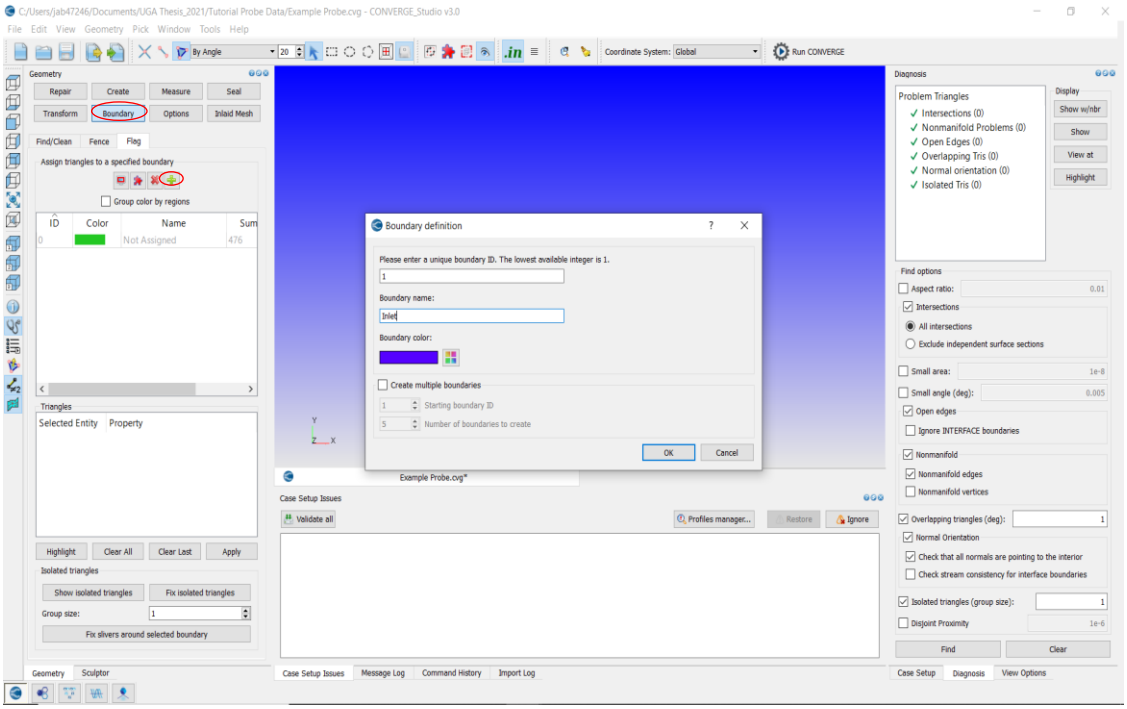

11. The next steps are to tell the software where each of the boundaries that were created lie on the geometry. First, rotate the geometry so that the boundary that is going to be specified can be seen clearly. Then, choose ‘By angle’ in the upper left of the screen. This will allow us to select the face of the side that is chosen. After the portion of your mesh is highlighted with red, select the boundary that is to be associated with this area, and click ‘Apply’ in the bottom left. Finally, repeat this process after specifying ‘By angle’ to identify all portions of the geometry. (Multiple portions of the geometry can be selected at once and if something was selected accidentally, press esc on the keyboard to deselect everything and start over.)

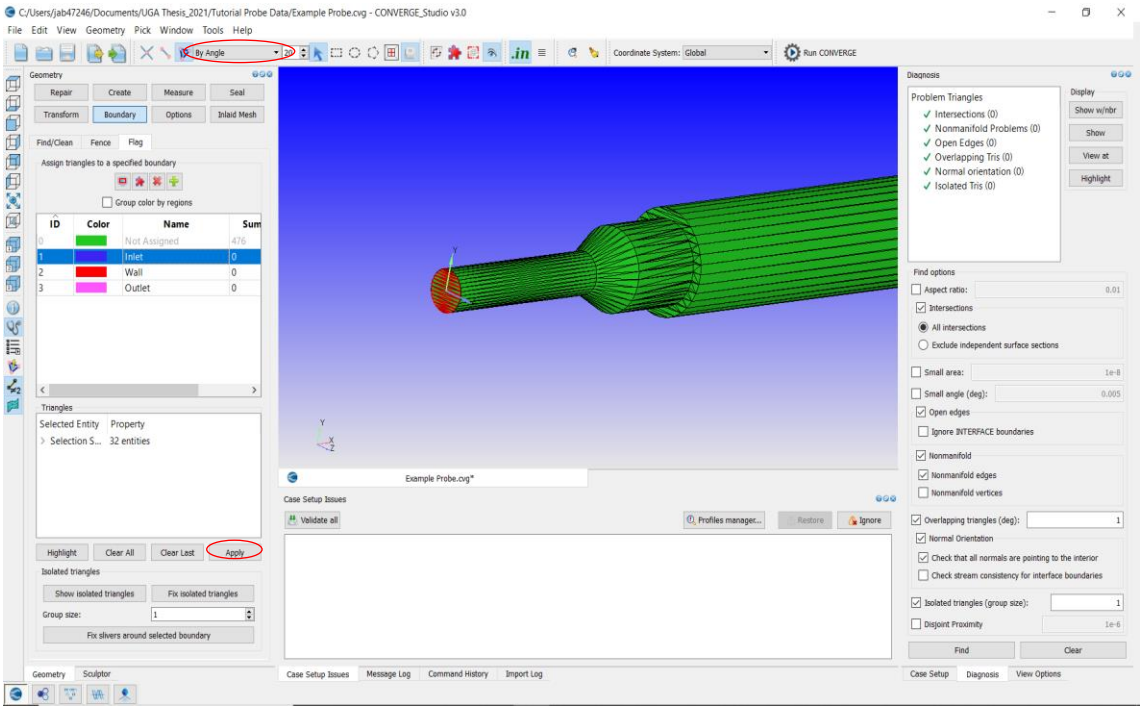

12. If the previous step was done correctly, the boundaries should be clearly identified and the ‘Not Assigned’ boundary should have a sum of 0. This indicates that all boundaries in the geometry have been specified and make sure that each boundary is identified properly. This completes the 2nd phase of the process and is probably a good place to save.

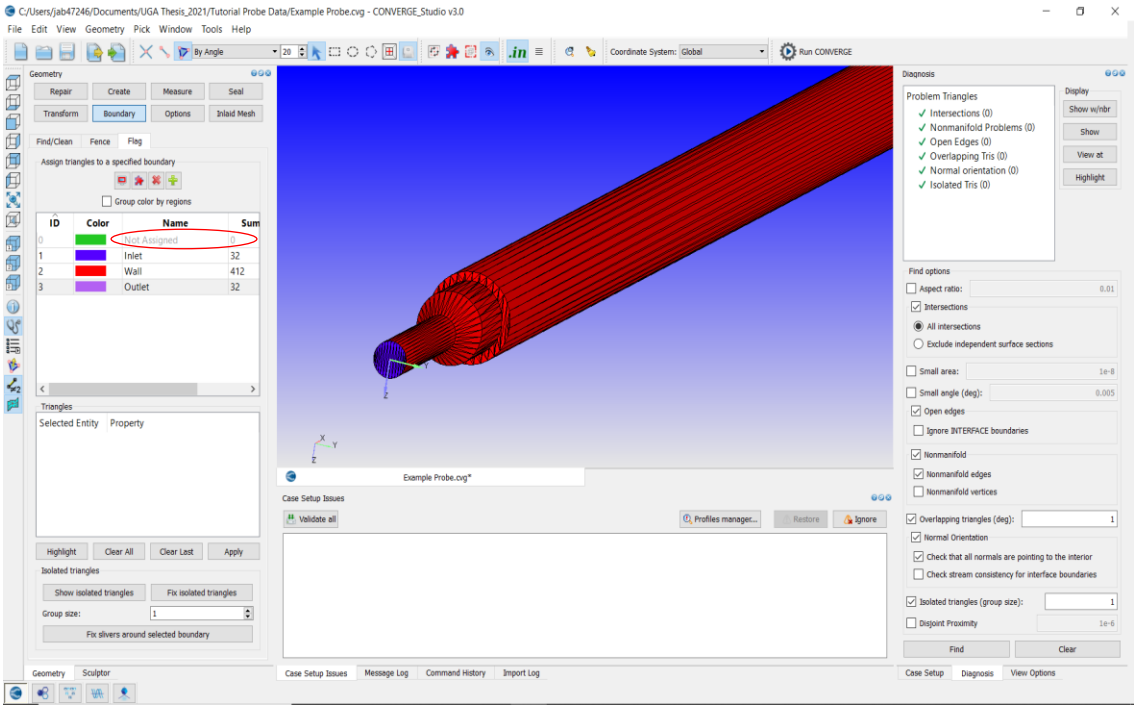

13. To begin the 3rd phase, select ‘Case Setup’ in the bottom right. Then select, ‘Begin Case Setup’. A pop-up box should show and the ‘Application Type’ tab will be up. Ensure that the ‘Time based’ option is selected.

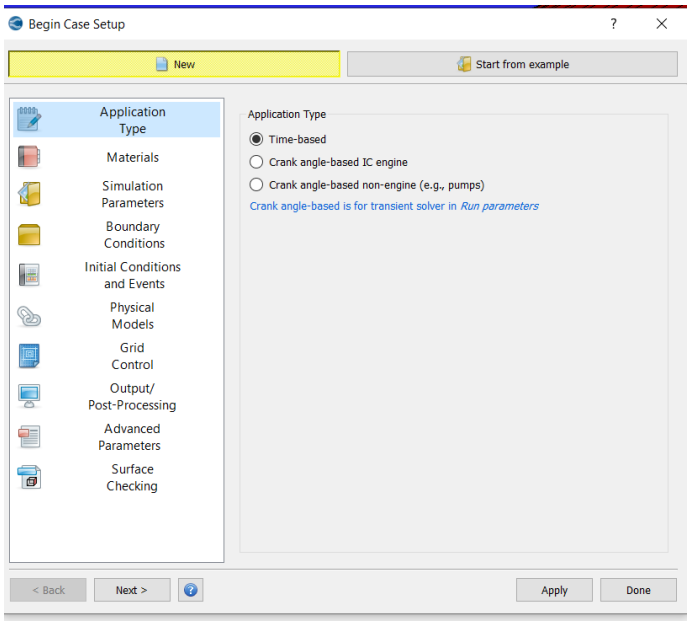

14. Now, select the ‘Materials’ tab and uncheck the ‘Reaction mechanism’ box. Next, check the box for ‘Species’.

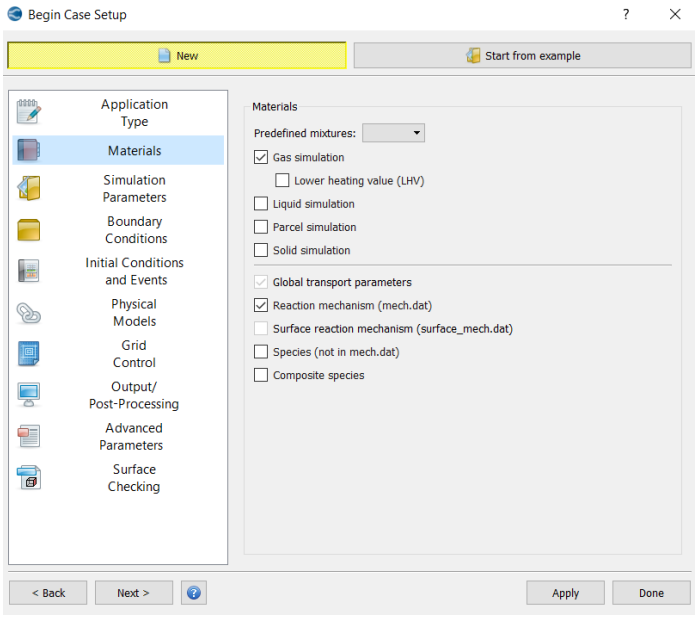

15. Next, select the ‘Initial Conditions and Events’ tab and check the ‘Events’ box. Finally, press ’Done’ at the bottom of the pop-up.

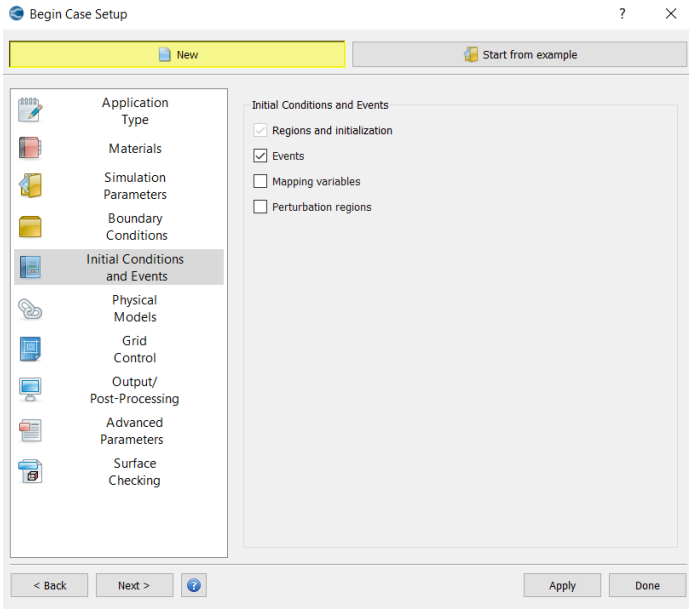

16. Then, select the ‘Gas simulation’ under the ‘Materials’ tab on the right. In this section, thermodynamic data can be imported here to match the data in the lab. (in this case, no data is being imported.) Next, press ‘OK’ on the pop-up.

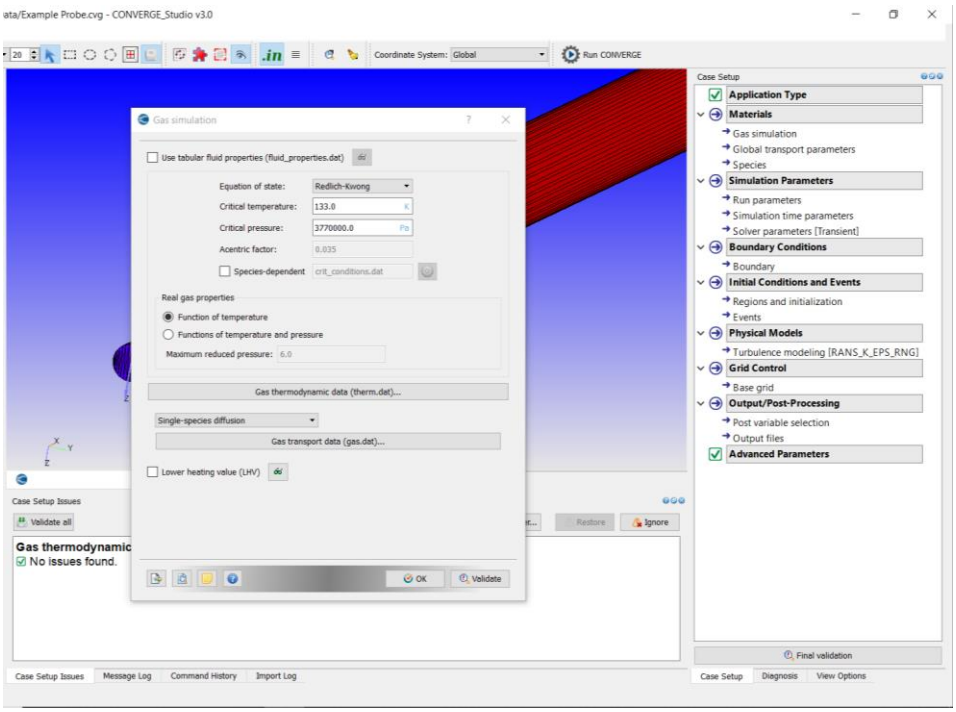

17. On the next tab, ‘Global transport parameters’, select ‘OK’ on the pop-up.

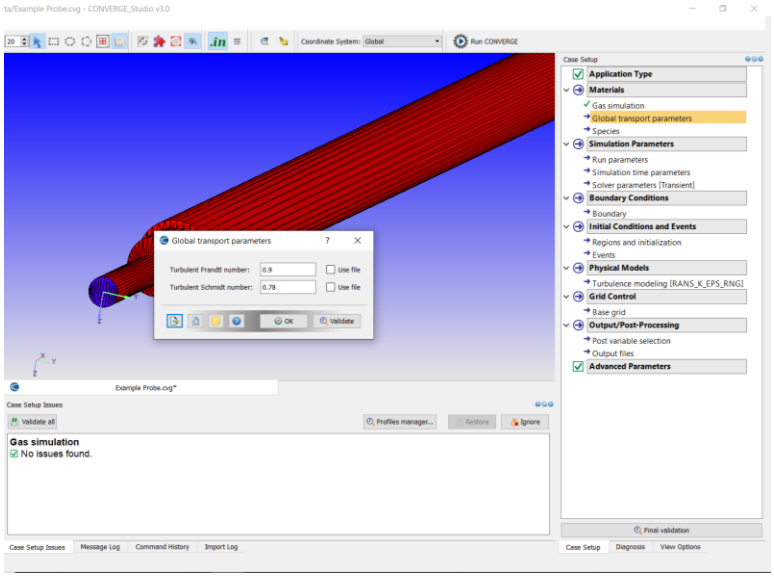

18. Select the ‘Species’ tab and when the pop-up shows, select the green button. This is where the fluid is specified based on the thermodynamic data. In the search bar, find the species that will be used in the simulation (in this case, N2 will be used). Finally, press ‘OK’.

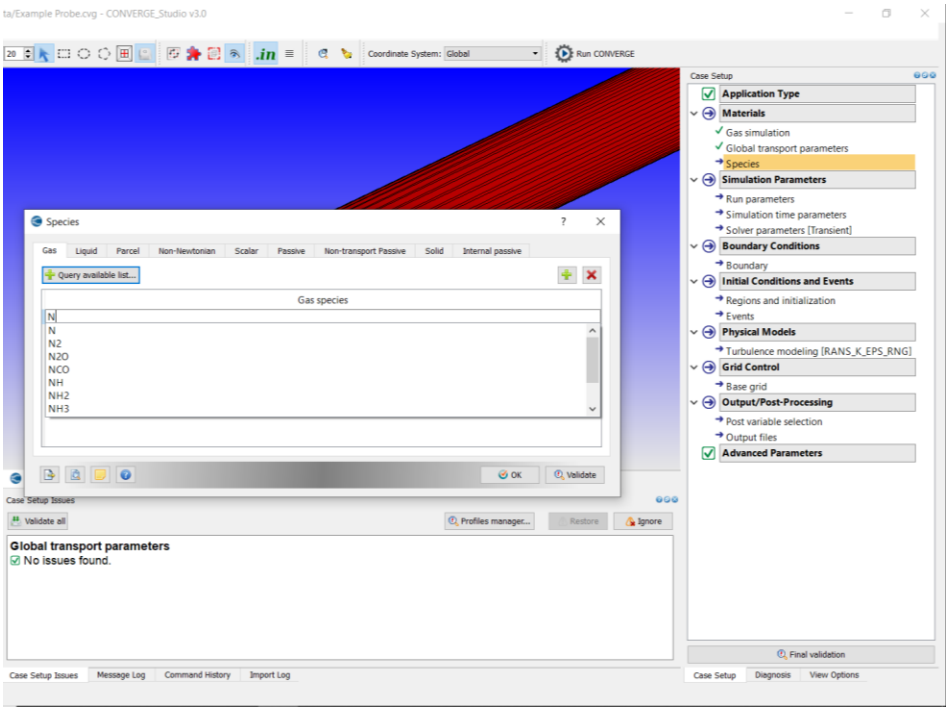

19. In the ‘Run parameters’ tab, if steady-state is one of the assumptions in the problem, then specify it here.

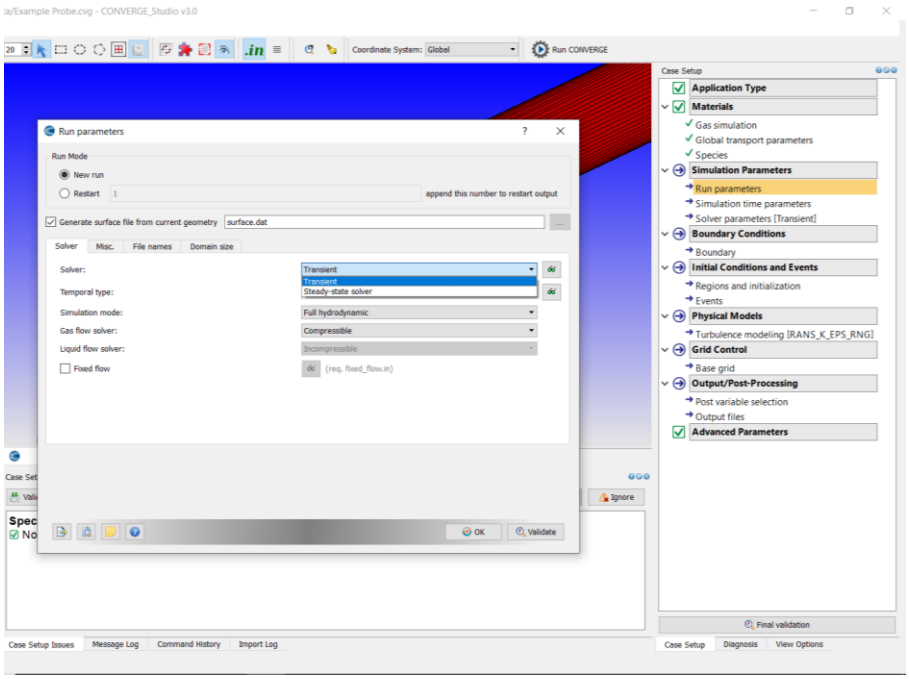

20. Then, on the ‘Misc’ tab of the same pop-up, turn on the ‘Steady-state monitor’ and press ‘OK’.

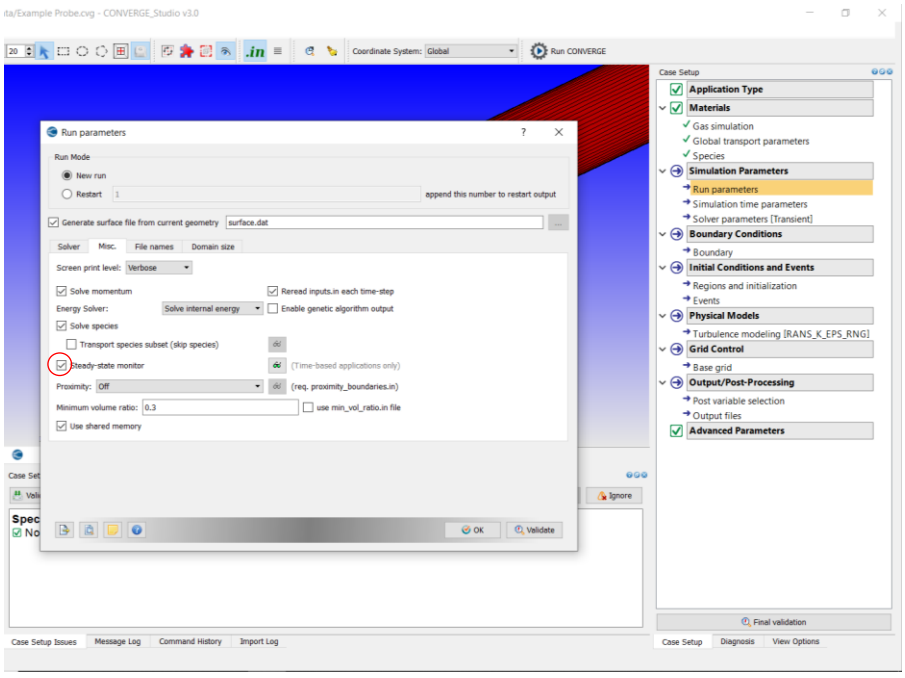

21. Click ‘Confirm’ on the new pop-up.

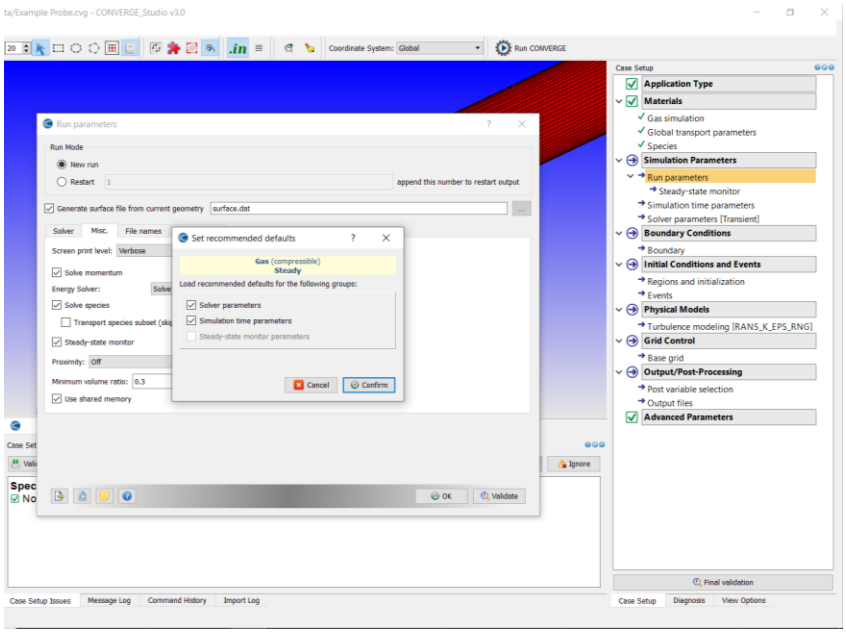

22. In the ‘Steady-state monitor’ pop-up that should have opened (it’s also now under the ‘Simulation parameters’ tab), select the green plus to add configuration. Then, press the green plus at the bottom of the pop-up and select a variable to monitor such as the mean temperature.

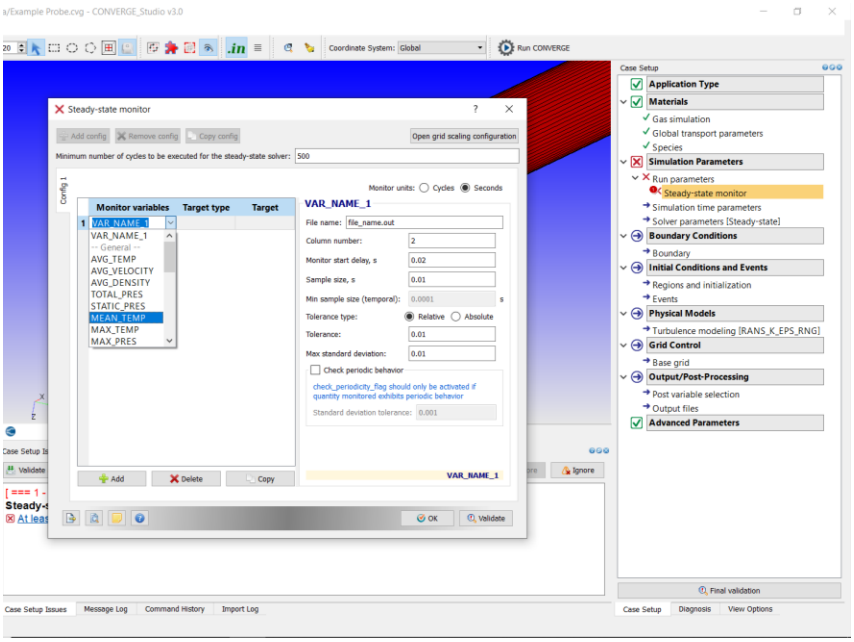

23. Then, under ‘Target type’ select region, and under ‘Target’ select ‘All regions’. Finally, press ‘OK’.

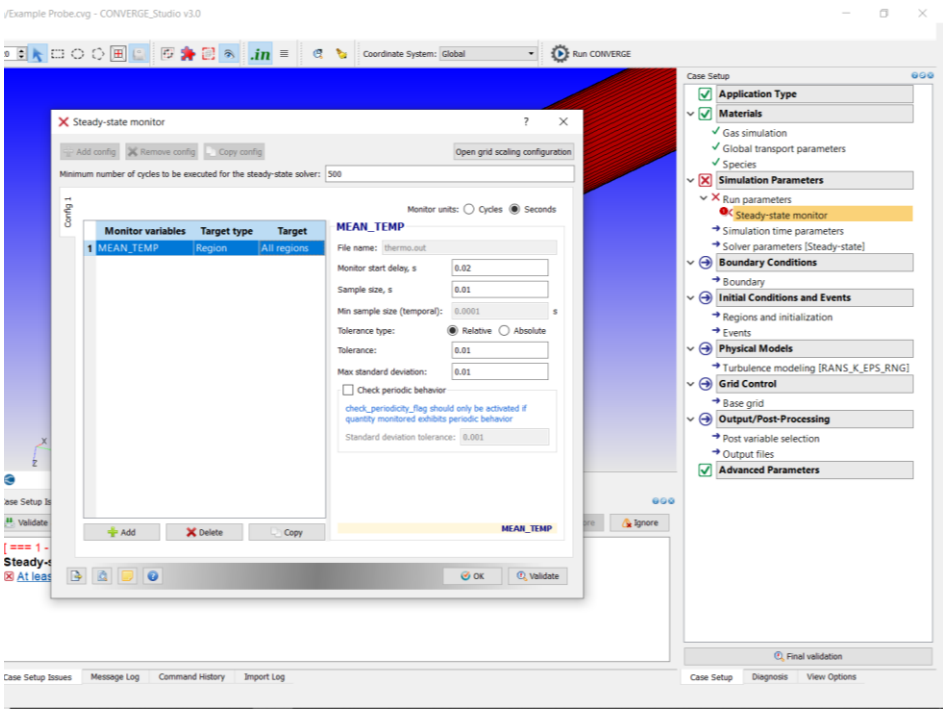

24. Now, under the ‘Simulation time parameters’ a guess must be made for how long the simulation will run and for the time steps in the problem. The values here will potentially work fine but, can be adjusted later for optimal run time. Here, 1000 (not 5000 as shown in image) is used for the ‘End time’ while 1e-06 is used for the ‘Initial time-step’, 1e-07 for the ‘Minimum time-step’, and .001 for the ‘Maximum time-step. Once the values are specified, select ‘OK’.

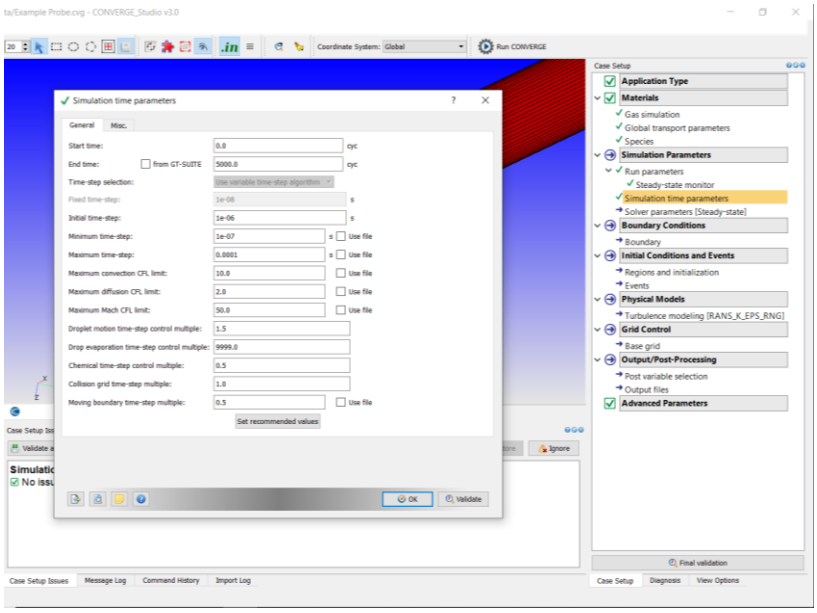

25. Under the ‘Solver parameters’ pop-up, select ‘OK’.

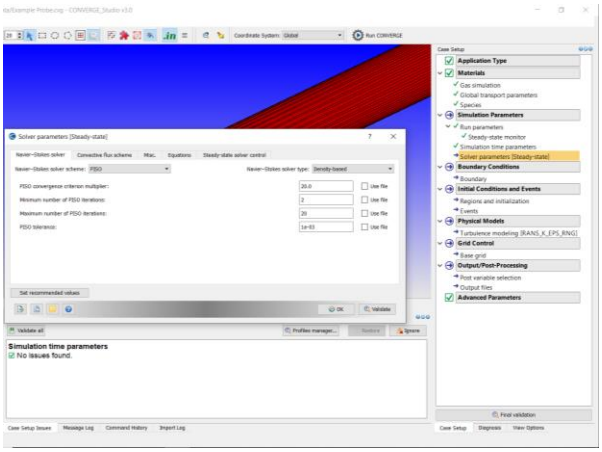

26. Next, instead of going to boundary, go to ‘Regions and initializations’ first. Then, add 2 regions with the green plus and these regions do not have to be renamed. Under the ‘Region 0’ tab these conditions must be made consistent with the inlet boundary conditions. Here, an inlet velocity of 500 m/s in the x-direction is used along with an inlet pressure and temperature of 100,325 Pa and 700 K respectively. Then, go under ‘Species Name’ and add item with the green button. Finally, specify the species that was selected earlier with the mass fraction of that species as well.

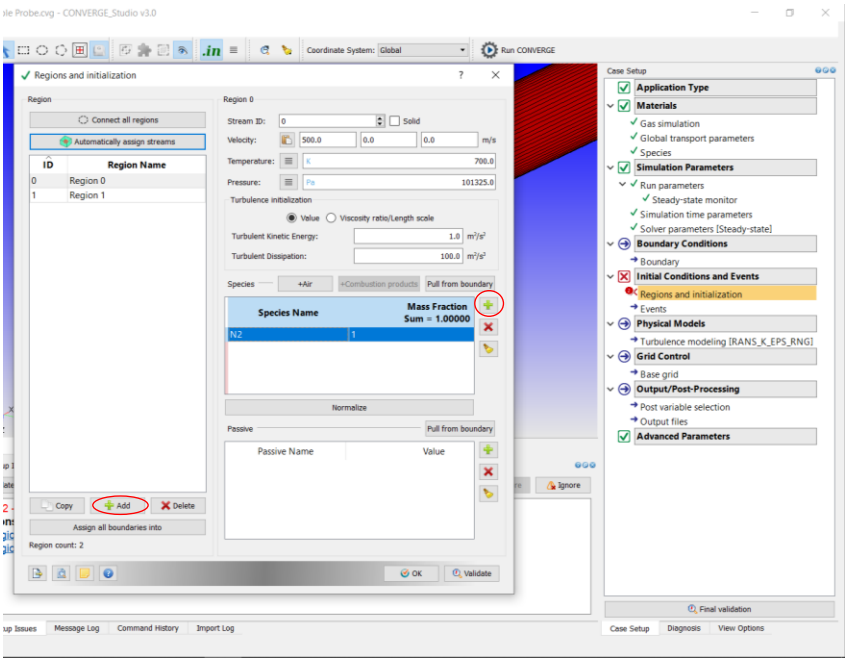

27. Here, do the same thing for the species. It should be consistent throughout the problem and this section will match the outlet boundary conditions. In this case, 8,000 Pa is used as the outlet pressure and the outlet temperature is 300 K. After this is specified, press ‘OK’ at the bottom of the pop-up.

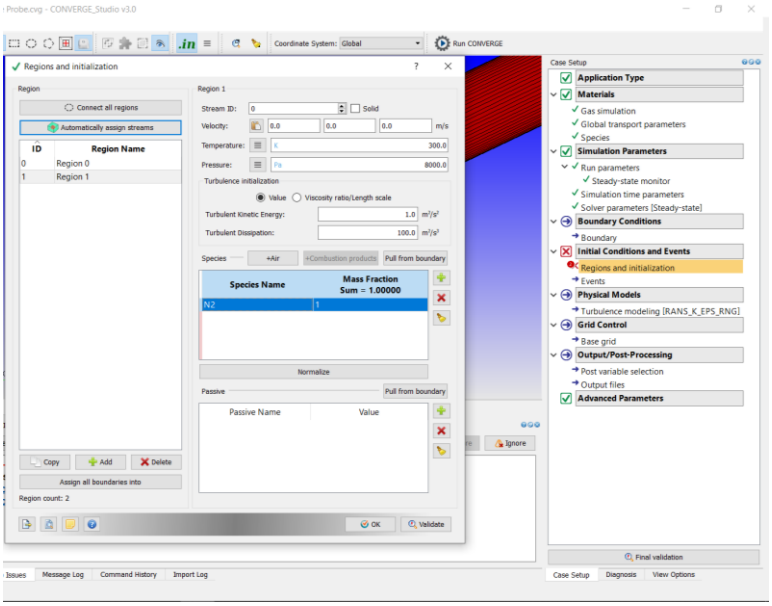

28. Now, go to the ‘Boundary’ tab and define the region for each boundary. Ensure that the wall boundary is consistent with the inlet. Next, select the ‘Inlet’ (or whatever name was used here) to specify the inlet boundary. Select ‘Inflow’ in the drop down menu.

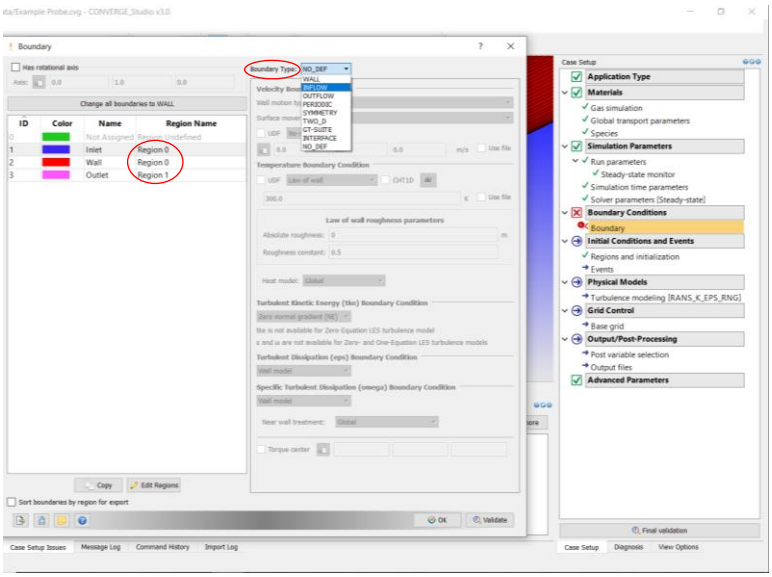

29. After ‘Inflow’ was specified, set the temperature and pressure values to be consistent with what was set in the corresponding region. Also, specify the species and check the ‘Supersonic’ box. Once this was selected, under the ‘Velocity Boundary Condition’ tab, select ‘Specified Value’ in the drop down menu which will allow for the velocity to be set as well *another reminder to set values to what was set in the corresponding region*.

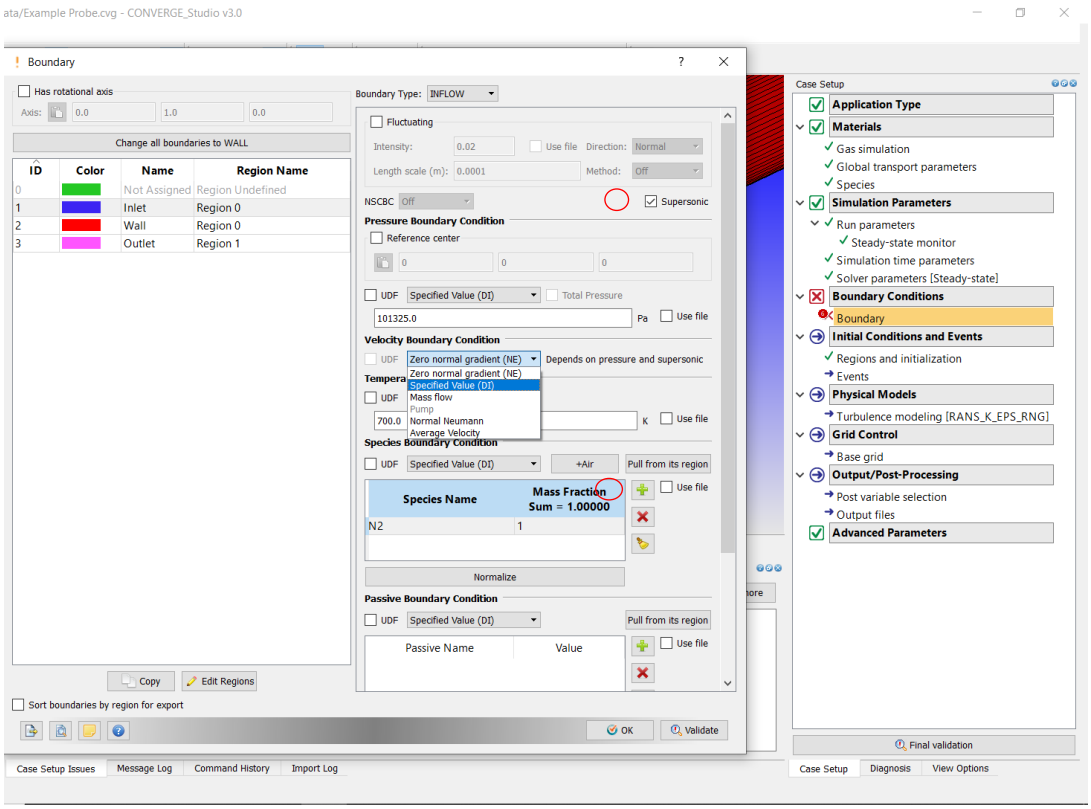

30. Next, specify ‘Wall’ with the drop down ‘Boundary Type’ menu. Once specified, ensure that the velocity and temperature boundary condition is specified by ‘Law of wall’. Finally, in the tke boundary condition, specify ‘Zero normal gradient’.

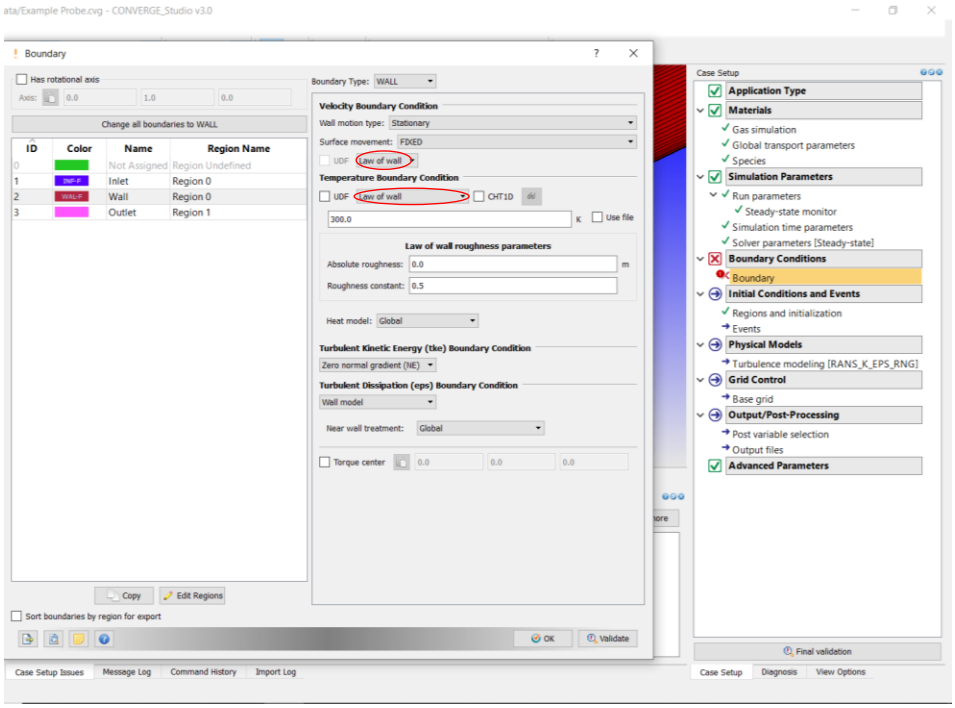

31. In the last step, specify the ‘Outflow’ with the boundary type drop down menu. Make sure the velocity boundary condition is specified as ‘Zero normal gradient’ and the pressure boundary condition has ‘Specified Value’ so that outlet pressure and temperture can be consistent to the corresponding region. Finally, press ‘OK’. This may be a good spot to press save as well.

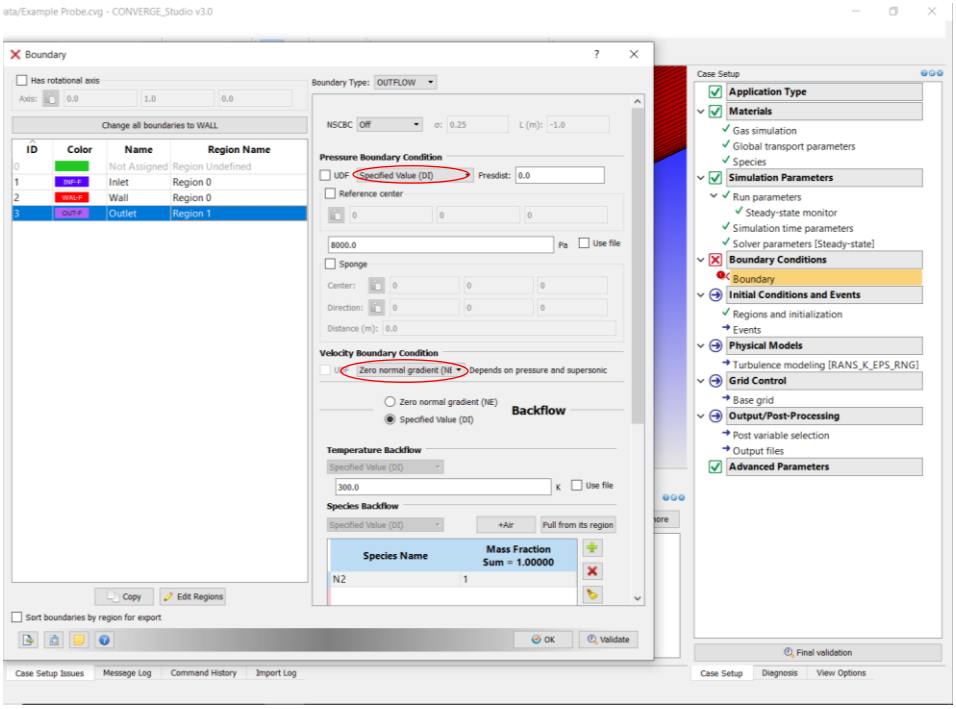

32. Next, in the ‘Events’ tab, select the ‘Permanent’ tab and check the box next to it. Then, add an item with the green button and specify each section accordingly; ‘Event by’ with Regions, ‘Region A’ with the region corresponding to the inlet, and ‘Region B’ with the region corresponding to the outlet. Finally, press ‘OK’.

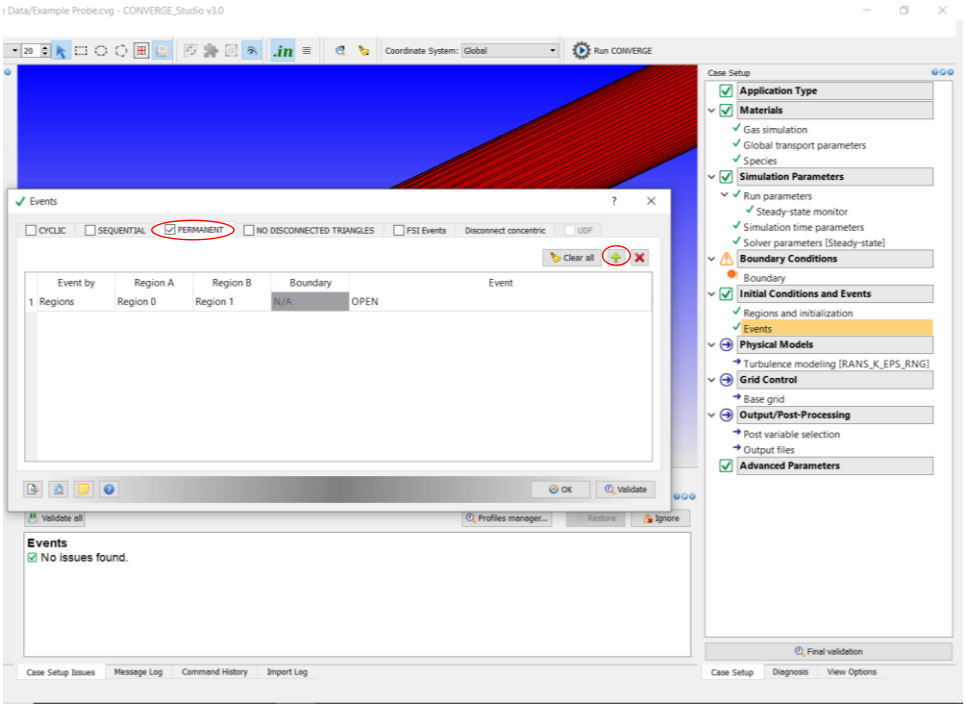

33. Next, under ‘Turbulence modeling’ make sure the RANS is selected in the top right of the pop-up. Then press ‘Set recommended model values’ and press ‘OK’.

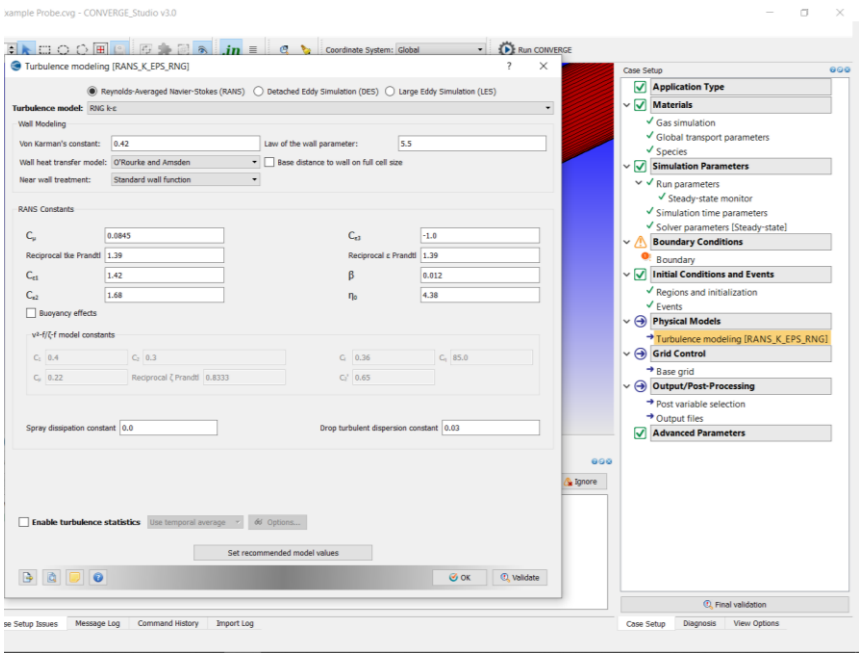

34. Select ‘Base grid’ and select ‘OK’.

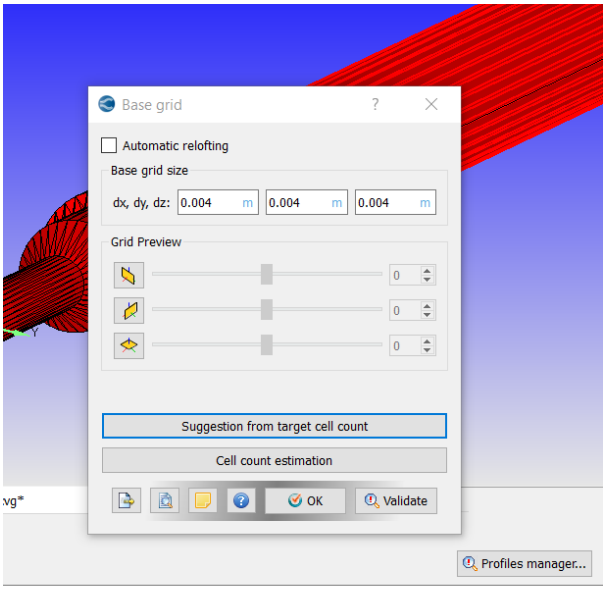

35. Select ‘Post variable selection’ and select ‘OK’.

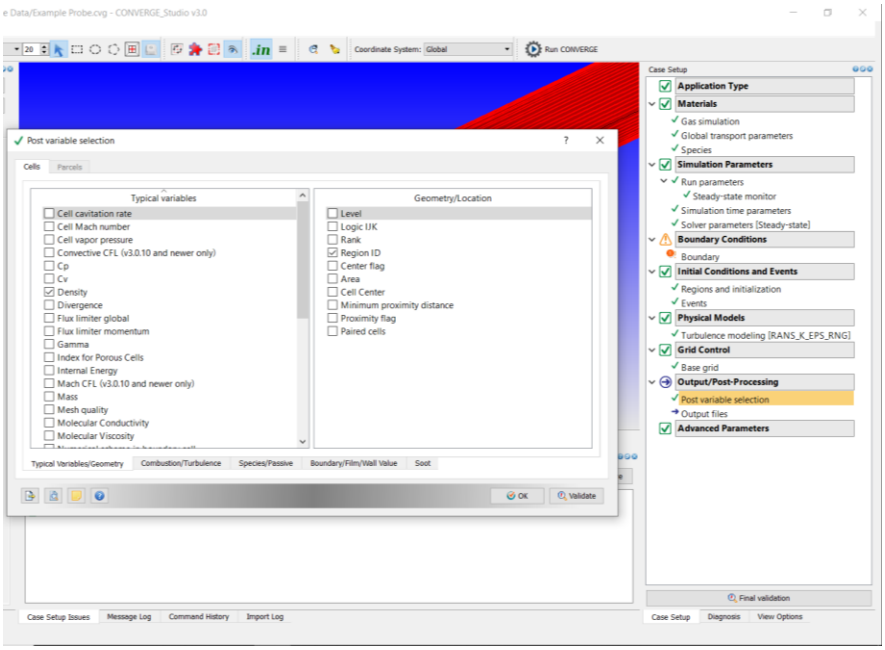

36. Finally, press the ‘Output files’ tab and select ‘OK’.

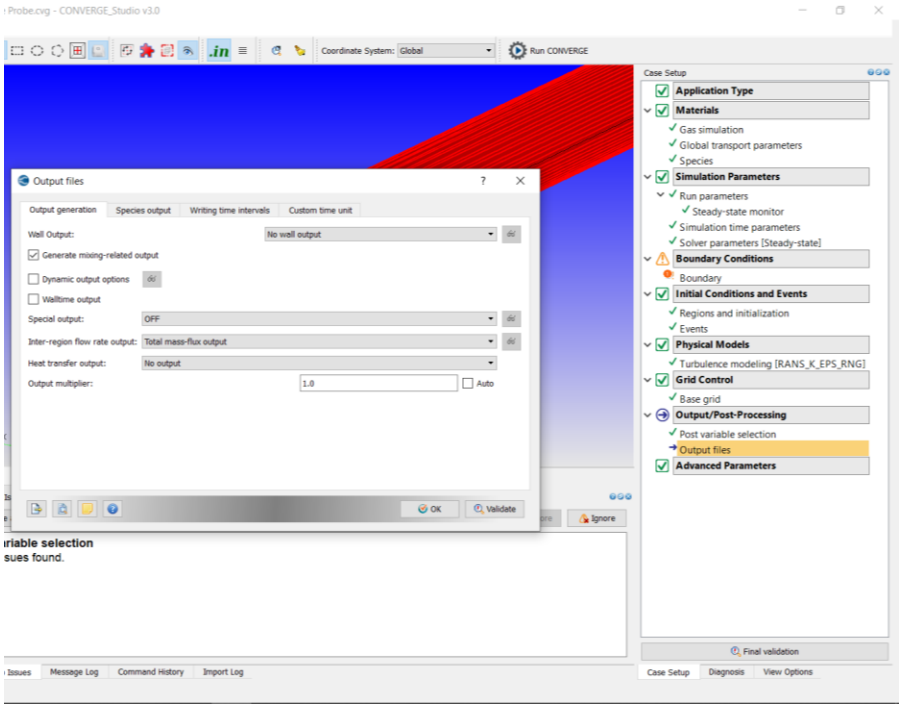

37. Now, press the ‘Final validation’ button in the bottom right and select yes on the pop-up. This will tell us if there are any warnings or errors in the case setup. Converge will run with errors which are identified by an orange exclamation point while errors are identified with a red coloring. If there, is some issue, then a parameter in your case setup is wrong so double-check everything. In this case, a warning will be shown because of the really low pressure value but, that is ok. This is a good point to save and it is the end of phase 3.

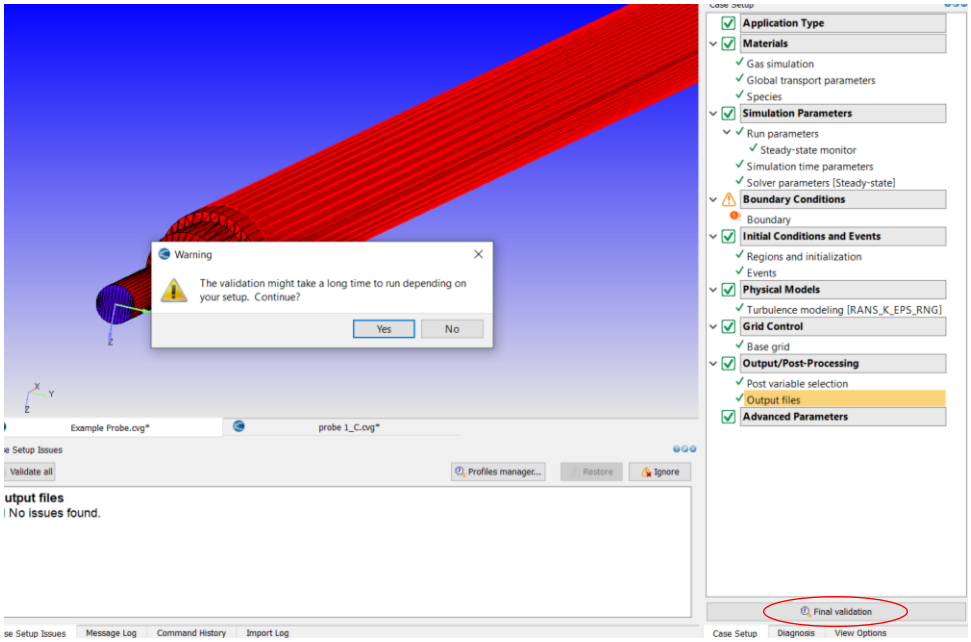

38. Now, in the 4th and final phase, the simulation can be ran and post-processing can start. At the top right, press ‘Run CONVERGE’ to commence the simulation.

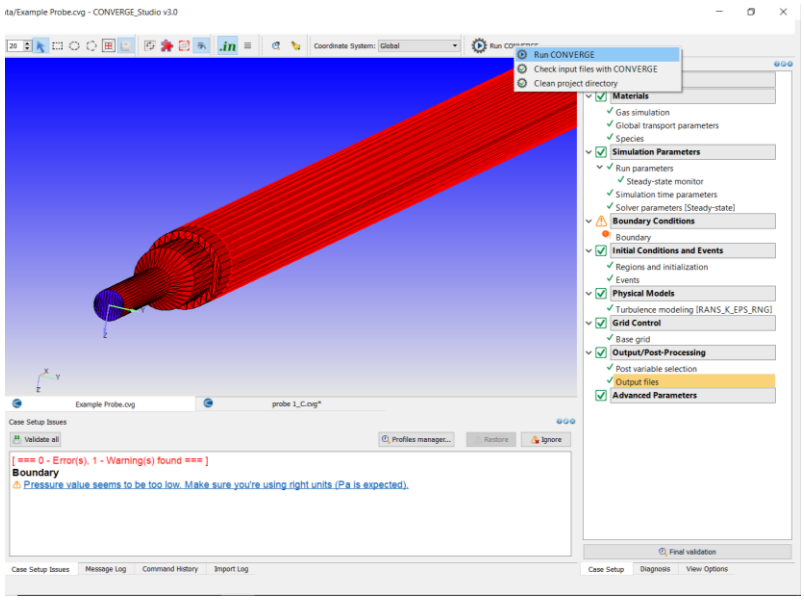

39. Next, on the pop-up, make sure the data is going to the correct output folder and select ok so the simulation can start.

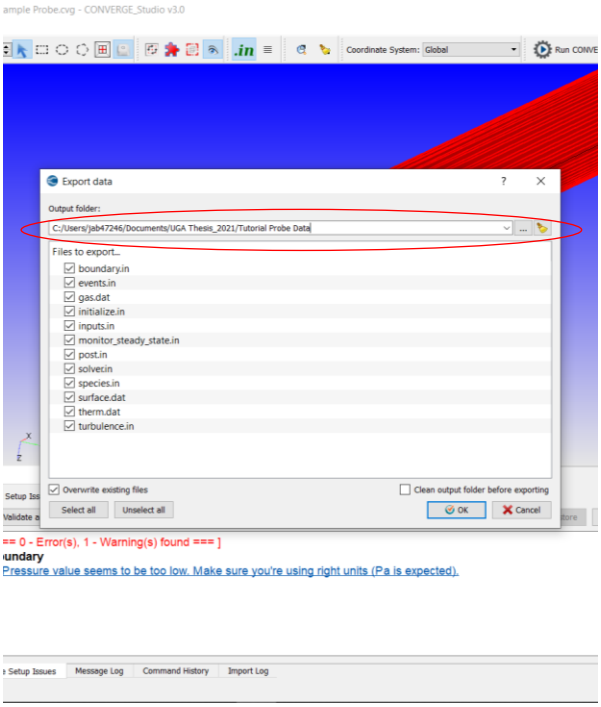

40. Now, the simulation should start. In some cases it may stop early because of some error and it will usually address this by referring to the issue in the case setup. If it doesn't start but, everything is correct, try to run it again and it should run properly. This pop-up will show the status and progression of the simulation. Run times vary for different simulations.

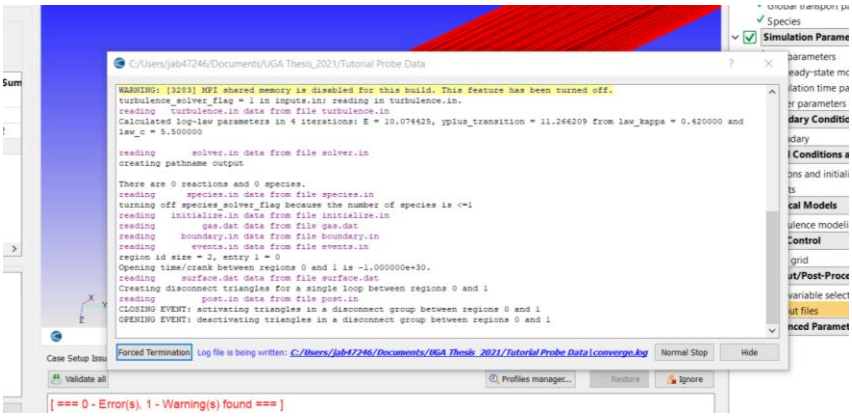

41. Once, the simulation is complete, this pop-up will show finished. If, this pop-up isn't shown, go to the 'Tools' tab in the upper left and click 'CONVERGE status'. One thing to note is that this status can show finished even if the process didn't reach 100%. Also, the time shown here is how long it took the simulation to run and has nothing to do with the output data.

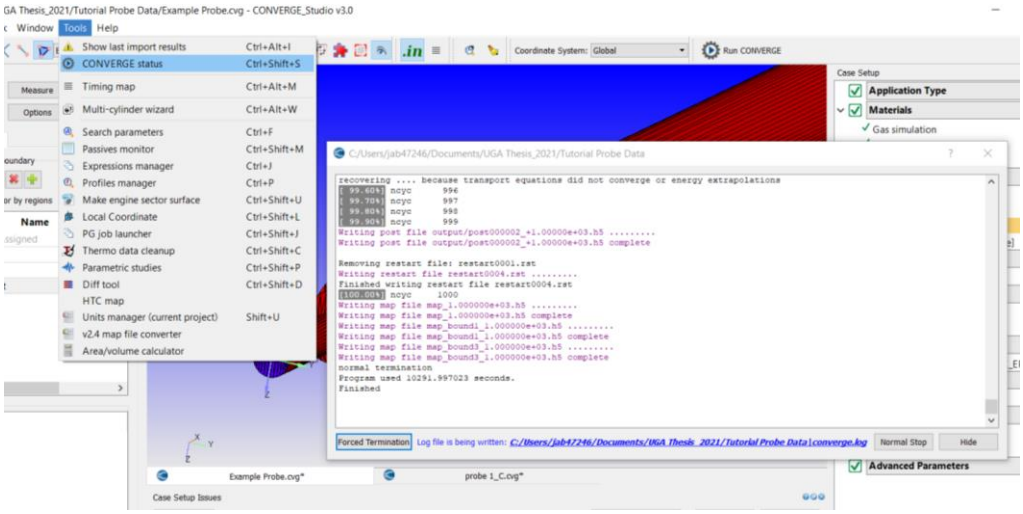

42. Once the simulation data is completed, the ‘Line plotting’ tab can be selected in the bottom left to begin post-processing. Next select ‘Open’ and select the folder that the output data for this case is in. Finally, a pressure plot should show up on the graph with cycles on the x-axis. This will be listed under the thermo.out files.

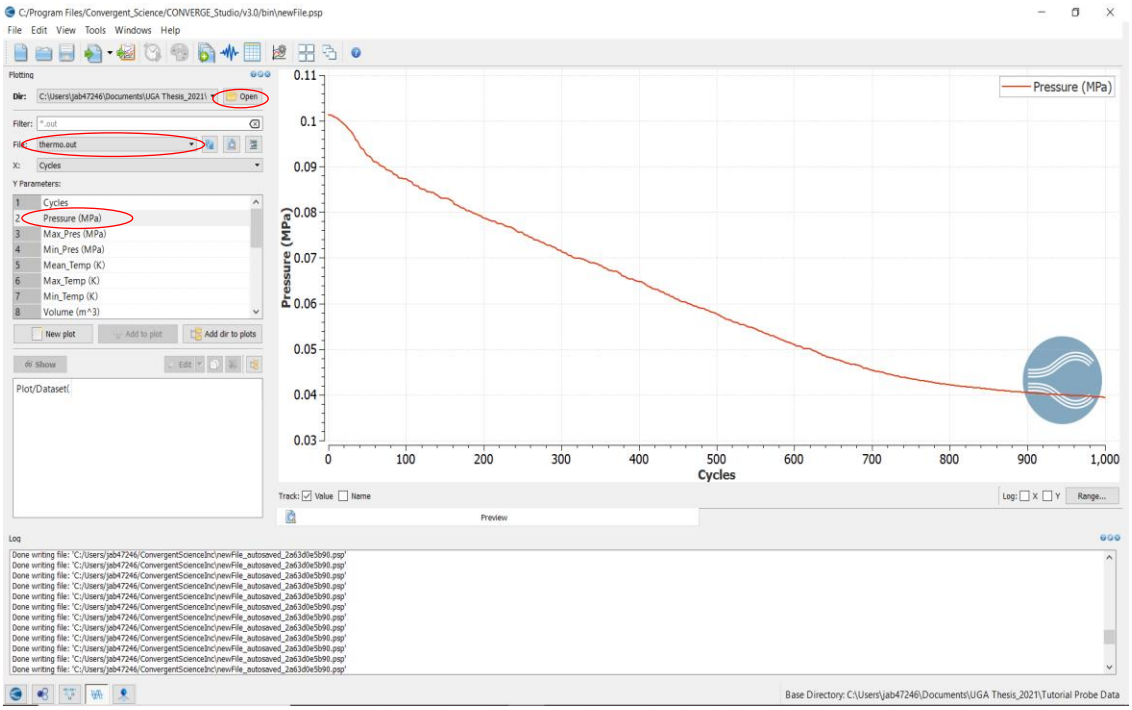

43. Next, I would suggest creating an excel file to help compile all of the data. Then click on the ‘preview plot data’ option to bring up the data for what is shown on the graph. Then highlight all of the data and select ‘copy to clipboard’.

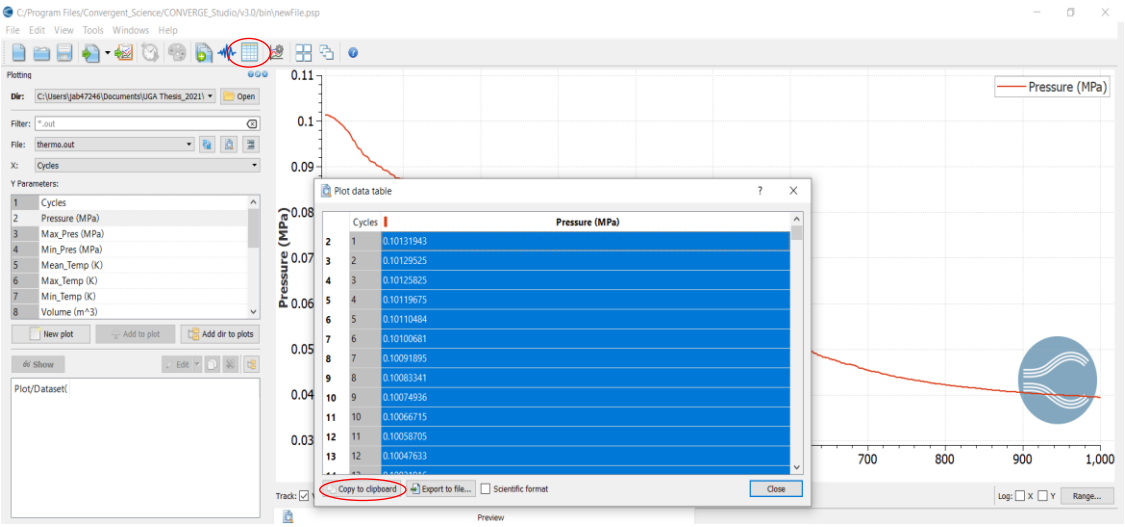

44. With the data copied to the clipboard, paste it directly into an excel sheet. Then make sure to label the data and pay attention to units.

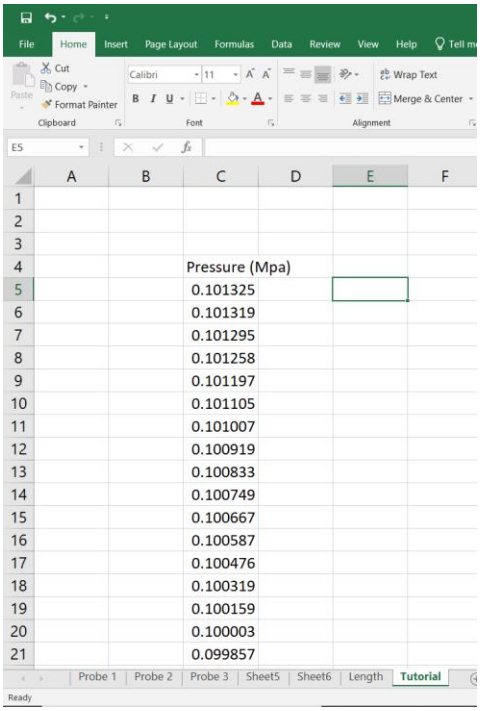

45. Next, repeat steps 43-44 for the mean temperature data which is also listed under the thermo.out data.

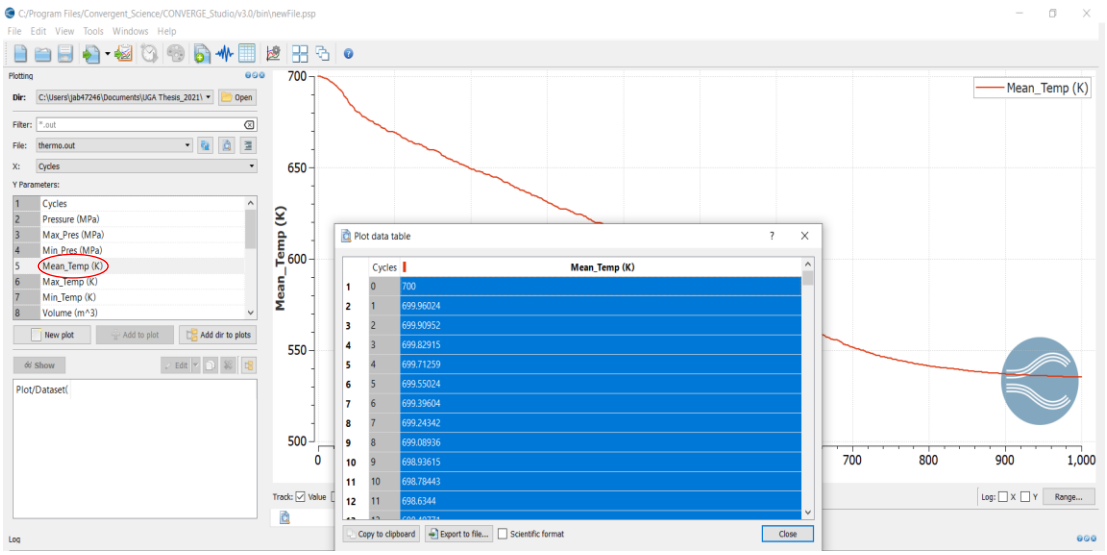

46. After that is completed, the excel sheet should look like this…

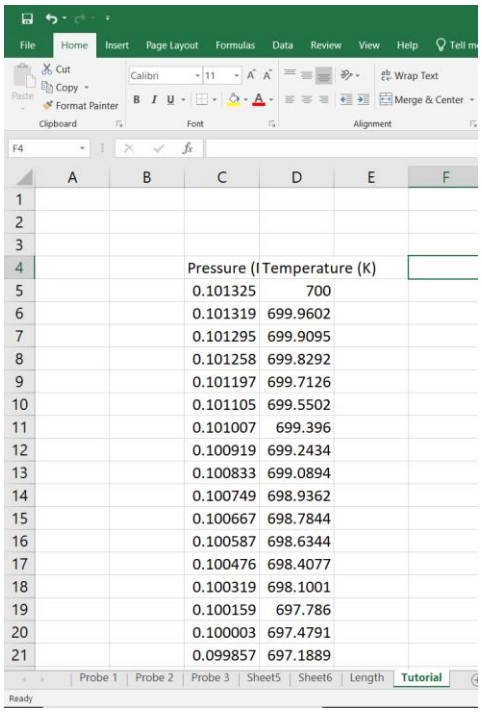

	A	B	C	D	E	F
1						
2						
3						
4			Pressure (I	Temperature (K)		
5			0.101325	700		
6			0.101319	699.9602		
7			0.101295	699.9095		
8			0.101258	699.8292		
9			0.101197	699.7126		
10			0.101105	699.5502		
11			0.101007	699.396		
12			0.100919	699.2434		
13			0.100833	699.0894		
14			0.100749	698.9362		
15			0.100667	698.7844		
16			0.100587	698.6344		
17			0.100476	698.4077		
18			0.100319	698.1001		
19			0.100159	697.786		
20			0.100003	697.4791		
21			0.099857	697.1889		

47. Next, change the file from ‘thermo.out’ to ‘time.out’ or ‘steady_state.out’ to extract the ‘Pseudo_Time’ data.

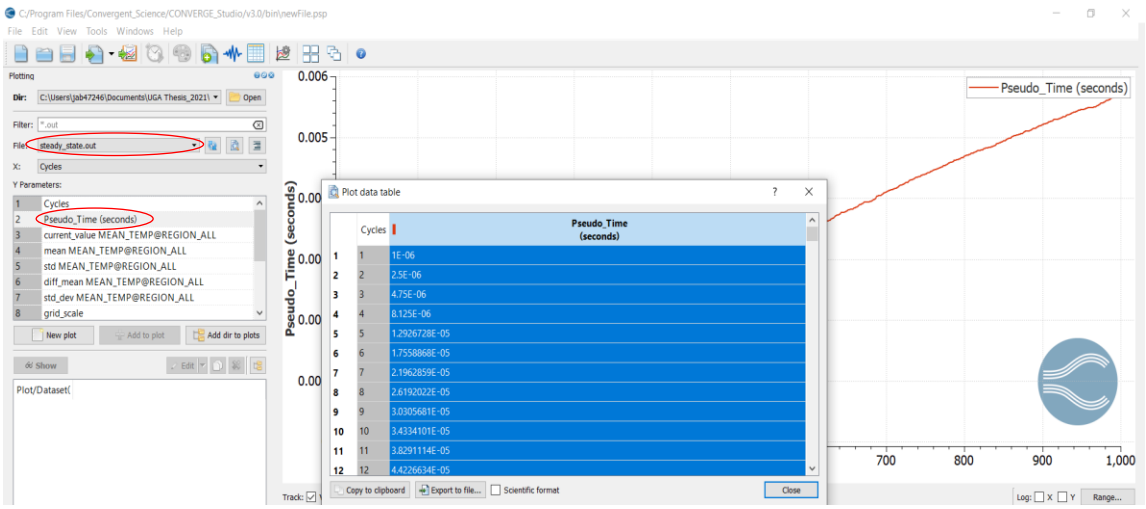

48. Then, take the time data and put it in excel.

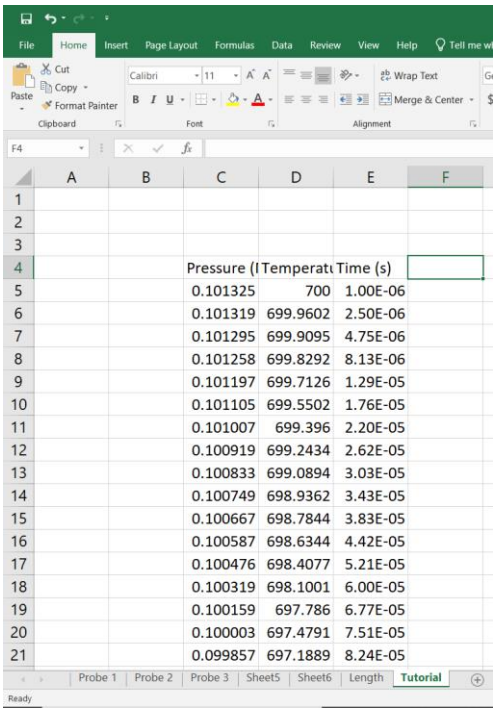

	A	B	C	D	E	F
1						
2						
3						
4			Pressure (I	Temperat	Time (s)	
5			0.101325	700	1.00E-06	
6			0.101319	699.9602	2.50E-06	
7			0.101295	699.9095	4.75E-06	
8			0.101258	699.8292	8.13E-06	
9			0.101197	699.7126	1.29E-05	
10			0.101105	699.5502	1.76E-05	
11			0.101007	699.396	2.20E-05	
12			0.100919	699.2434	2.62E-05	
13			0.100833	699.0894	3.03E-05	
14			0.100749	698.9362	3.43E-05	
15			0.100667	698.7844	3.83E-05	
16			0.100587	698.6344	4.42E-05	
17			0.100476	698.4077	5.21E-05	
18			0.100319	698.1001	6.00E-05	
19			0.100159	697.786	6.77E-05	
20			0.100003	697.4791	7.51E-05	
21			0.099857	697.1889	8.24E-05	

49. Finally, change the file from ‘time.out’ or ‘steady_state.out’ to ‘turbulance.out’ then, extract the ‘lengthscale’ data.

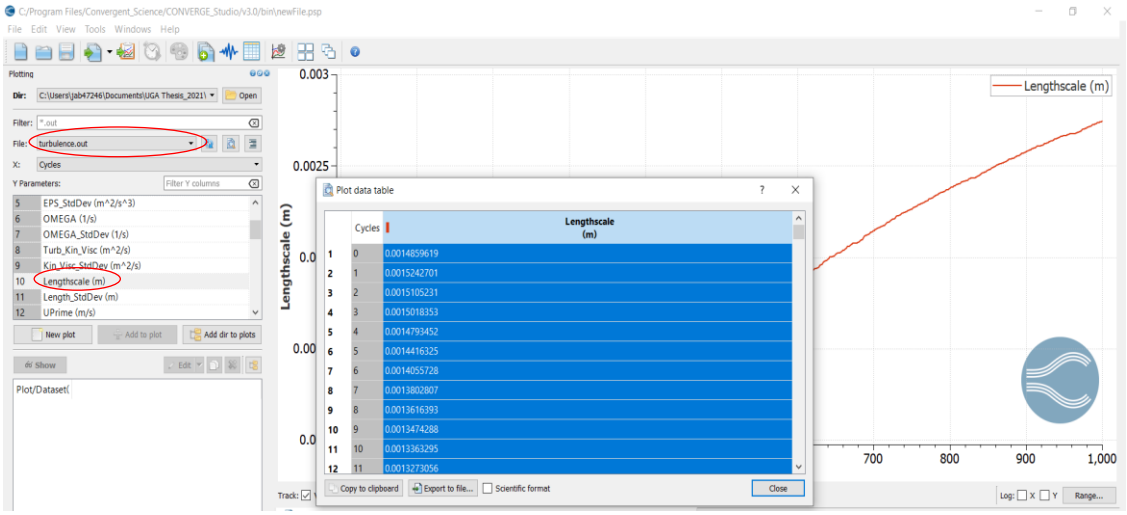

50. Once the ‘Lengthscale’ data is in excel, this data is essentially the ΔX data. So, an equation must be input to get the actual X data.

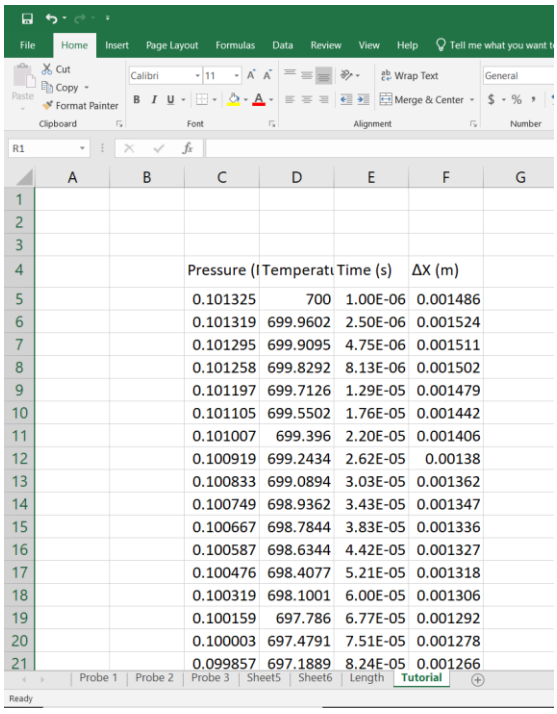

51. By inputting the formula below in excel, extend this formula down to the following sections.

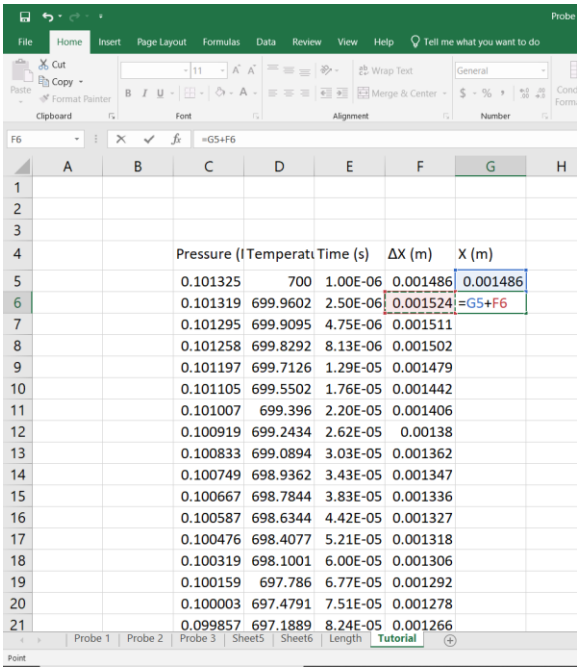

	A	B	C	D	E	F	G	H
1								
2								
3								
4			Pressure (I	Temperati	Time (s)	ΔX (m)	X (m)	
5			0.101325	700	1.00E-06	0.001486	0.001486	
6			0.101319	699.9602	2.50E-06	0.001524	=G5+F6	
7			0.101295	699.9095	4.75E-06	0.001511		
8			0.101258	699.8292	8.13E-06	0.001502		
9			0.101197	699.7126	1.29E-05	0.001479		
10			0.101105	699.5502	1.76E-05	0.001442		
11			0.101007	699.396	2.20E-05	0.001406		
12			0.100919	699.2434	2.62E-05	0.00138		
13			0.100833	699.0894	3.03E-05	0.001362		
14			0.100749	698.9362	3.43E-05	0.001347		
15			0.100667	698.7844	3.83E-05	0.001336		
16			0.100587	698.6344	4.42E-05	0.001327		
17			0.100476	698.4077	5.21E-05	0.001318		
18			0.100319	698.1001	6.00E-05	0.001306		
19			0.100159	697.786	6.77E-05	0.001292		
20			0.100003	697.4791	7.51E-05	0.001278		
21			0.099857	697.1889	8.24E-05	0.001266		

52. Next, the formula below can be input to find dT/dt. Next, this equation can be extended to the following iterations.

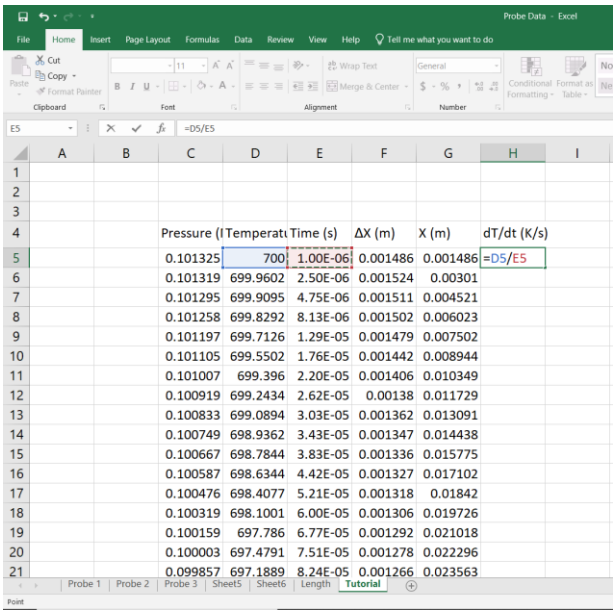

	A	B	C	D	E	F	G	H	I
1									
2									
3									
4			Pressure (I	Temperati	Time (s)	ΔX (m)	X (m)	dT/dt (K/s)	
5			0.101325	700	1.00E-06	0.001486	0.001486	=D5/E5	
6			0.101319	699.9602	2.50E-06	0.001524	0.00301		
7			0.101295	699.9095	4.75E-06	0.001511	0.004521		
8			0.101258	699.8292	8.13E-06	0.001502	0.006023		
9			0.101197	699.7126	1.29E-05	0.001479	0.007502		
10			0.101105	699.5502	1.76E-05	0.001442	0.008944		
11			0.101007	699.396	2.20E-05	0.001406	0.010349		
12			0.100919	699.2434	2.62E-05	0.00138	0.011729		
13			0.100833	699.0894	3.03E-05	0.001362	0.013091		
14			0.100749	698.9362	3.43E-05	0.001347	0.014438		
15			0.100667	698.7844	3.83E-05	0.001336	0.015775		
16			0.100587	698.6344	4.42E-05	0.001327	0.017102		
17			0.100476	698.4077	5.21E-05	0.001318	0.01842		
18			0.100319	698.1001	6.00E-05	0.001306	0.019726		
19			0.100159	697.786	6.77E-05	0.001292	0.021018		
20			0.100003	697.4791	7.51E-05	0.001278	0.022296		
21			0.099857	697.1889	8.24E-05	0.001266	0.023563		

53. The final product of the excel data should look similar to what is shown below. By using this data, the dT/dx, dP/dx, dT/dt, dP/dt, and (dT/dt)/dt plots can be created. This concludes the post-processing section.

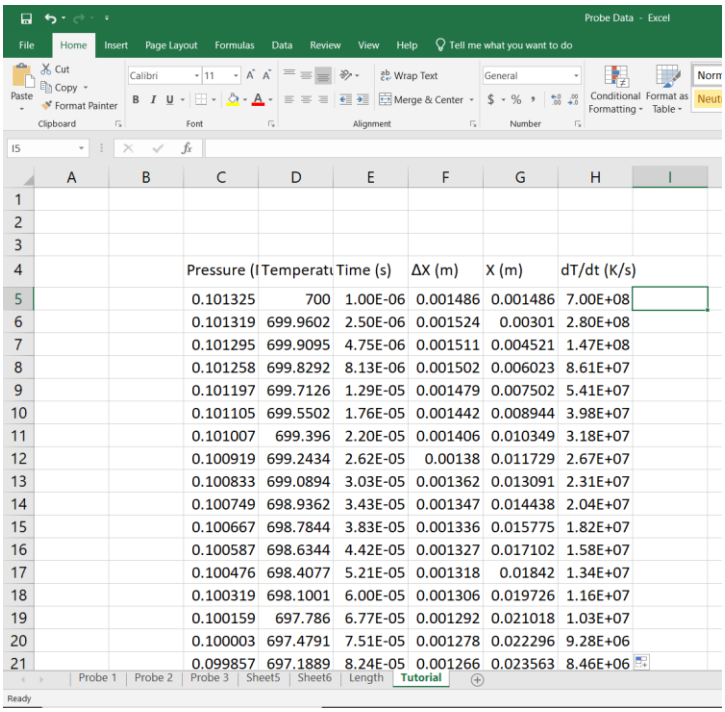

	A	B	C	D	E	F	G	H	I
1									
2									
3									
4			Pressure (I	Temperatı	Time (s)	ΔX (m)	X (m)	dT/dt (K/s)	
5			0.101325	700	1.00E-06	0.001486	0.001486	7.00E+08	
6			0.101319	699.9602	2.50E-06	0.001524	0.00301	2.80E+08	
7			0.101295	699.9095	4.75E-06	0.001511	0.004521	1.47E+08	
8			0.101258	699.8292	8.13E-06	0.001502	0.006023	8.61E+07	
9			0.101197	699.7126	1.29E-05	0.001479	0.007502	5.41E+07	
10			0.101105	699.5502	1.76E-05	0.001442	0.008944	3.98E+07	
11			0.101007	699.396	2.20E-05	0.001406	0.010349	3.18E+07	
12			0.100919	699.2434	2.62E-05	0.00138	0.011729	2.67E+07	
13			0.100833	699.0894	3.03E-05	0.001362	0.013091	2.31E+07	
14			0.100749	698.9362	3.43E-05	0.001347	0.014438	2.04E+07	
15			0.100667	698.7844	3.83E-05	0.001336	0.015775	1.82E+07	
16			0.100587	698.6344	4.42E-05	0.001327	0.017102	1.58E+07	
17			0.100476	698.4077	5.21E-05	0.001318	0.01842	1.34E+07	
18			0.100319	698.1001	6.00E-05	0.001306	0.019726	1.16E+07	
19			0.100159	697.786	6.77E-05	0.001292	0.021018	1.03E+07	
20			0.100003	697.4791	7.51E-05	0.001278	0.022296	9.28E+06	
21			0.099857	697.1889	8.24E-05	0.001266	0.023563	8.46E+06	